PALEOECOLOGICAL STUDY OF COASTAL MARSH IN THE CHENIER PLAIN, LOUISIANA: INVESTIGATING THE DIATOM COMPOSITION OF HURRICANE-DEPOSITED SEDIMENTS AND A DIATOM-BASED QUANTITATIVE RECONSTRUCTION OF SEA-LEVEL CHARACTERISTICS

By

KATHRYN E.L. SMITH

A DISSERTATION PRESENTED TO THE GRADUATE SCHOOL
OF THE UNIVERSITY OF FLORIDA IN PARTIAL FULFILLMENT
OF THE REQUIREMENTS FOR THE DEGREE OF
DOCTOR OF PHILOSOPHY

UNIVERSITY OF FLORIDA

2012

To my son, Leo

ACKNOWLEDGMENTS

I gratefully acknowledge the logistical support of the U.S. Geological Survey Center for Coastal and Marine Science in St. Petersburg, Florida, and the National Wetlands Research Center in Baton Rouge and Lafayette, Louisiana. In addition, staff from Rockefeller Wildlife Refuge and Louisiana Department of Natural Resources for granting access to the refuge and aid in sampling. In particular, I wish to thank Molly McLaughlin, Meghan Maraia, Tom Harmon, Carl Taylor and Chandra Dreher for assistance in the lab; Marcy Marot for radioisotope analyses; Sarai Piazza and Greg Steyer for answering countless questions on CRMS and sending me the mud; Leigh Ann Sharp, George Melancon, and Mark Mouledous for assistance in the field; Brady Couvillion for providing access to spatial data; Jim Flocks for letting me run with this project; and Jimmy Johnston and Kim Yates who got me started down this path.

I wish to thank the members of my committee: Drs. John Jaeger, Melanie Riedinger-Whitmore and William Wise; you are truly the best group of advisors I could have ever hoped for. Not many people can say they came out of their qualifying exams feeling inspired and excited, but I can. Thank you for your enthusiasm and support. I also want to thank Tom Whitmore for sharing his passion and knowledge of diatoms, and asking for nothing in return. I would not have been able to do any of this if it wasn't for your help. Most importantly, I thank Dr. Clay Montague for accepting me as a student, inspiring me when I was floundering, sticking with me when I faced challenges, helping me see the bigger picture, and providing an example of the exact type of scientist and educator I will strive to be.

My heartfelt thanks go to the following: my parents for never letting me doubt my abilities and making me your first and foremost priority; my brothers, who encouraged

my imagination and without which I would not be nearly as resilient and resourceful; to some wonderful friends who provided a much needed compassionate ear and backed me up over the years, each in your own way, when I faced parent-work-school-life challenges: Marti McGuire, Theresa Burress, Kelly Shotts, and Kristine Martella. No matter how far apart we are now or in the future, you'll always be a part of this journey.

And to my son, Leo, thank you for being patient and forgiving me for all those times I couldn't do what you wanted to do because I had to work on my 'desert-tation'. I know I have some making up to do. You are my heart and my treasure.

TABLE OF CONTENTS

LIST OF TABLES

LIST OF FIGURES

LIST OF ABBREVIATIONS

Acc	vertical accretion
BD	bulk density
°C	degree Celsius
CCA	canonical correspondence analysis
CF:CS	constant flux : constant sedimentation
cm yr^{-1}	centimeters per year
g cm^{-3}	grams per cubic centimeter
CRMS	Coast-wide Reference and Monitoring Station
CRS	constant rate of supply
DCCA	detrended canonical correspondence analysis
DIC	Differential interference contrast
DSI	diatom salinity index
Grain	mean sediment grain size
km^2	square kilometers
LDNR	Louisiana Department of Natural Resources
LOI	loss-on-ignition
m	meters
mL	milliliters
MSO	multi-scale ordination
NAVD88	National Vertical Datum 1988
MDS	multidimensional scaling
NOAA	National Oceanic and Atmospheric Administration
PCA	principal components analysis
pRDA	partial redundancy analysis

RDA	redundancy analysis
RSET	rod-surface elevation table
RWR	Rockefeller Wildlife Refuge
Sed	sediment elevation change
SD	Hill's standard deviation units of compositional turnover
Spp	primary species cover
USGS	U.S. Geological Survey
Veg	total vegetation cover
WA	weighted average
WA-PLS	weighted averaging partial least squares
WL	water level
VAR	vertical accretion rate
^{210}Pb	lead-210
$^{210}Pb_{xs}$	excess (unsupported) lead-210
^{137}Cs	cesium-137

Abstract of Dissertation Presented to the Graduate School
of the University of Florida in Partial Fulfillment of the
Requirements for the Degree of Doctor of Philosophy

PALEOECOLOGICAL STUDY OF COASTAL MARSH IN THE CHENIER PLAIN, LOUISIANA: INVESTIGATING THE DIATOM COMPOSITION OF HURRICANE-DEPOSITED SEDIMENTS AND A DIATOM-BASED QUANTITATIVE RECONSTRUCTION OF SEA-LEVEL CHARACTERISTICS

By

Kathryn E.L. Smith

December 2012

Chair: Clay L. Montague
Major: Environmental Engineering Sciences

Combined paleoecological and geochronological analyses can provide a critical tool for understanding coastal marsh development and ecological response to perturbations, such as sea-level rise and tropical storms, particularly in regions like coastal Louisiana, where high rates of wetland loss threaten an ecologically and economically important ecosystem. Analysis of sediment cores from Rockefeller Wildlife Refuge identify sediment deposition from storm surge and show that diatom assemblage of hurricane sediments are dissimilar from non-storm sediments and have the potential for examining historical frequency of storms. Chronology and vertical accretion rates calculated from ^{210}Pb radioisotope using the constant flux : constant sedimentation method provided the best match to an independent tracer (^{137}Cs), and indicate that marsh rates of vertical accretion are generally lower than regional estimates of mean sea-level rise, despite recent hurricane deposition. Contemporary diatom samples from 46 sites located throughout the Chenier plain were examined to test the relationship between diatom assemblage and environmental parameters.

Results showed that diatom assemblage was strongly influenced by salinity, but less strongly by water level, bulk density, and organic matter. Analyses which partition the variance indicate a significant overlap between salinity, bulk density, and organic matter, while water level explains a portion of diatom variability independent of the salinity influence. Spatial autocorrelation was significant only for samples closer than 3 km, which in this study affected only a few sample pairs, but demonstrates a possible problem for studies where samples are closer in proximity. Transfer functions relating diatom assemblage to salinity had a high r^2 and salinity reconstructions for three sediment cores suggest a good correspondence to historic data and information. However, the model tended to under-predict high salinity samples and was sensitive to removal of sites (r^2_{jack}= 0.45). Water level and elevation transfer functions were not recommended because an insufficient number of diatom species had their optima located within the data set. Future work should involve increasing the number of samples to build a more robust salinity transfer function and testing the model on a sediment core from a location where a longer historic record is available.

CHAPTER 1
INTRODUCTION

Motivation

The goal of this study is to investigate diatoms as a paleoecological indicator for identifying hurricane sediment deposition and examining sea-level history in the coastal marsh of southwest Louisiana. The influence of storm sedimentation on vertical accretion is a critical research question in southern Louisiana because marsh loss is increasing under rising sea level and a sedimentary deficit is considered to be one of the primary causes (Boesch et al., 1994; Hatton et al., 1983; Turner, 1997). In southwest Louisiana, sediments are delivered into the marsh in largely three ways: freshwater inflow from upland areas, tidal flooding, or wind-driven currents from storms (Gosselink et al., 1979). Storm-derived sedimentation may be the dominant source of mineral sediments to some marsh areas, particularly the interior marsh (Delaune et al., 1986; Rejmánek et al., 1988; Stumpf, 1983). Storm sediments have been shown to positively influence marsh elevation and slow submergence through delivery of sediments and stimulation of root matter production (McKee and Cherry, 2009). However, tropical storms can also have a negative influence on marsh elevations, through erosion and saltwater intrusion (Guntenspergen et al., 1995; Morton and Barras, 2011; Stone et al., 1997). Paleoecological methods can provide a substantial tool to understanding the role of hurricane sedimentation on marsh elevation and the influence of rising sea level on marsh ecology. Specific questions addressed in this study are:

- Is the diatom assemblage of storm deposited sediments different from non-storm sedimentation? If so, can diatom assemblage be used as a proxy for identifying past storms?

- Are estimates of vertical accretion rate and chronology using radioisotope tracers ^{210}Pb and ^{137}Cs valid in an event-driven system? Do radioisotope depth profiles and inventories reflect these events through deviations from expected profile patterns and inflated radioisotope inventories?
- Is variation of diatom assemblage influenced by sea level parameters, such as water level and elevation?
- Does a regionally-based diatom transfer function produce a reasonable reconstruction of sea-level?

Background

Louisiana Wetland Loss

Coastal wetlands are among the most productive ecosystems in the world and are under increasing threat due to anthropogenic and natural environmental pressures. They provide numerous services to society, including nursery habitat for many species of fish and crustaceans (Boesch and Turner, 1984) and protection from storm surge, flood attenuation, and shoreline mitigation (Costanza et al., 2008). Coastal wetlands also play an important role in biogeochemical processes (Harvey and Odum, 1990; Hemond et al., 1984). Coastal wetlands can improve water quality of adjacent coastal waters by intercepting surface and groundwater, and reducing suspended sediments, nutrients, and contaminants through bioaccumulation in wetland soils and plants (DeLaune et al., 1981; Merrill and Cornwell, 2002). Intertidal wetland loss has accelerated in the United States in recent years (Dahl, 2011; Stedman and Dahl, 2008), which will likely have long-term consequences on ecosystem services (Nicholls et al., 1999). Coastal Louisiana is home to one of the largest intertidal wetland ecosystems in the world, but also the most extensive loss of wetlands since the 1970s (Britsch and Dunbar, 1993; Dahl, 2011). A majority of the wetland loss has been attributed to submergence from subsidence and sea level rise (Boesch et al., 1983; Penland et al.,

1996; Reed, 1995), but the interrelated factors contributing to loss is a combination of many factors including deficiencies in sediment, artificial waterways, wave erosion, land subsidence, and salt water intrusion. Vertical accretion is an important facet of wetland submergence since both organic production and inorganic sedimentation are important controls for marsh elevation, and marsh elevation in relation to sea level is the critical element of wetland persistence.

Hurricanes have both physical and chemical impacts on coastal marsh through a combination of high-velocity wind and water level. Wind is the primary force that generates storm surge and surface waves (Ebersole et al., 2010), which alters marsh surface elevation through erosion and deformation. Chemical stress from inundation and prolonged retention of storm-surge water can have adverse impacts on wetland plants, potentially leading to plant death and peat collapse (due to decomposition of root material and sediment compaction; Cahoon et al., 2003). Although, physical removal and salinization from hurricanes have been cited as causes of wetland loss (Barras, 2006; Day et al., 2000; Stone et al., 1997), hurricanes are also a source of inorganic sediments (Michener, 1997; Turner et al., 2006a) and may positively influence marsh elevation. Paleoecological or geophysical methods for identifying storm-derived sediment deposition can provide critical information on the role of storms and their influence on past marsh elevation, further clarifying the challenges which will be faced in future climate change and sea-level rise scenarios.

Wetland loss has been well documented in recent history using aerial and satellite imagery (Barras et al., 2003; Britsch and Dunbar, 1993). Field studies provide a robust body of knowledge on the interrelated processes causing wetland loss (Boesch

et al., 1994; Cahoon et al., 1999; Cahoon et al., 1998; Day et al., 1994). Geologic models provide the foundation for subsurface processes and controls on subsidence (Gagliano et al., 2003; Kulp et al., 2005). However, we still have very little knowledge of the long-term ecology of wetlands and how they respond to environmental and climate-driven stimuli because continuous environmental monitoring of Louisiana wetlands has only just recently been initiated (Steyer, 2010). Paleo-indicators can provide a useful tool for bridging the gap between recent monitoring efforts, snap-shot spatial mapping, and the longer-term temporal dynamics of intertidal marsh.

Paleoecology

Diatom assemblages have been successfully used to reconstruct long-term ecological histories in both fresh and marine systems (Battarbee, 1986). Diatoms are particularly useful paleo-indicator because: species often have identifiable ecological niches, their species-distinctive frustule preserves well in most sediment, they are sensitive to environmental conditions, and they respond rapidly to environmental change. Phytoplankton doubling is on the time scale of a few days (Reynolds, 1984) and species assemblage have been shown to respond to different times scales, from days to weeks to seasonal events (Pannard et al., 2008). Diatoms have been used to reconstruct many variables of environmental change, including sea level, water quality parameters, and extreme events, such as tsunamis or tropical storms (Smol and Stoermer, 2010).

The reconstruction of past environments has long been the objective of paleontology. Earlier research on diatoms was largely qualitative or semi-quantitative, attempting to reconstruct past conditions using the varying abundances of particular species (e.g. Fletcher III et al., 1993). Some studies rely on indices, developed from

knowledge of the distribution or characteristics of species (such as a ratio of marine to estuarine species) based on some qualitative grouping of species or characteristics (e.g. Parsons et al., 1999a).

Paleoenvironmental transfer functions are a quantitative approach to reconstructing past environmental conditions. A transfer function is an empirically derived equation based on relationships between modern environmental data and the distribution of a paleoindicator, such as diatoms, foraminifera, and pollen (Sachs et al., 1977). The implementation of numerical techniques for calculating these functions is accredited to Imbrie and Kipp (1971), but was also independently introduced by Fritts et al. (1971) and Webb & Bryson (1972). The methodology of paleoecological transfer functions has been thoroughly evaluated and described in the work of several authors (Birks, 1995; Birks et al., 2012; Birks, 2010; Guiot and de Vernal, 2007; Juggins, 1992; Sachs et al., 1977). Briefly, two data sets are needed: the modern analogue (also called training data or calibration data) and fossil species data from a sediment core. The modern analogue provides species responses to specific environmental variables, which are used to construct the response models (Chapter 4). Data for the modern analogue are typically obtained by measuring both the environmental variables and diatom species assemblage for locations throughout the range of the environmental parameters of interest and calculating a transfer function, which is essentially a multivariate regression model. Species data are obtained from surface sediments samples, which represent diatom thanatocoenoses (both allocthonous and allochthonous remains, present at a particular time in the sediment), the assumption being that this assemblage integrates the spatial and temporal variation of

environmental perturbations and represents more faithfully the fossil assemblage. Diatoms have excellent preservation and high site fidelity in estuarine environments (Hassan et al., 2008) and the surface sediment sampling technique likely provides an appropriate analogue in coastal marshes as well. The transfer function, which is the inverse of the multivariate response function, enables the calculation of the environmental parameter (e.g. salinity) from the known biological response (e.g. diatom assemblage) found in fossil samples (Chapter 5). The assumptions of this technique are: 1) the environmental variable of interest is a primary driver of the distribution of species assemblage, 2) the modern observations contain all the necessary information (the species found in the modern samples are the same as those within the fossil assemblage), 3) the modern record of species niches have not shifted/changed over time and are an accurate representation of the fossil data. These assumptions are partially satisfied by collecting data on diatom species distribution and examining it against fossil material. With well-defended assumptions, paleo-indicators can be applied to many areas of coastal research and management, including interpreting the effects of accelerated sea level rise on coastal marsh, and examining the impact of human activities on wetlands over the past century (Orson, 1996). Intertidal wetlands have become a focus of paleoecological research on sea level because their sediments retain records, in the form of microfossils of sea level (Gehrels et al., 2001; Horton et al., 2006; Horton and Edwards, 2006; Horton et al., 2007; Kemp et al., 2009; Roe et al., 2009; Sherrod, 1999; Szkornik et al., 2006). Microfossils are microscopic remains, or imprints, of plants or animals that existed in the past and are extracted from the soil, such as diatoms, foraminifera, or pollen. In addition, studies focused on the

identification and preservation of episodic events, such as tropical storms and tsunamis, have also encouraged paleoenvironmental studies of coastal marsh (Hayward et al., 2004; Hemphill-Haley, 1995; Hippensteel et al., 2005; Parsons, 1998). This study will apply the transfer function technique to examine marsh parameters of sea level for a coastal marsh in southwest Louisiana.

The Louisiana coastal marsh provides an ideal location for comprehensive studies of paleoecological evidence of both hurricanes and sea level rise, and this study focuses on the Chenier plain of southwest Louisiana (Figure 1-1). Coastal monitoring sites located throughout the region provide ideal sampling sites for modern calibration data and for sediment cores representing 100-200 years of Holocene record. Such information can be collected using hand push-cores. However, no paleoenvironmental studies have yet been published from Louisiana using a diatom transfer function technique, yet the utility of such a study is applicable to many areas of scientific research and coastal marsh planning.

Hurricanes and Sedimentation

Hurricanes have played a significant role in the geomorphology of the Louisiana coastline, and are both destructive agents and sources of sediment for declining wetlands (Baumann et al., 1984). Forty-one hurricanes and countless tropical storms have made landfall in coastal Louisiana since 1850. Thirteen hurricanes made landfall on the Chenier plain with approximately half of these storms classified as a category 3 or higher on the Saffir-Simpson scale (http://www.csc.noaa.gov/hurricanes/ ; accessed September 30, 2012). Hurricane Andrew (1992) encouraged a significant amount of research on tropical storms and storm impact on the geomorphology of the coastal marsh (e.g. Cahoon et al., 1995b; Dingler et al., 1995; Doyle et al., 1995;

Guntenspergen, 1998; Guntenspergen and Vairin, 1996; Parsons, 1998; Ramsey et al., 1994; Sallenger and Williams, 1993; Stone et al., 1995; Turner et al., 2007), but it was Hurricanes Katrina and Rita (2005) that highlighted the severity of high-frequency, catastrophic storms can have on an already weakened coast. Return history for major storms is one every 12 years (Rybczyk and Cahoon, 2002), but with the anticipated effects of climate change and ocean warming, hurricane frequency or storm intensity may increase (Goldenberg et al., 2001; Webster et al., 2005), resulting in potentially greater impacts for Louisiana coastal wetlands.

Numerous field surveys have documented the addition of hurricane-deposited sediments onto the surface of the coastal marsh. The thickness of storm-deposited sediment ranges from just a few centimeters to up to 70-cm thick (Table 1-1) and is dependent on many factors, such as storm track, wind speed, and height of storm surge. Although storm deposition is often considered an influx of mineral sediments to the coast from intercontinental waters (Turner et al., 2006a), the deposited sediment could be from inland waters (shallow bays or marsh lakes) or transported and re-deposited marsh sediments.

Sediment deposition from tropical storms may provide a substantial source of mineral sediments to coastal marshes, particularly for interior marshes or locations where flood waters are obstructed from levees or impoundments. Storm deposition has been shown to alleviate marsh loss by stimulating below-ground productivity and positively impact marsh elevation (McKee and Cherry, 2009). However, storm deposition has been shown to increase elevation loss through subsurface compaction (Cahoon et al., 1995a), thereby annulling the sedimentary increase in marsh elevation

from deposition. Overall, the uncertainty of where the sediments are coming from and how they impact marsh development requires further research.

Paelotempestology is the study of past tropical cyclone activity by means of geologic proxies and historical documentary evidence (Liu, 2004). Since hurricane impacts and frequency are spatially dependent, understanding the long-term history of storms and the influence of storms on coastal geomorphology is vital for examining the impact of future climate changes and sea-level rise on coastal habitats and examining the susceptibility of wetlands to storm damage. In the northern Gulf of Mexico, sand layers are a common proxy used to isolate historic storms in the geologic record (Liu, 2004; Liu and Fearn, 2000a; Liu and Fearn, 1993, 2000b; Otvos, 1999; Stone et al., 2004; Williams, 2010). Sand layers are caused by overwash from storm surge and wind currents that transports sand from barrier islands and beaches into coastal lakes and marsh located interior of the shelf margin. Sand layers are found within sediment cores since they are uncharacteristic of regular sedimentation patterns and have distinct, boundaries or “contacts”. Since compaction and decomposition over time influences porosity and organic matter composition of sediments, non-storm sediments have a general trend of slightly increasing bulk density downcore. However, sharp, distinct boundaries between sedimentary deposits indicate an abrupt change in sedimentation processes and an abrupt return to the former sedimentation pattern suggests an “event”. Since the continental margin of southwest Louisiana is dominated by fine-grained sediments deposited from the Mississippi and Atchafalaya Rivers (Draut et al., 2005; McBride et al., 2007; Roberts et al., 2002), the sand layer proxy may not provide a well-defined indicator of historic storms for this region. Diatoms have been used to

identify past extreme events, such as hurricanes or tsunamis (Hayward et al., 2004; Hemphill-Haley, 1995; Parsons, 1998; Zong et al., 2003). Diatoms may provide a more reliable indicator of past tropical storms than sand layers in southwest Louisiana.

Study Area

Chenier Plain

The Louisiana coastal zone can be divided into two basic geomorphic zones: the Mississippi delta plain on the southeast coast and the Chenier plain of the southwest with the dividing line located near Vermillion Bay (29°43'11" N, 91°58'34" W). The Chenier plain extends from Vermillion Bay to the Texas state border and includes over 6,000 km^2 of coastal marshes. It was formed by the deposits of fine-grained sediments of the Mississippi River during the Middle to Late Holocene. A series of regressive-transgressive phases created relict beach ridges (called 'cheniers') within a 30-km wide coastal plain of low-energy fresh, brackish, and saline marshes (McBride et al., 2007). The cheniers act as barriers, reducing tidal flow to some areas of the marsh. The sediments are largely fine-grained silts and clays, with large amounts of organics and peat. Vegetation follows a general north-south salinity gradient of fresh to brackish to saline marsh. Visser et al. (2000) identified seven marsh types within the three salinity zones, with half of the marsh types being classified as oligohaline. The marsh types include: fresh maidencane, fresh bulltongue, oligohaline bullwhip, oligohaline paspalum, oligohaline wiregrass, mesohaline wiregrass, and mesohaline mixture.

The marshes of the Chenier plain are experiencing fewer declines than the Mississippi delta plain, with 20% of the total wetland loss in coastal Louisiana (Barras et al., 2003). However, these microtidal marshes receive limited sedimentation and alterations to natural hydrology have caused salinization. An estimated 360 km^2 of

wetlands have been lost in the Chenier plain from 1978 to 2000, and an additional 100 km^2 of loss is expected in the coming decades (Barras et al., 2003). Wetland loss rates will be an even greater problem given the increased human-impact on the environment, growing coastal populations, climate change and sea-level rise.

To mitigate the problem of wetland loss, state and federal partners have initiated one of the largest coastal restoration and monitoring programs in the nation. Various restoration projects have been initiated, with most projects targeted at restoring natural hydrology and stabilizing shorelines (Twilley, 2003; U.S. Army Corps of Engineers, 2003). To monitor and evaluate restoration efforts, the Coast-wide Reference and Monitoring Stations (CRMS) were created (Steyer et al., 2003; Steyer, 2010). CRMS is a network of 390 stations located throughout the coastal area where biological, hydrological, and physical data are being collected. Data collection includes water level, salinity, vegetation species and, sediment accretion, and elevation change.

Rockefeller Wildlife Refuge

Rockefeller Wildlife Refuge (RWR) is a state-owned refuge located in southwest Louisiana. Much of the area is managed for waterfowl and fishery habitat and a primary mission of the refuge is to promote scientific research (Louisiana Coastal Wetlands Conservation and Restoration Task Force, 2002). RWR has several constructed levees that are intended to moderate salinity and water level fluctuations for wildlife. However, the southeast portion where cores were collected is largely unaltered and receives natural tidal flows. Freshwater flow from upland marshes, however, was largely obstructed since the 1950s due to the construction of a highway and canal along the northern border. Shortly after road construction, concern by landowners prompted the construction of several culverts and bridges to increase flow south of the highway.

Dilapidation of these structures and concern over wetland loss south of the highway prompted the initiation of a restoration plan that involved a freshwater diversion from the Chenier lakes sub-basin to the north (Clark and Mazourek, 2005), the assumption being that changes in wetland vegetation and recent wetland submergence was caused by saltwater intrusion from a lack of freshwater from upland habitats. Vegetation data from 1948 to 2007 show that saline marsh has gradually increased in area, moving from a narrow fringe along the Gulf of Mexico shoreline to covering large areas of the interior marsh at the refuge (http://lacoast.gov/crms_viewer/; accessed on October 10th, 2012). The observed vegetation change is likely a result of reduced upland freshwater flow, sea-level rise, and subsidence. This general trend is not unique to RWR, but is observed at many locations throughout coastal Louisiana.

Outline of Chapters

Each of the chapters in this dissertation were written as stand-alone studies to test hypotheses or methodology, however they are closely interrelated and organized into a unified whole with a final chapter tying everything together. The main objectives of Chapter 2 are: 1) to identify hurricane sediment layers from marsh sediment cores, and 2) if hurricane sediment layers are found, examine diatom microfossils from hurricane sediments to determine if the diatom assemblage is spatially and temporally consistent with storm deposits from multiple sediment cores.

Geochronology for the sediment cores is evaluated to gain a greater understanding of impacts of event-based sedimentation on radioistopes (Chapter 3). Sediment deposited on the marsh surface from storms may significantly influence radioisotope inventories and flux rates. Since radioisotopes are a common technique for

calculating vertical accretion rates and sediment chronology, the influence of hurricane deposits on these calculations merits further research.

Chapter 4 examines exclusively the contemporary diatom assemblage from surface sediments in the Chenier plain and conducts a thorough analysis of the environmental variables that seem to drive species distributions. The goal of this study is to determine if diatom microfossils sampled from a regional (non-transect) sampling scheme can be used to construct a sea-level transfer functions, by evaluating the correlation of diatom data to environmental variables (elevation, water level, and salinity) and examining the standard assumptions of the transfer function technique.

The goals of Chapter 5 are to reconstruct salinity from fossil diatom assemblages from three sediment cores using a diatom transfer function. The evidence gathered from a study of diatom assemblages in coastal marshes of Louisiana could provide new insight into the role of sea level rise and hurricanes on marsh ecology. The overall benefits and pitfalls of this approach will be evaluated and future directions revealed (Chapter 6).

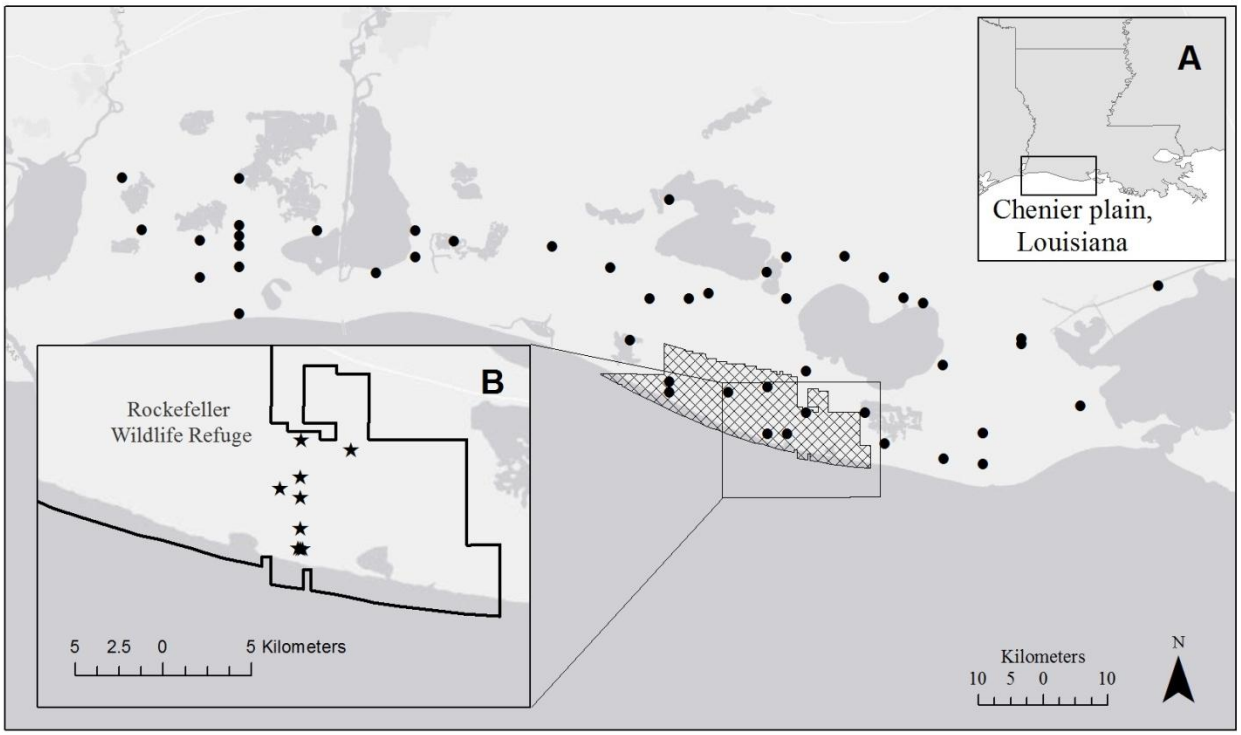

Figure 1-1. Map showing Louisiana Chenier plain and Rockefeller Wildlife Refuge showing surface sediment samples (black circles) and sediment cores (black stars). A) Location of the Chenier plain in southwest Louisiana, USA. B) Rockefeller Wildlife Refuge with locations of sediment cores.

Table 1-1. Measurements of sedimentation deposition from hurricanes in coastal Louisiana.

Hurricane (Year)	Depth of sediment	Publication
Hurricane Audrey (1957)	up to 70 cm of sediment deposition	(Morgan et al., 1958)
Hurricane Camille (1969)	up to 5 cm of sediment	(Wright et al., 1970)
Hurricane Andrew (1992)	2 to 6 cm greater vertical accretion than previous measurements	(Cahoon et al., 1995b)
Hurricane Rita and Katrina (2005)	averaged 5 cm of sediment deposition (ranged 0 to 68 cm	(Turner et al., 2006a)
Hurricane Ike (2008)	1 to 5 cm of sediment	(Williams, 2011b)

CHAPTER 2
STRATIGRAPHIC RECORD AND MICROFOSSIL ANALYSIS OF HURRICANE SEDIMENTATION IN SOUTHWEST LOUISIANA

Background

Hurricanes and tropical storms have a significant impact on the sedimentary processes of coastal marsh, both through erosion and sediment deposition (Conner et al., 1989; Stumpf, 1983). Along with organic primary production, inorganic sediment deposition is an important element of vertical accretion and therefore has an influence on marsh elevation. Vertical accretion, coupled with sea level rise and subsidence, is a critical element of marsh persistence, particularly in coastal regions like Louisiana where marsh loss has been largely attributed to insufficient inorganic sediment supply (Day et al., 2000).

The role of hurricanes in contributing or removing sediments from coastal marsh continues to be a leading concern of coastal managers as they make decisions on the management and restoration of coastal marsh. Climate change scenarios predict not only rising sea level, but research also indicates the possibility of increasing storm frequency and intensity due to warming sea surface temperatures (Intergovernmental Panel on Climate Change, 2007). If storms are a significant contributing factor of inorganic sediments and have a positive influence on marsh accretion (McKee and Cherry, 2009), then the increase in storms may provide a substantial contribution to marsh persistence under rising sea-level. However, if hurricane sediment deposition causes compaction or high storm intensity causes increased erosion, having a negative influence on marsh elevation, the added pressure in addition to sea-level rise could dramatically increase marsh loss. The response of wetlands to sediment deposition appears to vary, dependent on the shear strength of marsh soils, fetch of open water

during storm surge, and long-term rates of wetland subsidence (Morton and Barras, 2011).However, the most important questions for wetland resource managers are: What are the characteristics of the marsh that lead hurricane sedimentation to have a positive impact on marsh elevation and what are marsh characteristics that lead to negative storm impacts? Can specific management activities reduce wetland vulnerability to submergence or erosion from hurricanes? To answer these questions will require greater knowledge on wetland response to storm sedimentation and the factors influencing wetland resilience to erosion. Current efforts focus on continued monitoring and evaluation of future hurricane impacts or evaluating storm impacts using imagery (Morton and Barras, 2011). However, using paleoecological techniques, we may be able to examine sedimentation from past hurricanes and extrapolate changes in marsh ecology before and after historic storms, providing an additional tool for investigating the role and impact of storm sedimentation on coastal marsh.

Diatom microfossils have long been accepted as useful paleoindicators of oceanographic events (Jordan and Stickley, 2010) and environmental change in lakes (Battarbee et al., 2011). They have also been applied in coastal marsh for sea level investigations (Horton and Sawai, 2010). Sand layers are the standard method for identifying past tropical storms in geologic records, and numerous studies have employed microfossil foraminifera (Collins et al., 1999; Hippensteel et al., 2005; Horton et al., 2009; Williams, 2009). In Louisiana, hurricane sediments were found to be higher in bulk density (Turner et al., 2007; Williams, 2009), likely from a high composition of mineral matter due to the removal of organic matter during turbulent storm surge (Jackson et al., 1995). Few studies have investigated diatoms as evidence of tropical

storms, however the utility has been clearly articulated (Horton and Sawai, 2010). Storm surge can suspend sediments from the inner continental shelf, bays, or marsh lakes, delivering the sediments and component diatoms into the marsh. Turbulence from surge can also erode sediments from one area of the marsh and deliver it to another location, perhaps leading to a different diatom composition than sediments delivered from open waters. Intrusion of sea water from storm surge into otherwise fresh or brackish marshes can introduce allocthonous diatoms or change marsh salinity, resulting in a change in taxa. One notable study by Parsons (1998) examined Hurricane Andrew sedimentation in a Louisiana salt marsh pond. His research demonstrated a significant change in the diatom assemblage post-storm that persisted more than two years after landfall. Shifts in the diatom community may be a leading indicator of past tropical storms. Diatom analysis may be particularly useful in areas such as southwest Louisiana, where fine-grained sediments dominant both the marsh and the nearshore environment, making other proxies, such as sand content, less reliable. Hurricane sediment layers could be distinguished from non-storm sediments by increased composition of marine diatoms in a non-marine location, through valve preservation, or a change in species density, diversity, or evenness. If characteristics can be identified in recent storm-derived sediments, historic hurricanes might be identified from diatom analysis of fossil material from deeper within the sediment column.

The goal of this study was to determine if hurricane sediment layers could be distinguished from other sedimentary layers in marsh cores using x-radiographs, sedimentary characteristics, and diatom microfossils. If hurricane layers are found, then

comparisons between three different physiographic locations can reveal the utility of diatoms as an indicator of past storms.

Regional Setting

Rockefeller Wildlife Refuge (RWR) is a state-owned refuge located on southwest Louisiana. Much of the area is managed for waterfowl and fishery habitat. The primary mission of the refuge is to promote scientific research on wildlife and coastal marsh ecology and management (e.g. Chabreck, 1963; Joanen et al., 1970; Phillips, 2002; Wicker et al., 1983). RWR has several constructed levees that are intended to moderate salinity and water-level fluctuations for wildlife management and research. However, the southeast portion where cores were collected is largely unaltered and receives natural tidal flows.

Coastal Louisiana has been subject to several hurricanes that have had a great influence on marsh sedimentation and morphology (Stone et al., 1997). With hurricane landfall, currents rise and move in the windward direction, driving water and sediments onto land on the “right” side of the hurricane eye (Hayes, 1978). The opposite is true for the “left” side of the hurricane, where water and sediments are pushed out of the coastal zone, at times causing erosion. Due to the counter-clockwise rotation of hurricanes and the east-west coastline of Louisiana, coastal areas on the east side of hurricane landfall are the most likely to receive hurricane deposition and the west side are more likely to be eroded (Figure 2-1). Hurricanes Rita and Katrina in 2005 provided substantial sediment to coastal Louisiana (Turner et al., 2006a). Evidence of several recent hurricanes may also be represented within the surface sediments, including Hurricanes Lilli (2002), Humberto (2007), and Ike (2008). Hurricanes Lilli and Katrina made landfall east of the study site, making it less probable that significant deposition at RWR would

occur. Hurricane Humberto, a category 1 storm, made landfall just west of the Louisiana-Texas border. Landfall for Hurricane Ike was even further west, near Galveston. Nearby coastal monitoring stations with feldspar markers established in 2006 did not document a significant increase in post-Humberto vertical accretion (CRMS0610, 0609 and 0599; data downloadable from http://lacoast.gov/crms2/). Post-Ike measurements were approximately 2.5 to 4 cm higher than pre-storm measurements, indicating that surface deposition at RWR from Hurricane Ike was likely. Deposition from both Hurricane Rita and Ike may be reflected in the surface sediments of these cores.

Several historic storms have contributed sediment to the coastal marsh at RWR. In particular, Hurricane Audrey in 1957 made landfall in nearly the same location as Hurricane Rita. Sediment deposition from Hurricane Audrey was documented throughout the Chenier plain, including at RWR (Morgan et al., 1958). Hurricane Danny (1985) and Edith (1971) both have trajectories that took them directly over RWR, just west of sediment core sites. Rejmánek et al. (1988) documented an average of 2 cm of sediment deposition from Hurricane Danny in a *Phragmites* marsh located west of Atchafalaya Bay. Prior to 1950, a category 3 unnamed hurricane in 1918 and several other category 1 hurricanes made landfall west of the study site. All of these storms could have deposited sediments on the RWR site (Table 2-1).

The primary goal is to identify deposition layers for two (or three) specific hurricanes from the past hundred years that most likely deposited sediment. The first are recent storms Hurricane Rita (2005) and Ike (2008), which occurred just prior to core collection. If sedimentation occurred, it would be identified at or very near the

surface. Due to their trajectory and intensity, Hurricane Audrey (1957) and the unnamed hurricane of 1918 most likely deposited sediment at RWR. Using radioisotopes, we can refine the search for both hurricanes. Hurricane Audrey would likely be found below the ^{137}Cs peak (1964) and above first occurrence of ^{137}Cs fallout (approximately 1950). Sediment from the unnamed hurricane of 1918 would be located near or just above where unsupported ^{210}Pb (derived from in situ decay of ^{226}Ra) reduces to zero.

Methods

Stratigraphic evidence of hurricanes was determined for nine marsh sediment cores using x-radiographs and physical sedimentary data. Hurricane sediments are often higher in bulk density, coarser texture, and less organic matter than normal marsh sedimentation. Therefore, sedimentary data useful for identifying hurricane sediments include bulk density, total organic matter, and grain size. X-radiographs provide a visual interpretation of changes in soil density and the abruptness of these changes. Radioisotopes provide geochronology for designating approximate time frames for sedimentary layers and temporal windows for associating sedimentary layers to hurricanes. For three of the nine cores, sediment samples were also analyzed for diatom microfossils. The three cores were selected based on their physiography and sedimentary characteristics to represent the variability of the sedimentation processes observed at RWR.

Identification of Episodic Sedimentation

Since hurricane sediments are higher in bulk density than non-hurricane deposited sediments, x-radiographs and bulk density profiles can facilitate hurricane sediment layer identification. When x-radiographs are inverted, high density sediments are dark and low density sediments are light. Sharp, distinct contact boundaries (the

transition between sediment layers) also indicate episodic sedimentation, since an abrupt change in sedimentation pattern would cause a distinct boundary, whereas gradual changes would appear as a gradient from light to dark.

In addition, bulk density and organic matter profile data can also be used to identify storm sediments by identifying shifts or sharp increases in soil density or organic matter. Sharp or abrupt changes in bulk density or organic matter with depth may indicate storm deposition or an abrupt change in inorganic sedimentation. Bulk density and organic matter profile data are particularly useful when identifying storm deposition at sites where non-storm deposition is similarly high in mineral composition, such as locations that receive a regular supply of mineral sediments from tidal processes, because storm sedimentation is less visually distinct on x-radiographs. Even minor increases in bulk density can suggest changes in sedimentation processes. In comparison, at locations where organic matter is the dominant control in non-storm vertical accretion, storm sediments would be markedly different from non-storm sediments and will be visually distinct on x-radiographs.

Profiles of the radiometric isotope Lead-210 (^{210}Pb) provide additional information on both sedimentation rate and approximate date of sediment deposition (Appleby and Oldfield, 1978; Appleby and Oldfield, 1992) . The ^{210}Pb profile of a sedimentary system undergoing consistent, non-episodic sedimentation should follow an exponential decay rate consistent with time since deposition. Deviations from the standard decay pattern indicate a change in the sedimentation rate and/or a change in ^{210}Pb supply. Such deviations, in concurrence with x-radiograph or bulk density indications and sharp contacts, can provide additional support for episodic sedimentation.

Assignment of an approximate date using ^{210}Pb radioisotope in a non-steady state system is more difficult than determining geochronology for steady-state systems since standard ^{210}Pb age-dating models assume either a constant sedimentation rate or constant ^{210}Pb flux (Appleby, 2002; Appleby and Oldfield, 1992); where in coastal marsh, either or both may be variable. If fluctuations or severe deviations from the standard decay curve are apparent, the bottom of the curve, where unsupported or excess ^{210}Pb ($^{210}Pb_{xs}$) reduces to approximately zero, can be used to effectively date the sediment interval. The half-life of ^{210}Pb is 22 years; therefore, $^{210}Pb_{xs}$ will reduce to practically undetectable in 100-120 years.

Cesium-137 (^{137}Cs) isotope data can be examined in conjunction with ^{210}Pb to obtain additional date estimates. Cesium-137 in soils is primarily derived from nuclear fallout resulting from atmospheric bomb testing. The peak in the downcore ^{137}Cs profile indicates the date when atmospheric fallout was highest and initial occurrence is when atmospheric levels could first be detected. Based on atmospheric estimates of ^{137}Cs and ^{90}Sr by Milan (1995), the date of peak atmospheric levels in Louisiana was approximately 1964 and atmospheric levels were first detected in approximately 1950. The ^{137}Cs dating assumes that supply is primarily from atmospheric sources and downward or upward movement is negligible (Chmura and Kosters, 1994; Delaune et al., 1978).

Core Collection

Nine cores were collected in the coastal marsh at Rockefeller Wildlife Refuge (Figure 2-2) during April of 2009. Five core sites were located along a transect perpendicular to the Gulf of Mexico coastline, ranging from 0.5 to 5.75 km from the shoreline (cores 4, 6, 7, 8, and 9). To examine small-scale variation, two additional sites

were located 100 meters to the east and west of site 4 and parallel to the shore (sites 3 and 5). Two sites were located to the west and east of the transect (sites 1 and 2).

Landscape position and physiography, particularly distance from a tidal sedimentation source, can have an impact on marsh sedimentation processes and may influence episodic sediment identification as well (Reed et al., 1999). Sites 1, 2 and 9 are all located in brackish marsh dominated by *Spartina patens* (Aiton) Muhl. Site 1 is located approximately 3 km from the Gulf of Mexico in a largely unbroken marsh system, with a few open water marsh lakes and a tidal stream approximately 0.5 km away. Both sites 2 and 9 are located 6 km from the Gulf of Mexico. The marsh at site 2 is moderately broken, with several very small marsh lakes located within close proximity. A tributary is located 150 meters to the east and another 250 meters to the west of the coring site. Site 9 is 30 meters from a marsh stream and the intersection of two tributaries. Sites 3, 4, and 5 were located 0.5 km from the Gulf of Mexico and 300 to 500 meters east of a tributary. Sites 3 and 4 are in an unbroken saline marsh dominated by *Schoenoplectus robustus* (Pursh) Strong and *Distichilis spicata* (L.) Greene. Site 5 is located next to a small lake (area ≈ 0.05 km^2) in a slightly less saline marsh than sites 3 and 4 and dominated by smooth cordgrass (*Spartina alterniflora* Loisel). Site 6 is a polyhaline *S. alterniflora* dominated marsh located 1.5 km from the Gulf of Mexico and 50 meters from a wide tributary. Site 7 is a polyhaline marsh located nearby a small, low-flowing tributary in thickly vegetated *S. patens*. The site is only 14 meters from a small tributary and 3 km from the Gulf of Mexico. Site 8 is located in between a tributary and marsh lake (140 and 45 meters distant, respectively) in a *S. patens* marsh. Surface and pore water measurements signify mesohaline conditions.

Cores were collected by pushing a 10-cm diameter clear acrylic barrel into the sediment column. Cores were 45 – 60 cm in length and compaction was estimated by measuring difference in marsh elevation between the inside and outside of the top of the barrel before extraction. This measurement may be an over-estimation, since compaction may have occurred below or adjacent to core as the tube was pushed into the marsh, rather than within the sediments of the core tube. Geographic position, time of day, depth of the water, water salinity and porewater salinity were measured at each coring site (Table 2-2). Prior to core collection, porewater was sampled by driving a narrow plastic tube to 10-cm depth in the marsh sediment nearby the core collection site and drawing porewater into an attached syringe. The cores were sealed and transported to the lab, where they were x-radiographed (58-64 kV, 2.0 mAs) using a Torrex 120 portable X-ray unit and a ScanX CR2500 imaging system. The ScanX is a CR (computed radiography) digital imaging system that uses phosphor storage plates. The x-radiograph image files were imported into Adobe Photoshop CS5 (Version 12.5; Adobe Systems, Inc.) where they were merged and inverted. After imaging, cores were extruded and sliced at 2-cm intervals. Compaction from core transport and sampling (extrusion) were estimated by the difference between the measured lengths of the core before and after each procedure. Sedimentary characteristics (sediment texture, physical characteristics, presence of roots/shells/burrow, and stratification type) were described in detail during the sampling process.

Laboratory Analysis

Sediment samples were processed in the laboratory for bulk density, grain size, and radiometric dating (^{137}Cs and ^{210}Pb). A 30-mL sediment sample was weighed wet, dried in an oven at 60°C, and weighed again to calculate bulk density (dry mass divided

by volume). Loss on ignition (LOI) was determined by grinding the dried sample to a fine powder and combusting a subsample at 650°C for four hours (Dean, 1974; Lewis et al., 2002; Moore and Reynolds, 1989). Approximately 50% of the samples were measured in triplicate to calculate sample error.

Grain size was measured by laser diffraction using a Coulter *LS 200* particle-size analyzer after organic digestion. Digestion was accomplished by following the methods described in Soukup et al. (2008). Approximately 5g of sediment was placed in a 50-mL test tube, 15-mL of sodium hypochlorite was added, and placed in a warm water bath (80°C) for 15 minutes. The sample was then centrifuged and supernatant was carefully removed using a pipette as to not remove sediments. The sodium hypochlorite digestion was conducted at least three times to remove all organic matter. After digestion, 7% sodium hexametaphosphate solution was added to deflocculate clays. At minimum, three aliquots were analyzed three times to generate a total of nine grain-size distributions for each sample. Estimates of percent sand, silt, clay and mean phi were calculated from grain size distributions for each aliquot using Gradistat version 8 (Blott and Pye, 2001). The nine data sets were checked for any unusual variations (i.e., exceptionally high or low values which can be caused by partially undigested organics or debris) and data were removed if values deviated significantly from the majority of aliquots (1 standard deviation from the mean). The remaining data were average to create a single estimate of grain size (percent sand, silt, and clay, and mean sediment size) for each sample.

Lead-210 was determined for all core slice intervals by measuring the activity of ^{210}Po using alpha-spectrometry (Pheiffer Madsen and Sørensen, 1979). Polonium-210

is assumed to be in secular equilibrium with its parent ^{210}Pb. The fired sample from LOI analysis was transferred to a glass beaker and ^{210}Po was acid leached from the sediment. A known quantity of the tracer ^{209}Po was added to the solution prior to auto-plating and counted on low-level alpha spectrometer coupled to a pulse-height analyzer. Reported errors are the statistical counting errors at the 95% confidence interval. At least five samples per core were processed in duplicate in order to calculate relative standard deviation for an estimate of between sample errors.

Samples were selected for gamma-ray spectrometry (^{137}Cs) by examining ^{210}Pb profile data, isolating the depth where the detectable limit where excess ^{210}Pb reaches zero (provides a rough estimate 100 years before present), and estimating where ^{137}Cs activity would likely be detected (1984 to 1950; Milan, 1995). Approximately 15 g of dried, ground sample was sealed in a plastic jar and stored for at least 3 weeks to allow activity to reach equilibrium. Samples were counted using a germanium detector for low-energy gamma rays and a multi-channel analyzer was used for data collection. Samples were counted for at least 24 hours or until counting errors were less than 5 percent.

Microfossil Analysis

Samples from three cores (cores 4, 6 and 9) were processed for diatom microfossils. The three cores were selected because observation of their x-radiographs suggests they represent the diverse sedimentation patterns observed at the study site. Every other sample interval was selected for diatom analysis; however, additional intervening samples were added when sediment characteristics indicated storm deposition. Interpretation of x-radiographs and sedimentary profile data provided target zones for collecting microfossil data. To extract diatoms, approximately 0.5 mL of

sediment was digested in a 100-mL beaker using hydrogen peroxide and potassium dichromate. Samples were rinsed twice with deionized (DI) water (the beaker was filled with DI water; sample was allowed to settle overnight, decanted to 500-mL mark, and refilled, etc.). Since samples contained a significant fraction of fine-grained sediment (silt and clay), a 7% sodium hexametaphosphate solution was added to deflocculate fine-grained sediments. Each sample was continually rinsed until decant was clear. A known volume (5 or 10 mL depending on the density of diatoms and sand grains) of diatom solution was added to settling trays containing four cover slips and allowed to dry (Battarbee, 1973). Cover slips were sealed to microscope slides using Zrax diatom mountant (refractive index ~ 1.7+). A minimum of 300 diatoms were identified to species and counted using a Nikon Optiphot light microscope at 1000x magnification (Plan 100x / 1.25 oil DIC objective). The identification of species and autecology, including general salinity preferences, was determined from taxonomic literature (Krammer and Lange-Bertalot, 1990-2009; Patrick and Reimer, 1966a, b; Stidolph et al., 2012; Witkowski et al., 2000).

Statistical Analyses

Cluster analysis is the assignment of a set of observations into subsets or groups based on similarity of numerical data. Cluster analysis was used here to determine if microfossil species abundance data indicate the presence of distinctive sedimentary layers evidenced by sample grouping or creating “clusters” of similar samples and distancing dissimilar samples (Everitt, 2011). Several methods of hierarchical clustering were tested, including single, complete, and average agglomerative clustering. A cophenetic correlation computes the correlation between the original dissimilarity matrix and the cophenetic matrix (Borcard et al., 2011; Sneath and Sokal, 1973). The method

with the highest cophenetic correlation indicates the best clustering model for the distance matrix and was used to select the best clustering method. A silhouette width was calculated for all parameters. Silhouette width is a measure of the degree of membership of an object to its cluster. The highest average silhouette width for a cluster was used to indicate the optimal number of clusters (Rousseeuw, 1987). Once clusters were identified, species with the strongest association to the cluster were identified by calculating simple statistics on mean abundances from typologies obtained from the clustering method. All statistics were performed using R version 2.10.1 (http://cran.r-project.org/).

Results

Sediment Characteristics and X-radiographs

Cores ranged in total length from 45-60 cm and are depicted in positive x-radiographs as having a mixture of organic matter (light) and more dense, mineral sediments (dark) (Figures 2-3). Total compaction ranged from 3 to 34%, which is not uncommon for loosely consolidated marsh cores. In general, dry bulk density is low (< 0.60 g cm^{-3}), largely due to a composition of high organic matter and fine-grained mineral sediments. Grain size measurements confirm that sediments are predominately silt (50-80%) and clay (~20%). Sand layers have been shown to be indicative of storms (Liu, 2004; Liu and Fearn, 2000a; Liu and Fearn, 1993, 2000b; Otvos et al., 2002). In general, sand content is very low with a total mean of less than 7%; however, sharp increases of up to 30-40% sand content were found in several cores. Organic matter content is highly variable, demonstrated by LOI values ranging from 8 to almost 60%. Roots and small inclusions are detected in the x-radiograph for site 6.

A distinct sediment layer near the soil surface is present in all cores and varies in thickness from 5 to 14 cm. This sediment layer is relatively high in bulk density (0.3-0.6 g cm^{-3}) and low in organic matter (less than 25%) in comparison to sediments beneath. The boundary contact between this layer and the sediments beneath are distinct (the exceptions are core 7 and 8, where the contact appears more gradual). The surface sediments of some cores appear less dense than the underlying material, such as in core 2, 5, 6, and 9. However, for many cores the entire surface layer appears to have significant inorganic content which is substantially higher in some cases than sediments found below this layer.

Each core has distinct textural and compositional features. Sites 1, 2, and 9 have the greatest range in bulk density (Figure 2-3A, B, and I). All three locations show distinct dense sediment deposits on the x-radiographs, which are reflected in bulk density measurements. Additional dense layers can easily be identified on all three cores in x-radiographs. The core collected at site 1 has four distinct deposition layers above the ^{137}Cs peak. The x-radiograph for site 9 shows only two slightly dense layers prior to the ^{137}Cs peak, however there is no indication of increases in bulk density data. Site 2 exhibits no record of such events in either the x-radiograph or bulk density. Below the ^{137}Cs peak, there are indications of two events in all three cores: one occurring between the peak and first appearance of ^{137}Cs (between 1964 and 1950), and the second occurring prior to the first appearance of ^{137}Cs (before 1950).

Sites 3, 4, and 5 are located approximately half a kilometer from the Gulf of Mexico shoreline, and sediment composition is largely composed of dense, mineral soils (Figure 2-3C, D, and E). Site 5 is near a small lake (Figure 2-2) with the other two

sites to the west spaced 100-meters apart. Core 5 is the densest of the three cores and has the lowest organic matter content. All three cores have a gradual increase in bulk density from the deepest depth to a depth of 11-15 cm, where bulk density rapidly increases to illustrate a dense mineral layer at the surface. This dense layer is more difficult to discern on the x-radiograph than the same layer from cores collected at other locations because the composition is similar to the subsurface; however, the bulk density profile indicates changes where the x-radiograph is less clear.

Sites 6, 7 and 8 are located in the middle of the north-south transect amongst a natural channel system (Figure 2-3F, G, and H). Organic matter generally increases with distance inland, averaging 17, 20, and 35%, respectively. The x-radiograph indicates that site 6 is dominated by mineral deposition, with relatively dense sediments and low organic matter. A dense deposition layer with a sharp contact can be identified at the surface on x-radiograph. Several other dense layers can be identified from the x-radiograph and most are reflected in bulk density data. However they lack distinct contact boundaries. The bulk density profile and x-radiographs for site 7 is generally uniform, with only slight variations. An increase in sediment density is noted near 17 cm and from 21-35 cm, however distinct demarcation is absent. Grain size is also uniform, with a slight increase toward the very bottom of the core. Organic matter content increases gradually with depth at site 8, until 35 cm depth where it decreases. Sediment layers of high bulk density are discernible on the x-radiograph only at the very top and bottom of the core. A dense layer appears near the surface from 0-5 cm. Several less distinct layers are indicated on the x-radiograph, whereas bulk density data shows little variation. Below 37cm depth, several dense layers are clearly identified.

Grain size for the dense surface layer can be generally classified as mud (silt and clay) and does not differ greatly from subsurface samples of many cores. Some increases in sand content are observed at specific depth intervals indicating the possibility of “sand layers” often described as hurricane deposits; however, most sand layers sampled were less than 25% sand.

Identified storm deposits contributed approximately 15 to 50% of total vertical accumulation in the past century (Table 2-3). The estimate uses the sum of all identified storm deposits divided by the total depth where $^{210}Pb_{xs}$ reaches zero (an estimate of 100 years before present). Sites 7 and 8 have the least contribution of storm sediments, whereas sites 1, 2, and 3 have the greatest portion of vertical accretion attributable to storms. Storm sediments are often 1.5 to 2 times higher in bulk density than non-storm sediments; the difference between bulk density for storm and non-storm sediments is least apparent at sites 6 and 7.

Microfossils

Cluster analyses of sediment samples results in several groups with distinct diatom assemblages in all three cores. The samples in each group have a diatom assemblage that is more similar to each other than they do to samples in separate groups. Cophenetic correlations identified the best clustering method for all three core data sets is the unweighted pair group method with arithmetic mean (UPGMA). Silhouette widths indicate core 4 is best described by four groups (Figure 2-4A). Cluster group 1 contains two samples found within the upper portion of the core and one sample found lower in the core (at 27 cm). The main diatoms found in these samples include *Tryblionella granulata*, *Actinocyclus senarius*, *Cyclotella meneghiniana*, and unknown species of *Thalassiosira,* which is not well-represented in any of the remaining

clusters. The 27-cm sample also contains high bulk density and, though difficult to discern, x-radiographs indicate the presence of a distinct sediment layer through an increase in sediment density and distinct boundary between layers.

The samples of cluster group 2 are closely related to group 1. Samples included in this group were 3, 13, 15, and 21 cm. Diatom species identified in this cluster were similar to group 1, but had a higher density of *T. granulata* and included *Achnanthes brevipes*. Group 3 (31 and 37 cm) have lower bulk density values and there is no indication of high density sediments on x-radiographs. Diatom species were also similar to group 1 and 2, containing *A. senarius* and *C. meneghiniana*, but few *T. granulata* and the addition of the species *Navicula peregrina*. Group 4 contains samples found in the lower portion of the core (intervals 41, 45, 47, 49 and 53). These samples are more closely related to samples from group 3, with the inclusion of N. peregrina and C. meneghiniana, but with the addition of *Nitzschia scalaris* and *Pinnularia viridis*.

Cluster analyses of diatom assemblages for 13 samples from core 6 indicate only two cluster groups (Figure 2-4B). The entire core was dominated by the species *T. granulata*. The first cluster is exclusively for the two three samples (1, 5 and 7 cm) and contained *A. senarius*, *C. menghiniana*, and *D. crabro*. The other cluster contains all remaining samples downcore (11 through 47 cm). Although silhouette widths indicate group 2 is similar, the dendrogram does indicate two possible sub-groups. One sub-group comprises of samples 13 through 31 cm dominated by *T. granulata* and *Diploneis* cf. *bombus*; the other sub-group includes the sample from 11-cm and 35 through 47 cm, which is composed of the distinctive species *Caloneis formsa* and *Navicula peregrina*.

Cluster analyses of core 9 diatom assemblages indicate three distinct clusters of diatom assemblages (Figure 2-4C). Four samples were classified into the first cluster, which was differentiated in x-radiographs, bulk density and organic matter data as a very distinct inorganic layer near the surface. Diatom species found within this cluster include *T. granulata*, *A. senarius*, *C. meneghiniana*, and *Thalassiosira* sp4. Group 2 assemblage is aligned with sediments found within a very high organic-rich zone above the ^{137}Cs peak (15, 17, and 19 cm) and is exemplified by *Amphora proteus* and *Seminavis eulensteinii*. The final cluster contains all remaining samples, including those that indicate increased bulk density at 25 and 35 cm. Group 3 samples are more closely related to those from group 1 than group 2, however diatom species are quite unique and include *N. peregrina*, *Diploneis smithii* var. *dilatata*, *Nitzschia obtusa* and *N. scalaris*.

To examine consistency between sample sites, a cluster analysis was conducted on all 43 samples from the three cores (Figure 2-5). The data set was clustered into six groups. Group 1 contained samples near the surface of all three cores, indicating that the diatom assemblages from these sediments are more closely related to each other than they are to assemblages from samples downcore. Group 2 indicates a resemblance diatom assemblage from three samples of core 4 (13, 15 and 27 cm) with the remaining samples of core 6. An interval from core 9 at 23 cm was also classified within this group. According to x-radiographs, the sample at 23 cm is on the edge of a dense sediment layer. Group 3 is composed of samples from lower depth intervals of core 4 and 9 (pre-1964 based on the depth in relation to the ^{137}Cs peak), indicating a similar diatom assemblage for these two sites prior to 1964. Group 6 is composed of

three samples from core 9, the remainder from lower depths and is not so distant from group 3. Diatom assemblages for group 4 (core 9 samples from 15, 17, and 19 cm) are very distinct from any of the other groups, which is mirrored in the highly organic sediments, indicating very different marsh processes during this period than historically.

Discussion

The presence of sharp boundary between sediment layers and increased bulk density support the hypothesis that sediment on the surface of all nine cores is derived from recent hurricanes. Bulk density of storm sediments were typically from 0.40 to 0.55 g cm^{-3}, whereas non-storm sediments were around 0.30 g cm^{-3} or lower. Reduced organic matter is a characteristic of hurricane sediments due to the winnowing or loss of plant material from turbulent storm surge (Jackson et al., 1995). Though higher in bulk density, grain size for only a few sample intervals exhibited a larger increase in sand content and lacked consistency within the observed deposition layer, contrary to results found in other areas where sand layers were used as evidence for hurricane sedimentation (Donnelly et al., 2001; Liu and Fearn, 2000b). Spatial variability in grain size of hurricane sediments was also noted by Nyman (1995) in his study of Delta plain sedimentation from Hurricane Andrew. He attributed the observed variability to differences in the source of the sediment. Since the likely sources of hurricane sediment to RWR are the inner continental shelf or redistribution within the marsh system itself (including tributaries and marsh lakes) and all these locations are dominated by fine-grained sediments (Beall, 1968; Draut et al., 2005), the lack of distinct sand layers is not altogether surprising. In addition, Draut et al. (2005) describes post-storm deposition for the intercontinental shelf as sand-mud couplets resulting from decreasing intensity of the storm. Sand-mud layers characteristic of this pattern can be identified in several

cores and may explain a few of the 6 samples with greater than 25% sand content. However, not all of these samples could be associated with storms. The 2-cm depth sampling interval may be insufficient (too thick) to identify this pattern for all hurricane sediments in all cores. Since cores were collected three years after Hurricane Rita, the absence of a defined return to pre-storm sediments at the surface and the documentation of hurricane sedimentation in nearby monitoring sites suggest that Hurricane Ike deposition is likely reflected in this top layer.

Ancillary data also support the conclusion that surface sediments were deposited from recent storms. Phillips (2002) collected sediment cores at RWR in 2000 and 2001. Two of her sites (RE13 and RE1) were located nearby site 1 and 2 in this study. The difference in the depth of the ^{137}Cs peak from the pre-hurricane cores and these data is equivalent to the depth of storm deposition (13 and 7 cm, respectively), evidence that the sediment identified at the surface was deposited between 2000 and 2009.

Sedimentation from historic hurricanes can be identified in sediment cores using bulk density profiles and x-radiographs, and were clearly distinguished at sites where organic matter accretion is the dominant control on marsh elevation. Marsh locations with sediments composed of over 50% organic matter content (Sites 1, 2, and 9) show distinct dense sediment layering. A mineral sediment layer in between the ^{137}Cs peak and first occurrence (at approximately 26, 19, and 25 cm for sites 1, 2, and 9, respectively) can be attributed to Hurricane Audrey. Bulk density increases at the 35, 25 and 35 cm intervals may be indicative of the 1940 storm, and at depths 49, 35, and 55 cm are indicative of a 1918 hurricane. The consistency amongst these sites suggests significant regional events. All three of these cores are located more than 2 km from the

Gulf of Mexico and most are not located near a potential tidal sedimentation source. The exception is site 9, which is 30 m from a marsh stream. However, water level data from a nearby monitoring station indicate a low tidal-amplitude and infrequent marsh flooding relative to marsh elevation (water levels are above the marsh surface only 30% of the time), likely due to the sites distance (6 km) from the Gulf of Mexico, since tidal range would decrease with distance from the coast. The high organic matter and low bulk density content of the cores, combined with the isolated location, suggest a dominance of organic matter for recent (past 100 years) non-storm accretion. The contrast between organic matter accretion and storm sedimentation provide a clear record on x-radiographs. Increases in bulk density data also indicate event-derived sedimentation, with storm sediments having up to two times the density of non-storm sediments. These sites also have between 25 and 50% of their vertical accretion attributable to storms. Site 8 is also dominated by organic matter accretion, but with fewer storm deposits. The density of sediments is highly variable in x-radiographs, but there are no distinct mineral layers found within the profile to the depth of decayed $^{210}Pb_{xs}$. Below 40 cm, laminations of dense layers are present, indicating that event-driven sedimentation had a greater influence on marsh accretion than at present. The presence of historic storm sediments at site 9, which is further inland than site 8, is interesting and might be due to backflow from storm surge or upland runoff rather than overwash.

Historic hurricanes are difficult to identify in x-radiographs of cores collected from sites where tidal processes supply regular mineral deposition. Reed (1999) demonstrated that distance from a tributary has a significant impact on tidal

sedimentation, particularly inorganic sediments, where distant locations receive fewer sediments overall and a greater percentage of those sediments deposited are composed of organic matter. Tidal sedimentation is also influenced by other factors, such as floodwater velocity and vegetation morphology (Leonard and Luther, 1995; Stumpf, 1983), so distance from a tidal source is not the only consideration. In addition, factors such as event layer thickness, burial rate, and mixing, have an influence on storm sediment preservation (Wheatcroft and Drake, 2003). The three cores in close proximity to the Gulf of Mexico (sites 3, 4, and 5) have sediment profiles with high bulk density (≈ 0.30 g cm^{-3}) and low organic matter content (less than 25%) suggesting regular mineral sedimentation, likely due to their proximity to the Gulf of Mexico. X-radiographs for all three sites show fine laminations, which is likely attributable to winter storms and regular flux of tidal sediments. Despite a composition of approximately 80% mineral sediments, x-radiographs and sedimentary profile data for several cores show variations in soil density that can be attributable to storms, such as the sediment layers at 27- and 35-cm depths at site 4, chronologically reflecting Hurricanes Edith and Audrey. However, there is less confidence in identification of sedimentation from historic storms for these high mineral marsh locations. Alternative methods, such as microfossil analysis, that identify storm sediments would greatly aid interpretation.

Diatom microfossil assemblages found in recent storm deposited sediments are different from pre-storm sediments found deeper within the sediment core. Diatom assemblages of storm sediments from three different physiographic locations are more similar to each other than they are to non-storm samples and are composed primarily of *Tryblionella granulata*, *Actinocyclus senarius*, and *Cyclotella meneghiniana*. These

analyses are consistent with data presented by Parsons (1998) on sediment cores of marsh lakes from Louisiana's Delta plain in that the diatom assemblage was compositionally different. However, his results indicate an estuarine sediment source (from Terrebonne Bay) while the presence of these three species indicate a marine or highly saline source. In addition, since diatom composition of storm sediments from the three locations were similar, whereas non-storm sediments were dissimilar, hurricane-derived sediments for all three sites may have the same fundamental source and processes affecting hurricane sediments may be more uniform and less dependent on small-scale processes than non-storm sedimentation.

This study was not able to confirm if diatom assemblages from sediment deposits of recent storms can be used to identify past storm deposits. Based on the results of cluster analysis, the diatom assemblage of one subsurface sample (core 4, depth 27 cm) was similar to the assemblage of recent storm-derived sediments identified on the surface of each core. At this depth, the x-radiograph shows a sediment layer with higher in bulk density and lower in organic matter than sediments above and below, supporting the conclusion that these sediments were deposited by a historic storm. Chronological markers indicate the sediment was deposited after 1964, possibly in the 1970s, which indicate deposition from Hurricane Edith (1971). However, no other samples were classified as being similar to diatom composition of recent storms. A diatom paleoindicator of historic storms would be the most valuable at marsh locations with less than 20% organic matter accretion (high mineral composition) and at depths greater than 50 cm since organic matter decomposition increases soil bulk density at deeper

soil depths, likely making storm sediments more difficult to discern in x-radiographs and sedimentary profiles.

Additional samples from cores with similar depositional characteristics would be required to substantiate the hypothesis that the diatom assemblage found in the sediments of recent storms can be used to identify sediment deposits of past storms in the sediment record. Samples from storm deposits identified in in cores 1, 2, 5 and 6 (at depths 25, 17, 39, and 29 cm, respectively) could provide sufficient data for looking at diatom composition of Hurricane Audrey. Deposits for the 1940 hurricane can be seen in cores 1, 2, 5, 6, and 7. Analysis of these samples and selected non-storm samples should provide sufficient data to test the hypothesis that diatom composition is unique to storms. Processes influencing storm deposition may be unique to each storm or factors influencing storm sediment preservation may have an influence on diatom assemblage through mixing or dilution. In addition, sample depth may be too coarse to identify the more frequent, smaller storms which would deposit less sediment on the marsh surface. In conclusion, sediment deposition from hurricanes appears to have an influence on diatom assemblage, which is supported by these results and that of Hurricane Andrew and marsh lake samples by Parsons (1998) showing a difference in diatom composition between hurricane sediments and non-storm sediments. Future work should focus on analyzing and comparing samples from historic storms identified deeper in the geologic record to resolve patterns in diatom composition that can be used to identify storm signatures from pre-recorded history, and also examine post-storm changes in diatom assemblages which can elucidate characteristics of wetland change and development post-storm. The data from these studies can improve our understanding of the impacts

of future climate change and sea-level rise on coastal wetlands, as well as provide essential data for predictive modeling of the impacts of future hurricane events and climate scenarios.

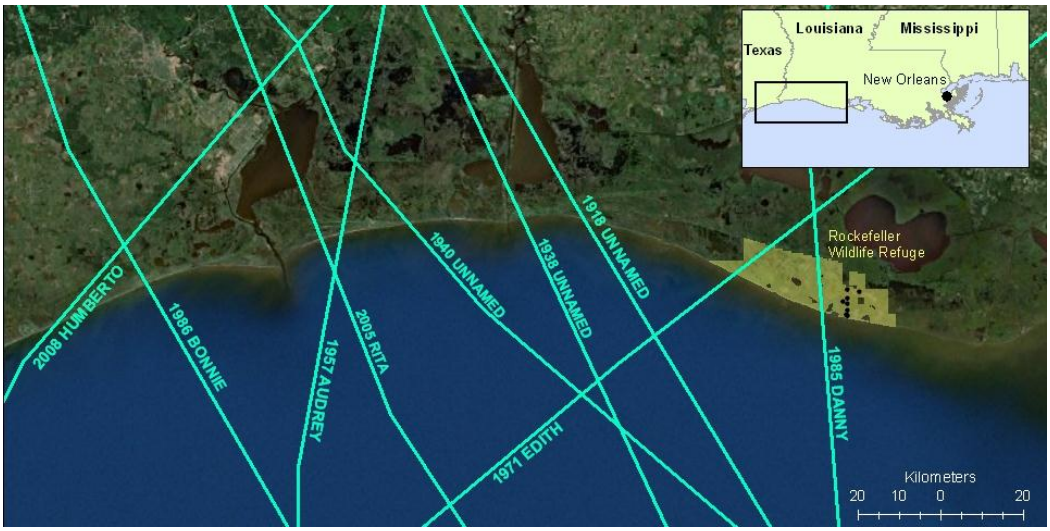

Figure 2-1. Map of category 1 or higher hurricane tracks with landfall to the west of marsh core sites at Rockefeller Wildlife Refuge since 1900.

Figure 2-2. Map of sediment core sample locations. Nine cores were collected on Rockefeller Wildlife Refuge in the Chenier plain of southwest Louisiana, U.S.A. during April 2009.

Table 2-1. List of hurricanes with probable sediment deposition impacts to Rockefeller Wildlife Refuge in southwestern Louisiana (1900 to 2009). Data for each storm includes wind speed and designated Saffir-Simpson scale.

Year	Hurricane	Wind (knots)	Saffir-Simpson Hurricane Wind Scale
**2008	Ike	94	H2
2007	Humberto	80	H1
2005	Rita	100	H5
*2002	Lilli	80	H1
*1992	Andrew	119	H4
**1989	Chantal	69	H1
**1986	Bonnie	75	H1
*1985	Juan	69	H1
1985	Danny	80	H1
1971	Edith	85	H2
*1977	Babe	65	H1
*1974	Carmen	130	H4
*1964	Hilda	100	H3
**1963	Cindy	65	H1
1957	Audrey	125	H4
**1947	Unnamed	69	H1
**1943	Unnamed	75	H1
**1942	Unnamed	69	H1
1940	Unnamed	69	H1
1938	Unnamed	65	H2
1918	Unnamed	105	H3

*Hurricane landfall was to the east of Rockefeller Wildlife Refuge (RWR).
**Hurricane landfall was to the west and greater than 100 km distant from RWR.

Table 2-2. Characteristics of sediment core sampling locations, including core depth, marsh type and dominant vegetation, surface water and porewater salinities, and core compaction.

Core	Core depth (cm)	Marsh Type	Dominant Vegetation*	Surface water**		Porewater**		Estimated Compaction (%)
				Salinity (‰)	Temp (°C)	Salinity (‰)	Temp (°C)	
1	55.75	Mesohaline	S.pat	6.0	23.2	10.1	24.9	15
2	45.00	Mesohaline	S.pat, S.rob	14.9	29.2	16.5	25.6	28
3	46.00	Polyhaline	S.rob, D.spic	NS	NS	22.0	24.8	34
4	55.00	Polyhaline	D.spic, S.rob	NS	NS	22.3	24.3	34
5	56.00	Mesohaline	S.alt	10.4	23.2	17.9	25.8	28
6	49.00	Mesohaline	S.alt, D.spic	9.8	24.5	19.0	25.5	29
7	50.00	Polyhaline	S.pat thick	13.3	27.0	22.1	27.2	29
8	54.25	Mesohaline	S.pat patchy	14.0	28.4	16.1	27.4	21
9	60.00	Mesohaline	S.pat, S.lat	11.7	26.2	14.2	25.4	3

*Dominant vegetation are abbreviated, where D.spic = *Distichlis spicata*, S.pat = *Spartina patens*, S.rob = *Schoenoplectus robustus*, S.alt = *Spartina alterniflora*, S.lat = *Saggittaria latifolia*, Mix = a mix of D.spic, S.pat, and S.rob
**NS= No standing water to enable sampling; Porewater was sampled at 10-cm depth.

Table 2-3. Characteristics of sediment deposition from hurricanes for nine marsh sites.

Site	Depth to $^{210}Pb_{xs}$ first occurrence (cm)	Thickness of all storm deposits (cm)	Accumulation attributable to storms (%)	Bulk density (g cm^{-3})	
				Storm	Non-storm
1	41	20	48.8	0.386	0.222
2	31	11	35.5	0.421	0.208
3	31	12	38.7	0.489	0.369
4	43	15	34.9	0.520	0.379
5	41	12	29.3	0.498	0.387
6	35	16	45.7	0.478	0.405
7	41	8	19.5	0.393	0.367
8	41	6	14.6	0.310	0.203
9	41	10	24.4	0.327	0.181

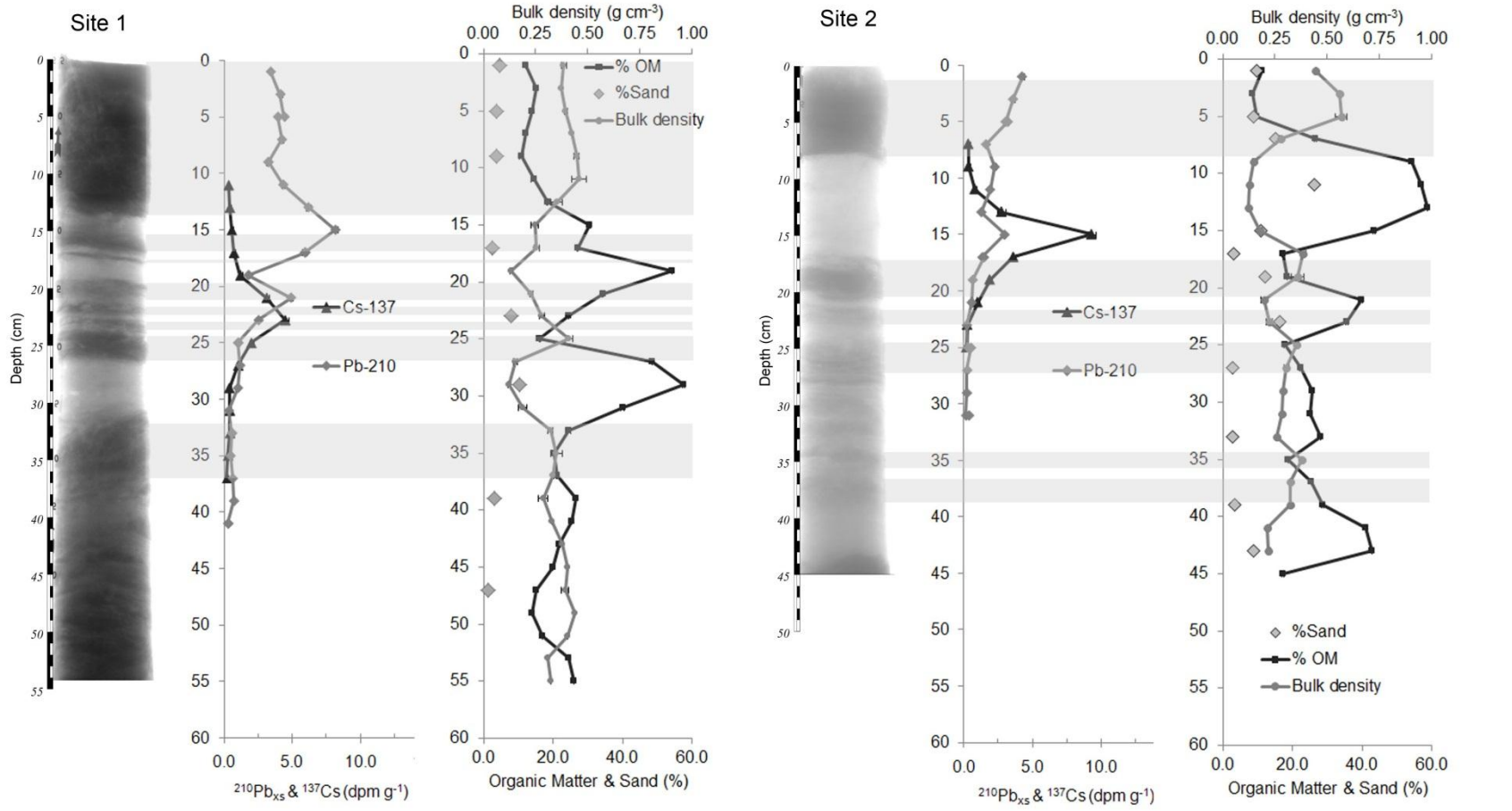

A B

Figure 2-3. X-radiographs and vertical profile data for sediment cores show measured changes in organic matter, bulk density, grains size, and radioisotopes ($^{210}Pb_{xs}$ and ^{137}Cs). Shaded areas indicate sequences of higher density (dark gray on the x-radiograph), indicating possible hurricane deposition. Vertical scale is present as a linear distance at depth from surface (cm). A) X-radiograph and data for site 1. B) X-radiograph and data for site 2. C) X-radiograph and data for site 3. D) X-radiograph and data for site 4. E) X-radiograph and data for site 5. F) X-radiograph and data for site 6. G) X-radiograph and data for site 7. H) X-radiograph and data for site 8. I) X-radiograph and data for site 9.

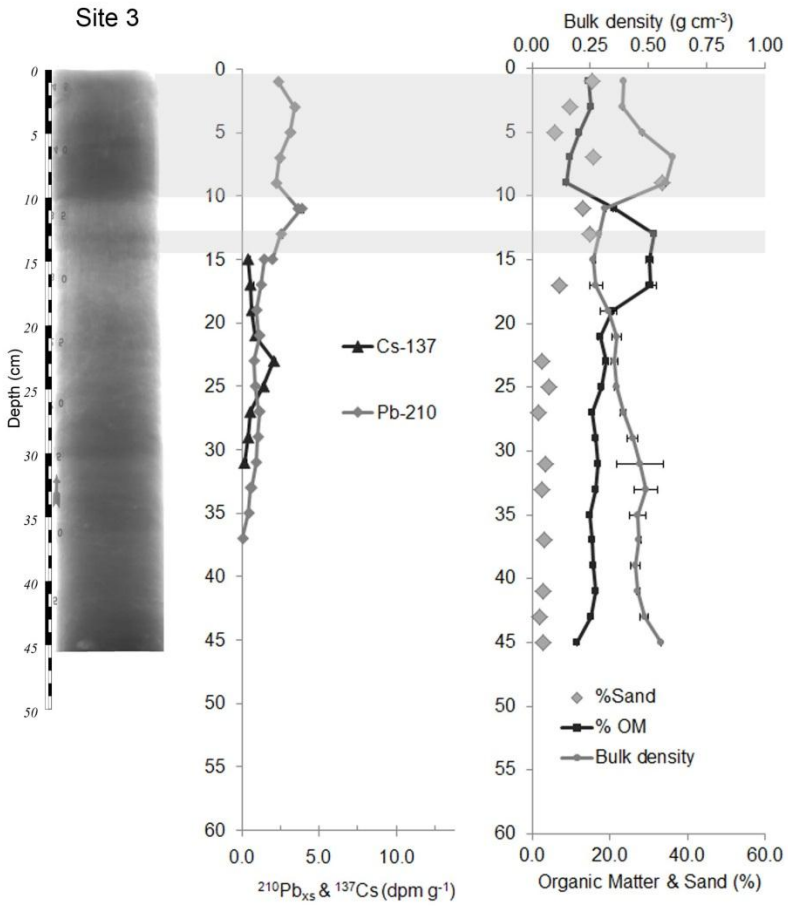

C

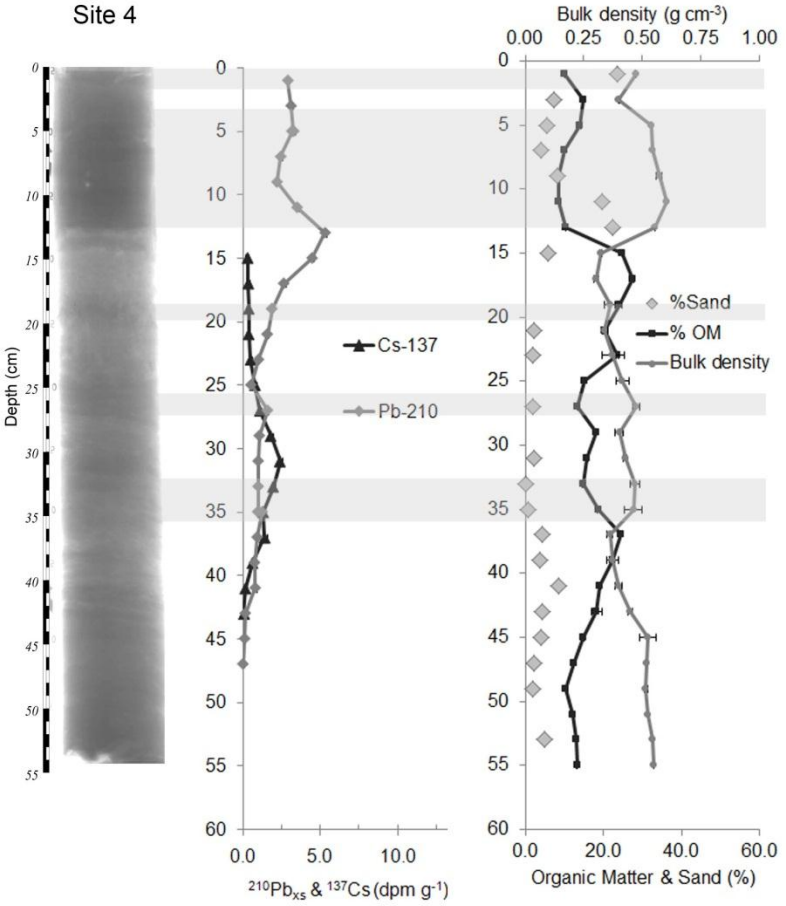

D

Figure 2-3. Continued.

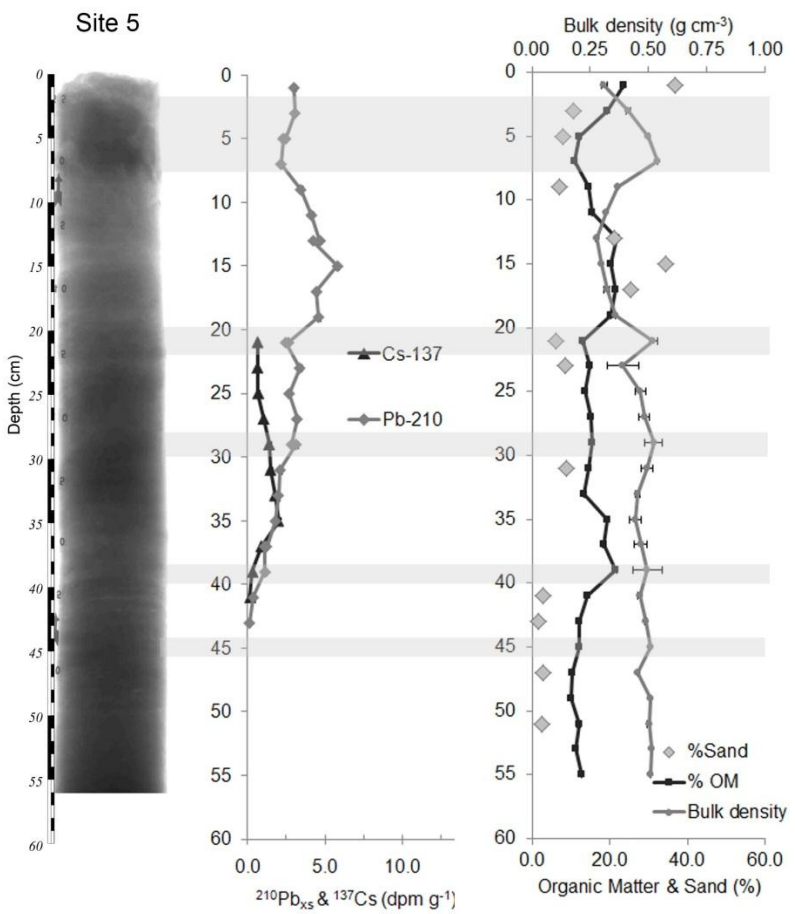

E

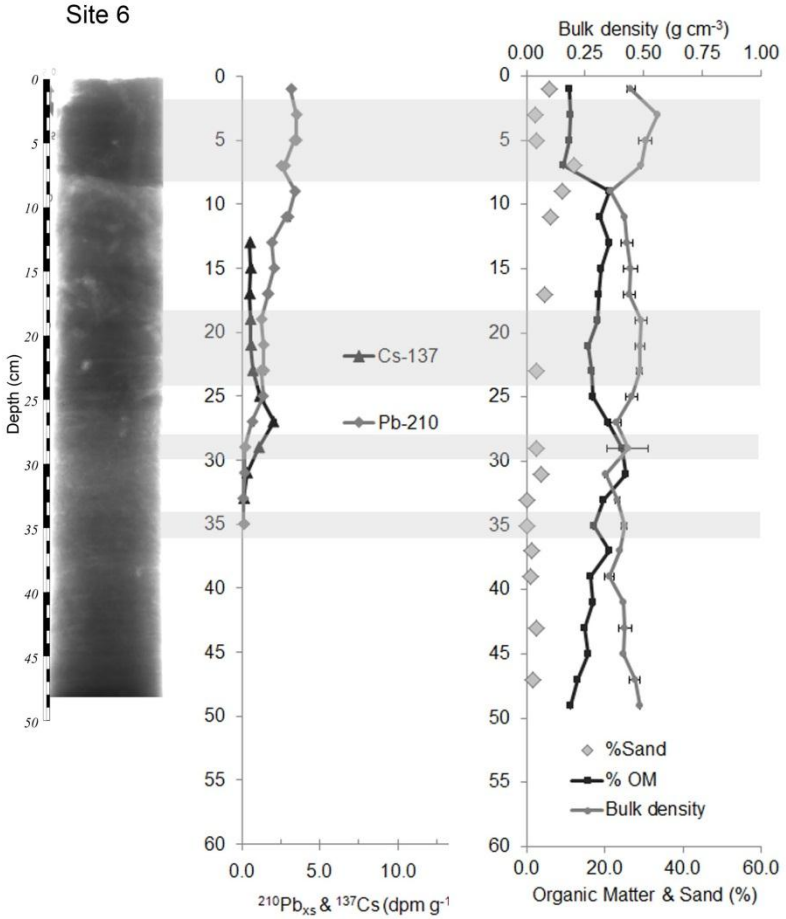

F

Figure 2-3. Continued.

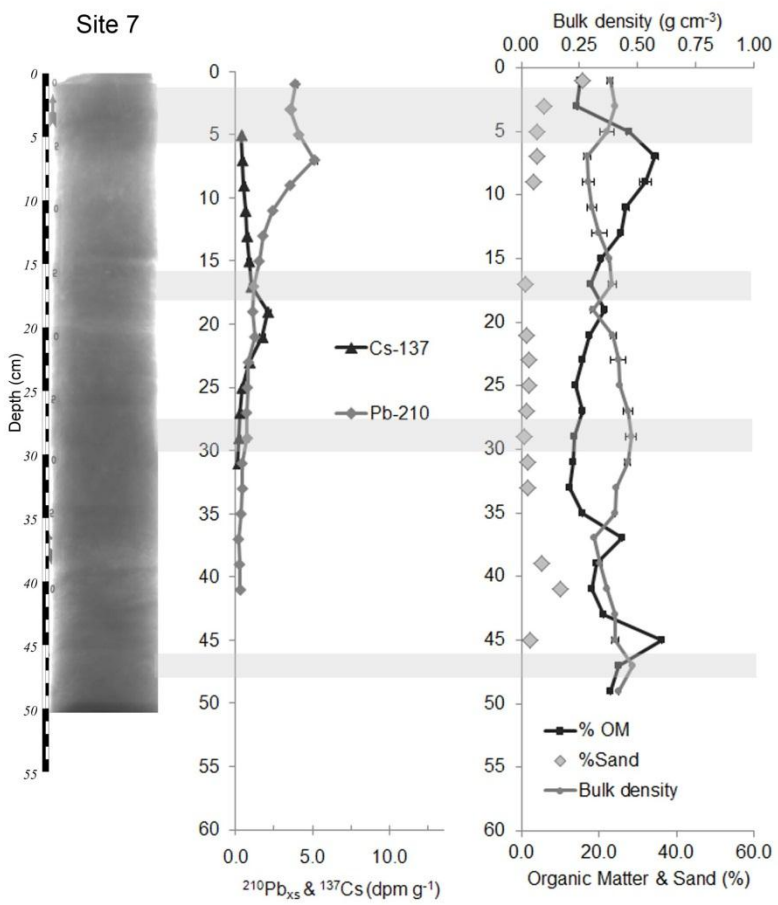

G

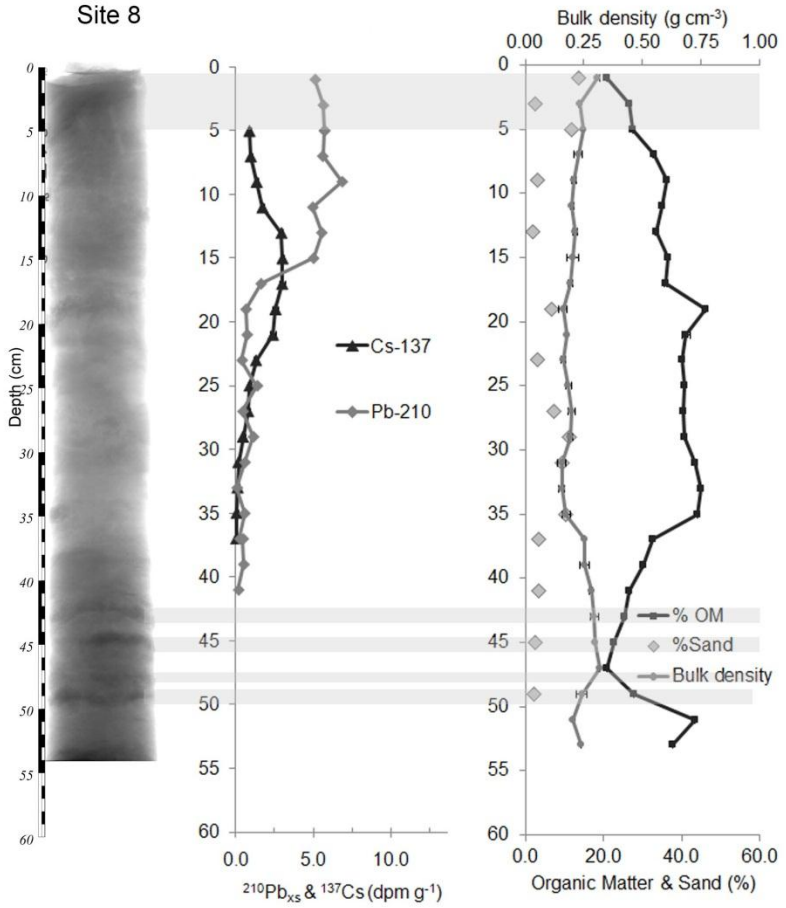

H

Figure 2-3. Continued.

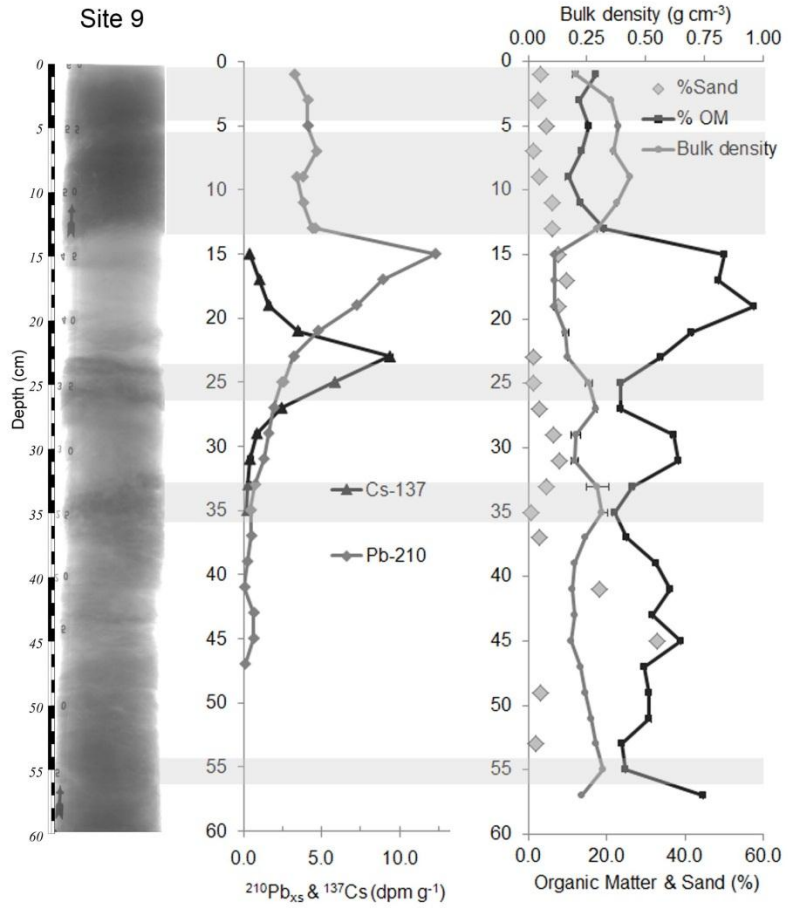

I

Figure 2-3. Continued.

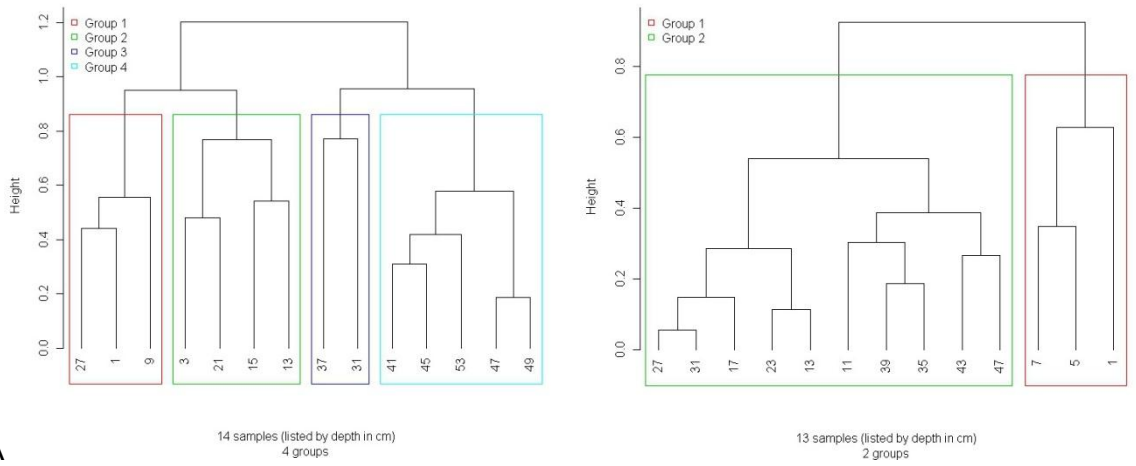

A B

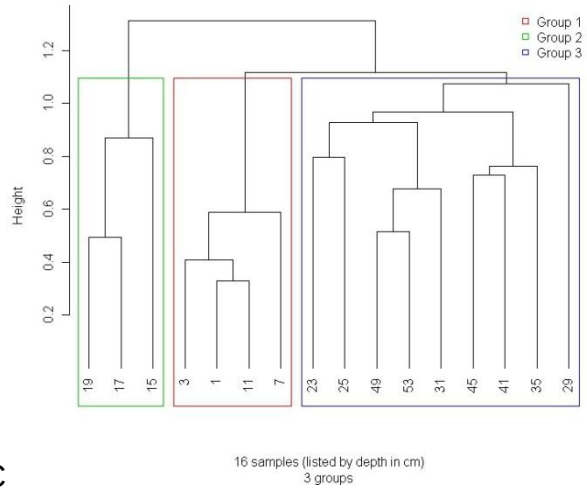

C

Figure 2-4. Cluster dendograms of diatom microfossil assemblage for depth intervals. Numbers along the bottom of each dendogram are the sample depth (cm). Height shows the distance clusters were joined. Colored boxes indicate the optimal cluster groups using maximum silhouette widths. A) Dendrogram of diatom microfossils for site 4. B) Dendrogram of diatom microfossils for site 6. C) Dendrogram of diatom microfossils for site 9.

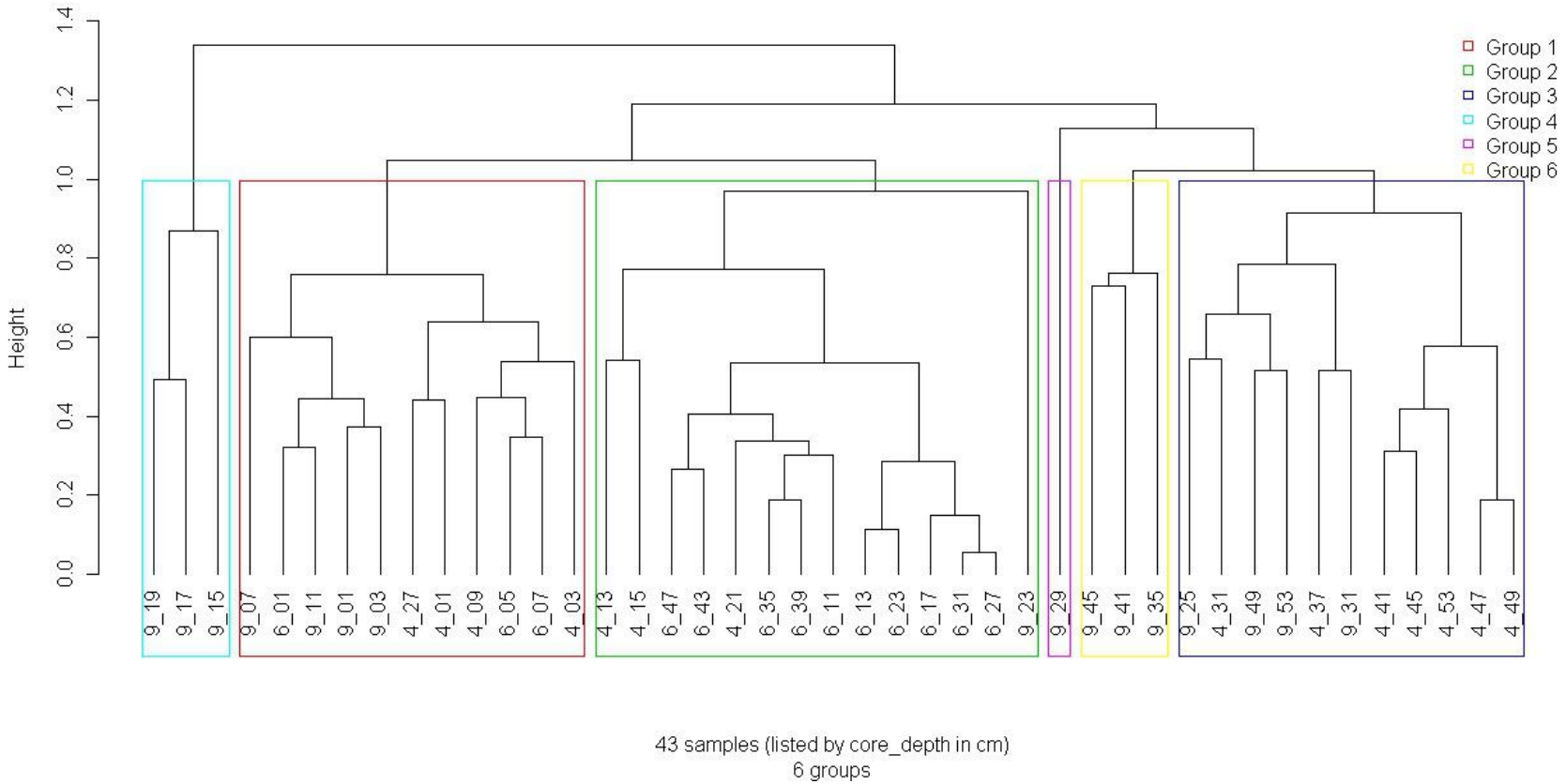

Figure 2-5. Cluster dendogram of diatom microfossil assemblage for depth intervals for all three sediment cores (sites 4, 6, and 9). Numbers along the bottom of each dendogram are the core number and sample depth (cm). Height shows the distance clusters were joined. Colored boxes indicate the optimal cluster groups using maximum silhouette widths.

CHAPTER 3
GEOCHRONOLOGY AND SEDIMENTATION IN AN EVENT-DRIVEN COASTAL MARSH OF SOUTHWEST LOUISIANA

Background

Rising sea-levels and increased tropical storm activity are expected to have substantial impacts on coastal wetlands in the coming decades (IPCC, 2007). Coastal marsh survival is dependent on their adaptive and transitional capacity and the ability to either retreat landward or accrete vertically in response to rising sea level (Scavia et al., 2002). If landward margins are developed preventing expansion inland, then wetlands can be lost if they are unable to gain elevation at rates sufficient to match sea-level rise. Higher water levels impact vegetation type, and under increasing relative sea level rise (RSLR), wetlands can change from freshwater marsh to brackish to open water. Marsh elevation controls tidal inundation and salinity, influencing both sedimentation and vegetative growth (Pethick, 1981). In turn, vertical accretion is dependent on two processes: mineral sediment deposition on the marsh surface and production of organic matter. Reduction in either processes can result in flooding, vegetation death, and marsh collapse (DeLaune et al., 1994).

Tropical storms have been seen as having both positive and negative impacts on marsh elevation, initially through sediment deposition or erosion (Michener, 1997), but also long-term changes in plant communities (Hook et al., 1991). Event-driven deposition in some marshes may be a significant, and potentially the only, source of mineral sediment, however deposited sediment must consolidate and resist re-suspension (Reed, 1989; Turner et al., 2006a).

Significant effort in the past two decades has been devoted to evaluation of coastal marsh elevation and the processes involved in vertical accretion. Long-term

coastal marsh stability is often evaluated by comparing estimates of accretion rates with regional estimates of relative sea-level rise (DeLaune et al., 1983; Kearney et al., 1994; Roman et al., 1997; Stevenson et al., 1985). If marsh accretion is equivalent to sea-level rise, the marsh is said to be stable. If marsh accretion is insufficient to keep pace with sea level, then the opposite is true and the marsh is identified as unstable or deteriorating (Cahoon et al., 1995a).

Understanding the dynamics of sea-level rise and vertical accretion are particularly important for coastal Louisiana where marsh loss rates have been calculated at an average rate of 77 km^2 $year^{-1}$ (Barras et al., 2003). Marsh loss has been attributed to both anthropogenic and natural processes. Wetland hydrology has been altered through impoundments (Reed, 1992), the building of levees, canals, and spoil bank networks (Davis, 1992; DeLaune et al., 1989), and below ground withdrawal of oil and gas (Ko and Day, 2004; Morton et al., 2001). Alterations to hydrology have reduced mineral sedimentation and plant productivity (Day et al., 2000), thereby impacting vertical accretion. Vertical accretion measurements in coastal Louisiana are highly variable and range from 0.20 to upwards of 2 cm yr^{-1} (Jarvis, 2010), and are dependent on many factors, such as tidal flooding, availability of sediment, and vegetation production.

A common approach to calculating vertical accretion rates and sediment chronology is the measurement of the radiometric tracers ^{210}Pb and ^{137}Cs in the soil. Cesium-137 is an anthropogenic impulse tracer that was produced as a result of nuclear weapons testing. Atmospheric input of ^{137}Cs to the soils began during 1954, peaked during 1963/1964, and has been declining ever since (Delaune et al., 1978; Milan et al.,

1995). Lead-210 is naturally occurring, and concentration in the soil at depth should follow a standard exponential decay curve (Robbins, 1978). Both tracers are chronological markers that rely on an expected deposition pattern and decay rate for calculating the time since the sediment was deposited. Based on that date, accretion rates are calculated using bulk density and depth (mass depth). Both ^{137}Cs and ^{210}Pb methods assume that supply is largely from the atmosphere and there is no significant vertical movement once deposited. A technique for determining their efficacy is to examine the total inventory against measured atmospheric deposition. Measurements of atmospheric ^{210}Pb flux in Galveston Texas have been conducted by Baskaran (2011) and calculation of long-term ^{210}Pb-flux for 20-30°N latitude is approximately 37 ± 8 dpm cm^{-2} for 120 years of deposition. Milan et al. (1995) estimated atmospheric deposition of ^{137}Cs from 1952 to 1986 for Houston/New Orleans and Miami at 83 and 89 mCi km^{-2}, respectively; decay corrected to 2009 (date of core collection), estimated inventory would be 6.6 to 6.8 dpm cm^{-2}, with 4.3 to 4.8 ± 1.1 (25% counting error) dpm cm^{-2} occurring prior to 1964. A higher inventory in the soil than from atmospheric levels from the same time period indicates supply in addition to that which is derived from the atmosphere, due to terrestrial or subtidal sources (Cochran et al., 1998). Since ^{210}Pb binds strongly to organics and ^{137}Cs to clay, organic or mineral inputs from tidal flooding and upland runoff can increase inventories. Erosion, dredging, and interception by vegetation are possible causes of depleted inventories. Organic matter decay can lead to loss of ^{210}Pb. Post-depositional mixing and molecular diffusion/advection can modify radioisotope concentrations either positively or negatively. Tropical storms can also

influence radioisotope inventories by introducing allochthonous sediments, vertical mixing, and erosion.

Hurricanes and storms can dramatically increase mineral sediment accretion by depositing several centimeters of sediment in a single event (Cahoon et al., 1995b; Morgan et al., 1958; Stone et al., 1997; Turner et al., 2006a; Williams and Flanagan, 2009). Since radiometric methods are influenced by allochthonous deposits, these events can have a significant influence on accretion rates and chronology. In southwest Louisiana, several hurricanes have occurred that can influence radioisotope inventories (Table 2-1). Hurricanes may be reflected in radioisotope inventories as an increase (sedimentation) or decrease (erosion) in radioisotope inventory. In addition, deviations from typical decay profiles (exponential decay for ^{210}Pb and subsurface peak for ^{137}Cs) can be indicative of events (Kang and Trefry, 2003).

Soil compaction can also have significant influence on vertical accretion (Cahoon et al., 1995a; Kaye and Barghoorn, 1964). Highly organic soils are particularly vulnerable to compaction due to compressibility of the root network, decomposition, and gasification (Knott et al., 1987). Sediment deposits from storms have also been shown to compress soils, resulting in a decreased overall net gain in elevation (Cahoon et al., 1995a). In addition, the collection and processing of a sediment core can cause compaction, which can influence vertical accretion measurements. Therefore, it is highly recommended that core compaction be considered in calculations, since it can have a substantial influence on resulting calculations of vertical accretion rates.

An approach that combines radioisotope data with x-radiographs and sedimentary data may provide stronger inference on sedimentation and chronology in

an event-driven system. X-radiographs provide information on soil density, depth of soil facies, and indications of mixing and bioturbation. They can also show evidence of hurricane deposition as distinct changes in soil density with a sharp boundary between adjacent sediment layers. Sedimentary data, including bulk density, organic matter, and grain size, provide quantitative records that aid the interpretation of x-radiographs. Storm events can also be identified in these data as increases in bulk density and decreases in organic matter. In this study, vertical accretion rates, chronology, and mass accumulation rates are determined for an event-driven coastal marsh in southwest Louisiana to answer the following questions: Are estimates of vertical accretion rate and chronology using radioistope tracers ^{210}Pb and ^{137}Cs valid in an event-driven system? Do radioisotope depth profiles and inventories reflect these events through deviations from expected profile patterns and inflated radioisotope inventories?

Regional Setting

The study site is located at Rockefeller Wildlife Refuge (RWR) in the Chenier plain, southwest Louisiana (Figure 2-2). The Chenier plain was formed from the tidal re-working of a series of progradational Mississippi River deltaic deposits, creating an undulating landscape of relic beach ridges (called cheniers) with marsh in between. Throughout the Chenier plain, man-made channels and water-control structures are prevalent and have greatly altered the natural hydrology, however the study site at RWR was selected because it is not impounded and subject to natural tidal conditions (Phillips, 2002; Twilley, 2003).

Sediment entering this region is almost entirely supplied by small tributaries, tidal flooding, and upland freshwater inflow. The Atchafalaya River, a tributary of the

Mississippi River, is located near the eastern edge of the Chenier plain and delivers fluvial sediment to Vermillion Bay and into the Gulf of Mexico intercontinental shelf. This deltaic deposit, composed primarily of fine-grain sediments, is transported west creating a mudflat from the river mouth to approximately the 93° latitude (Draut et al., 2005). This mudflat deposit is to the east of RWR; however, some sediment may be transported into the marsh during extreme events, such as hurricane storm surge. It is unlikely that tidal processes deliver the mudflat sediment into RWR marshes as the most severe shoreline erosion in the Chenier plain is occurring near RWR (Byrnes et al., 1995).

Recent studies shed light on the significance of episodic events on the vertical accretion rates caused by coastal storms and several storms have been documented to have deposited sediments in RWR. Deposition from Hurricane Ike (2008) was documented at monitoring stations near RWR (Chapter 2 Regional Setting). Hurricane Rita (2005) made landfall four years prior to core collection and five years prior to surface sediment samples. A significant sediment deposit by Hurricane Rita has been documented by previous researchers (Turner et al., 2006a) and a highly-dense sediment deposition is noted on x-radiographs of all nine cores. In addition, Hurricane Audrey (1957) occurred within the period of increasing atmospheric ^{137}Cs supply. This hurricane may be reflected as a deviation within the ^{137}Cs profile or as an inventory in excess of atmospheric levels, given deposition from storm surge. Since particle-bound isotopes are influenced by grain size, sediment composition of the storm deposition would also be an influential factor. Storm events may introduce a significant amount of mineral sediments from outside the system (such as off-shore), or sediments deposited from storms could be eroded sediments from other areas of the marsh. In addition,

smaller climatic events (such as cold fronts), seasonal flooding, and vegetation growth can also contribute sediments toward vertical accretion (Reed, 1989).

Methods

Coring and Laboratory Procedures

Push cores were collected using a 10-cm diameter clear, acrylic barrel with a sharpened edge to reduce compaction. Cores were capped and sealed. They were placed in large cylinder coolers, kept vertical and cold until they were x-rayed and sampled in the lab (Chapter 2 Methods). Compaction was measured by comparing the depth inside and outside the tube during core collection, and by measuring the distance again prior to extrusion. The total length of the extruded core was compared to these lengths to determine total compaction. Vertical accretion rates were calculated both with and without compaction, assuming that compaction influenced the sediments equally down the entire sediment column. This assumption may not be the case, since compaction characteristics of organic and mineral soils are not equivalent and compaction could have occurred outside of the sediment core; however estimates can show the possible influence of compaction on calculated rates.

Cores were sampled by extrusion at 2-cm intervals. Samples were processed for bulk density (dry mass by volume), organic matter (by loss-on-ignition), and ^{210}Pb using alpha spectrometry. Lead-210 in the soil can be divided into two components: supported and unsupported ^{210}Pb. Supported ^{210}Pb is the component in the soil which is derived from in situ decay of ^{226}Ra that is washed in from eroded material. It is considered as "background" levels and was calculated as the average of the ^{210}Pb values of the deepest samples where ^{210}Pb decreased to its lowest value (usually around or below 1 dpm g^{-1}). Unsupported (or excess) ^{210}Pb ($^{210}Pb_{xs}$) is the amount of ^{210}Pb contributed to

the soil from the atmosphere and was determined by subtracting supported ^{210}Pb. Select samples were processed for ^{137}Cs using gamma spectrometry and grain size using laser diffraction. See Chapter 2 Methods for a more complete description of lab procedures.

Chronostratigraphic Techniques

Sedimentation rates were estimated from profiles of radioisotopes (^{210}Pb and ^{137}Cs) and sedimentation models. Two primary models are commonly used to calculate chronology from ^{210}Pb data: Constant Flux-Constant Sedimentation (CF:CS) and Constant Rate of Supply (CRS) (Appleby and Oldfield, 1978). The model applied is dependent on sedimentation rate (accumulation) and chemical flux. The first model, CF:CS, assumes both a constant sedimentation rate and constant ^{210}Pb flux. The CRS model assumes that ^{210}Pb delivery is constant, but sedimentation rate varies. The assumptions applied to any one of the models may not be valid given possible hurricane and tidal influences on ^{210}Pb flux and sedimentation. Therefore, the results of both models were examined against x-radiographs, sedimentary characteristics, and ^{137}Cs data. In addition, the inventory of radioisotopes (both ^{210}Pb and ^{137}Cs) can indicate reliability of model results. These methods will be applied in tandem to estimate sedimentation rates and propose an appropriate chronology (Olsson, 1987).

The CF:CS model is a simple advection-decay model and is often used when the concentration of $^{210}Pb_{xs}$ plotted against depth shows generally an exponential decline. The specific $^{210}Pb_{xs}$ activity is calculated by

$$C = C_0 e^{-\lambda x/\omega}$$

where C_0 is the $^{210}Pb_{xs}$ at the surface (dpm g^{-1}), λ is the decay constant of ^{210}Pb (=0.03114 y^{-1}), x is mass depth (g cm^{-2}), and ω is the mass accumulation rate (g cm^{-2} y^{-1}). When $^{210}Pb_{xs}$ concentration is plotted on the logarithmic scale against mass depth, the profile becomes linear and the equation is transformed to

$$ln(C) = \ln(C_0) - \lambda x/\omega$$

where the slope of the line is λ/ω. Depth (z; cm) can be substituted for mass-depth and the slope of the line is then λ/r, where r is equivalent to the vertical accretion rate (VAR; cm yr^{-1}). Best-fit regression slopes (m) were estimated using Microsoft Excel 2010 (Version 14.0.6112.50000; Microsoft©).

For the CRS model, the age of the sediments at depth z (cm) is calculated by

$$t_{CRS} = \frac{1}{\lambda} ln\left(\frac{A_0}{A_z}\right)$$

where A_0 is the total inventory of $^{210}Pb_{xs}$ (dpm g^{-1}) and A_z is the total inventory of $^{210}Pb_{xs}$ below depth z (dpm g^{-1}). Both A_z and A_0 can be calculated by numerical integration of the concentration versus depth profile. If z denotes the depth of the sediment and C_z is the $^{210}Pb_{xs}$ at that depth, then

$$A_z = \int_z^\infty C_z \, \mathrm{d}z \quad \text{and} \quad A_0 = \int_0^\infty C_z \, \mathrm{d}z.$$

From the t_{CRS} equation, we can estimate the approximate age of the sediment interval. Using CRS method, VAR is calculated by dividing the depth of the interval by the age.

$$VAR = \frac{z}{t}$$

In addition to the two ^{210}Pb models, accretion rates from ^{137}Cs can be estimated by identifying the depth of the concentration peak. Atmospheric fallout began in the

1950s, peaked during 1964 (in this region, atmospheric fallout during 1964 was higher than 1963) and decreased to a very low level in 1982 (Milan et al., 1995). The maximum ^{137}Cs activity found within the sediments is interpreted as corresponding to the peak in fallout, and the depth where ^{137}Cs is first detected corresponds to the early 1950s. Since the number of sample intervals analyzed for ^{137}Cs varied between cores, inventories can only be estimated on all cores from the interval of first detection to the ^{137}Cs peak (the lower tail only; representing 1950 to 1964) since the upper tail (1964 to present) was not analyzed in its entirety for all nine cores.

Mass accumulation rates (MAR; g cm^{-2} yr^{-1}) is estimated by multiplying dry bulk density by vertical accretion rate. The overall contribution of organic matter is measured by the LOI fraction (f_{om}) and multiplied by MAR to estimate the organic matter accumulation rate (MAR_{org}). The mass deposition of mineral sediments (MAR_{min}) is the difference of MAR and MAR_{org}.

Results

Sedimentary Characteristics and X-radiographs

A summary of sedimentary characteristics for all nine cores can be found in Table 3-1. Sediments were predominately silt and clay size fraction and sand content was low, averaging approximate 7% for all nine sites. However, sites 4 and 5 each contained several samples with more than 20% sand. Bulk density for all nine cores was highly variable, and ranged from 0.112 to 0.340 g cm^{-3}. Organic matter content ranged from 8 to 60%, averaging at approximately 23%; the samples with the highest organic content were found in sites 1, 2, 9, and 8.

X-radiographs and bulk density, organic matter, and grain size data can be found in Figures 2-3 to 2-5 (Chapter 2). X-radiographs are inverted, therefore high-density,

high-mineral sediments are dark and low-density, high-organic sediments are light. Sites with intervals of high organic matter content were also reflected in x-radiographs as distinct light gray sediments as seen in x-radiographs. Multiple highly dense sediment layers can be identified on x-radiographs. All nine sites have a dense layer of sediment at the surface; however, sites 7 and 8 the layer is less distinct, but can be identified in the bulk density data. These deviations are similar in appearance to a mixing layer, however the presence in nearly all core sites, sharp contacts between lower sedimentary layers, and higher bulk density support the identity of event-based sedimentation from recent hurricanes.

Distribution of ^{210}Pb

Lead-210 distribution for five of the nine sites demonstrated the expected curve decreasing exponentially with depth (sites 2, 3, 6, 7, and 8); however, variations from this curve coupled with evidence of varying lithology indicate that sedimentation has not been constant through time or other factors, such as mixing or erosion have influenced ^{210}Pb profiles (Figure 3-1). Five sites (1, 3, 4, 5, and 7) had a moderate to sharp rise in ^{210}Pb below the surface that coincide with a dense surface layer identified in x-radiographs and bulk density profiles. Two sites (sites 5 and 8) show substantial variation in the upper portion of the ^{210}Pb profile. However, ^{210}Pb profiles at site 2 and 6 do not deviate significantly from the log-linear trend, despite the indication of dense sediment deposits at the surface.

Radioisotope inventories differed between sites, with several sites having less than or greater than expected levels based on atmospheric flux estimates for this region (Table 3-2; Baskaran, 2011; Baskaran et al., 1993). Five sites have a total inventory of $^{210}Pb_{xs}$ expected on the basis of regional calculations. The $^{210}Pb_{xs}$ inventory for site 2

was lower than expected. Site 2 contained the lowest inventory of $^{210}Pb_{xs}$ with approximately 48% of the inventory expected from direct atmospheric fallout, despite the presence of a thick layer of high inorganic sediment at the surface contributing half the total $^{210}Pb_{xs}$. Tidal flooding or hurricane sediment deposition may account for the large $^{210}Pb_{xs}$ inventory at site 5. When the $^{210}Pb_{xs}$ values for the dense sediment layer are removed from the total inventory, site 5 is within atmospheric levels (36.38 ± 1.15 dpm cm^{-2}).

Distribution of ^{137}Cs

Eight of the nine sites had a distinct peak in the ^{137}Cs distribution (Figures 2-3 through 2-5). Site 8 was the exception, with three sample intervals exhibiting similar ^{137}Cs values within the counting error. The lack of a distinct peak can indicate sediment mixing, bioturbation, mobilization of ^{137}Cs, or wash-in from tidal flooding or upland runoff.

Three sites (2, 4 and 9) contained a larger inventory of ^{137}Cs than would be expected based on regional calculations of atmospheric fallout of ^{137}Cs, indicating a source of cesium other than atmospheric fallout (Table 3-4; Milan et al., 1995). For both sites 2 and 9, the maximum value (peak) is very high (9.39 ± 0.34 dpm g^{-1} and 9.32 ± 0.27 dpm g^{-1}) and bulk density low in comparison to the other sites (with maximum ^{210}Pb ranging from 2 to 4.5 dpm g^{-1}). A low sedimentation rate could result in a high concentration of ^{137}Cs within the 2-cm sample interval designated as 1964 (the interval may contain several years of atmospheric deposition). However, the entire ^{137}Cs inventory (9.32 dpm cm^{-2} for site 2 and 10.18 dpm cm^{-2} for site 9) is also higher than atmospheric levels.

The ^{137}Cs inventory for site 6 is 35-40% lower than expected, suggesting erosion or upward mobilization. Total ^{210}Pb inventory is within error estimates of atmospheric levels suggesting that upward mobilization may be the most likely causal factor.

The five remaining sites have ^{137}Cs inventories within expected values given a 25% instrument error (3.23 to 6.0 dpm cm^{-2}; Milan et al., 1995), supporting sedimentation and chronological calculations from ^{137}Cs data. Since differences between the resolved and expected ^{137}Cs inventory are small (range from 20-40%) and a distinct peak can be identified for most sites (except for site 8), the depth of the peak ^{137}Cs value is a helpful independent marker for chronological analysis at these five sites.

Vertical Accretion Rates

Vertical accretion rates (VAR) estimated from ^{210}Pb and ^{137}Cs data taking into account compaction varied from 0.21 cm yr^{-1} to 1.03 cm yr^{-1} using the CRS model and 0.34 cm yr^{-1} to 1.84 cm yr^{-1} using the CF:CS model (Table 3-3). VAR calculations using ^{137}Cs indicate similar rates, from 0.38 cm yr^{-1} to 1.13 cm yr^{-1}. Using all three models, site 5 has the highest VAR and is also the most variable between model choices, with a mean 1.34 ± 0.44 cm yr^{-1}. Regardless of model or method, the VAR calculations are comparable and only site 5 has a VAR higher than local sea level rise estimates. When taking into account compaction, sites 4 and 5 has VAR values comparable to mean local sea-level rise trends of 0.92 ± 0.12 cm yr^{-1} (Eugene Island, LA; http://tidesandcurrents.noaa.gov/sltrends/sltrends.shtml, accessed on 9/1/2012).

With the exception of site 6, plots of log-linear $^{210}Pb_{xs}$ indicate a zone at the top of the cores not consistent with exponential decay. This zone, varying from 6-16cm in

depth, is consistent with the event/mixing layer identified in x-radiographs and bulk density data.

The regression coefficient of log-linear plots of $^{210}Pb_{xs}$ suggests that simple linear approximation does adequately explain depositional history for several sites (sites 2, 3, 6, and 7; Figure 3-1). After taking into account the uppermost horizon (the mixing or episodic sedimentation zone), linear approximation provides a satisfactory estimate for sites 1, 5, and 9. Sites 4 and 8 are the exception ($R^2 < 0.75$) where fluctuations in log $^{210}Pb_{xs}$ data indicate changes in either sedimentation or ^{210}Pb-flux.

Chronology

Chronology estimates using both ^{210}Pb models and ^{137}Cs peak and first occurrence intervals are shown in Tables 3-4 to 3-8. Three depth intervals (13-17cm) from site 8 are all equivalent to the maximum ^{137}Cs and the profile lacks a distinct peak, however both ^{210}Pb models estimate 1964 at 16-cm depth, which corresponds to the middle of the ^{137}Cs peak interval. For site 7, both ^{210}Pb models predict the ^{137}Cs peak and first occurrence. In four of the remaining sites (1, 2, 6, and 9), the CF:CS model approximates the ^{137}Cs peak more closely than the CRS model. However, date estimates from both models for sites 3, 4 and 5 do not correspond with ^{137}Cs data. For site 5, the downcore ^{210}Pb profile indicates deviation from a normal decay curve and the ^{210}Pb inventory is higher than would be expected if allochthonous sedimentation were introduced. Removal of hurricane sediments from CF:CS and CRS calculations does not improve calculations (Table 3-6).

Mass Accumulation Rates

Sediment core profiles of mass accumulation (MAR) with inorganic (MAR_{min}) and organic (MAR_{org}) fractions are found in Figure 3-2. Vertical accretion estimates from the

CF:CS model were used to calculate MAR for all nine sites because chronology estimates approximated the ^{137}Cs peak for most cores (the exceptions being sites 3, 4, and 5, where both ^{210}Pb model failed to accurately identify the 1964 peak). For a majority of the sites, organic matter contributions to mass accumulation appear consistent throughout the entire sediment core. There is some variability in MAR_{org} at site 5, which is also reflective in highly variable MAR_{min}. At site 3, there is a steady decrease in MAR_{min}, but MAR_{org} is stable. An abrupt increase in MAR_{min} between the ^{137}Cs 1964 peak and initiation of ^{137}Cs deposition in 1950 can be identified in sites 1, 2, 4, 5, 6, and 9. MAR is the least variable at site 8.

Discussion

This study used the vertical distribution and inventories of radioisotopes $^{210}Pb_{xs}$ and ^{137}Cs in marsh cores collected in southwest Louisiana to determine vertical accretion, chronology, and mass accumulation of both organic and inorganic matter coastal marsh. The primary goals were to 1) determine if the inventories of particle-reactive radionuclides can provide information on hurricane sedimentation and erosion, 2) determine if using two common ^{210}Pb depth-activity models and an event tracer (^{137}Cs) provided comparable vertical accretion rates and chronology given the varied and episodic sedimentation patterns, and 3) examine the importance of storm sedimentation on vertical accretion. Using x-radiographs and microfossils, hurricane sedimentation was identified at all sites and substantiated in Chapter 2.

The anticipated result, that the total inventory of $^{210}Pb_{xs}$ in marsh locations with storm deposits would be higher than atmospheric $^{210}Pb_{xs}$, was not observed at RWR because lead inventory of storm sediments was low at 1.5 to 3 dpm cm^{-2} and often well within the error estimate of atmospheric levels (^{210}Pb error estimate is ±8 dpm cm^{-2};

Baskaran 2011). Lead-210 inventories for most marsh locations were within the expected fallout inventory and do not indicate sediment focusing or $^{210}Pb_{xs}$ inputs other than atmospheric sources. The exceptions were sites 2 and 5, which were depleted and elevated, respectively. Olsen et al. (1985) examined $^{210}Pb_{xs}$ inventory in the marshes of Virginia and Tennessee and found generally larger inventories than expected from atmospheric deposition measurements. They attributed the excess to the location of the water table and aboveground vegetation creating a “trap” for particles containing sorbed $^{210}Pb_{xs}$. Elevated inventories in coastal areas have been attributed to sediment resuspension and repeated exposure to new $^{210}Pb_{xs}$ in the water column (Draut et al., 2005). Site 5 is located in close proximity to a marsh lake and the Gulf of Mexico and the highly dense nature of the soils indicate it likely receives a regular supply of sediments from diurnal and seasonal tidal flooding, which could cause elevated $^{210}Pb_{xs}$ inventory.

Erosion from storm events or diffusion may have caused the $^{210}Pb_{xs}$ inventory at site 2 to be half the expected inventory from atmospheric deposition. The low inventory was inconsistent with observed storm sedimentation patterns which would be a source of allochthonous sediments and provide $^{210}Pb_{xs}$ in addition to atmospheric fallout. The dense hurricane sediment layer contributed half of the total $^{210}Pb_{xs}$ inventory at Site 2. Also, comparisons of the $^{210}Pb_{xs}$ profiles for site 2 with sites 1 and 9, which have similar deposition patterns, indicate both sites 1 and 9 have a distinct peak in $^{210}Pb_{xs}$ just below the hurricane deposited sediment which is lacking in site 2, suggesting erosion as the cause of a depleted $^{210}Pb_{xs}$ inventory. In general, inventories for sites with substantial storm sedimentation were not consistently in excess in comparison to atmospheric

levels. Since $^{210}Pb_{xs}$ binds most strongly to organic matter and $^{210}Pb_{xs}$ inventory is often correlated with organic carbon (Paulsen et al., 1999; Ravens et al., 2009), it is possible that the high mineral composition of storm deposited sediment does not concentrate $^{210}Pb_{xs}$ in a such way as to cause the soil inventory to increase beyond the inherent error in the regional atmospheric calculations. $^{210}Pb_{xs}$ in these storm sediments in general are lower than $^{210}Pb_{xs}$ in sediments just below the storm layer. However, if storm sedimentation indeed increased $^{210}Pb_{xs}$ inventories, there must have been loss (possibly from erosion) equivalent to gain.

Cesium-137 binds strongly to illite clays, which are common in Louisiana marsh (Nyman et al., 1993) and the continental margin (Fisk and McClelland, 1959). Since ^{137}Cs bound to clay minerals is infrequently mobile and Chenier plain sediments have a significant clay composition, the ^{137}C dating method should be a reliable chronological marker. Eight of the nine sites sampled had a clear ^{137}C peak. In the case of site 8, where a distinct peak was not observed, it is possible that some mobilization of ^{137}Cs could occur due to decomposition, however the organic matter content of sediments is similar to (or lower than) several other sites which exhibit a ^{137}Cs peak, suggesting that organic matter content may not be the influencing factor. There is also no indication of bioturbation in the x-radiograph, however physical or biological mixing is still a possible explanation. Given these considerations, the absence of a distinct peak at site 8 is likely due to mixing (physical or biological).

Compared to estimates of atmospheric fallout, 1950-1964 ^{137}Cs inventory at three sites (2, 4, and 9) was elevated up to 40%. Sediment deposition from recent storms (Hurricanes Ike, Rita, and Katrina) would not influence the lower-tail (1950-1964) ^{137}Cs

inventory unless substantial erosion or deep mixing occurred. However, Hurricane Audrey delivered clay-mud sediments to RWR in 1957 (Morgan et al., 1958) and is hypothesized here as the cause of an increase in ^{137}Cs inventory. X-radiograph and bulk density data indicate the presence of a dense sediment deposit just below the ^{137}Cs peak (at the depths 19, 34, and 25 cm, respectively) for each of these three sites.

The nine cores within the Rockefeller Wildlife Refuge reveal a wide range of vertical accretion rates (0.33-1.84 cm yr^{-1} using the CF:CS, 0.22-1.03 cm yr^{-1} using the CRS method, and 0.33-0.90 cm yr^{-1} using ^{137}Cs) that reflect differences in the available mineral sediment supply. Vertical accretion estimates using ^{137}Cs tended to be higher than $^{210}Pb_{xs}$ methods, which was documented in other studies (Turner et al., 2006b) and explained by Mudd et al. (2009) as loss of ^{210}Pb from organic matter decomposition. In addition, locations that have higher mineral content, in general, have higher vertical accretion rates, suggesting mineral sediment deficits may be a cause for lower-than-sea-level-rise vertical accretion and marsh submergence. For sites located distant from an open water source, event-based sedimentation may be the main source of mineral sediments to these marshes, as seen in sites with predominately organic core profiles and dense mineral layering. However, hurricane surge can cause erosion. Moreover, the deposition of dense sediment on highly organic soils can lead to compaction (Delaune et al., 1986). Therefore, mineral deposition does not necessarily lead to an equivalent gain in marsh elevation.

Chronological estimates of non-steady state systems like coastal marsh are problematic since standard models assume consistency in either sedimentation or radioisotope flux and since the primary source of the radioisotope is from the

atmosphere. However, by using additional tools, such as x-radiographs and radioisotope inventories, a chronological model can be proposed that provides a satisfactory match with an independent tracer. For many marsh locations examined here, the CF:CS model approximates the ^{137}Cs peak more accurately than the CRS model, possibly because it captures general depositional trends over the long-term and is less influenced by year to year fluctuations in sedimentation or flux. Locations where evidence of episodic sedimentation is minimal (such as sites 7 and 8) had the greatest success using radionuclide techniques for chronological estimation since $^{210}Pb_{xs}$ and ^{137}Cs vertical accretion calculations were similar despite a non-steady state depositional pattern. Over the long-term (100 or so years) sedimentation seems relatively consistent. An exception may be in cases where marshes receive a steady supply of mineral sediments from tidal flushing in addition to event-based sedimentation (such as site 5). In those cases, examining the $^{210}Pb_{xs}$ inventory may help indicate the extent to which hurricane and tidal sedimentation contribute to vertical accretion.

Hurricanes do appear to contribute large amounts of mineral sediments to Chenier plain wetlands, as hypothesized by Turner (2006a). Contributions from recent storms (roughly 1900 to present) can account for up to 50% of the vertical accretion (as seen in site 1) or as little as 16% (site 6). However, in large part organic contributions to mass accumulation has not changed significantly over time, as demonstrated by relatively stable organic matter composition. Mineral contributions did vary significantly over time and, in the absence of storms, several marsh locations show a reduction by half in the accumulation of mineral sediments after 1950.

Radioisotope profiles and inventories provided information on accretion rates, chronology, and sediment source. Despite the common practice of calculating vertical accretion in coastal marsh using $^{210}Pb_{xs}$ and ^{137}Cs data, I can find no other studies in northern Gulf of Mexico marshes which examined radioisotope inventories and the effect of hurricane versus tidal sediment deposits on radioisotope data. Lead-210 flux models will be of greater import in the future, as ^{137}Cs decay reduces detectability in soils. Understanding the influence of sediment deposition and soil density, vegetation, tidal flooding, and storms on $^{210}Pb_{xs}$ flux is an important endeavor for future analyses of marsh development and susceptibility to submergence in a changing climate.

Table 3-1. The summary of sediment data (bulk density, organic matter, and grain size) for each marsh sediment core and the combined data set. Data are summarized as mean ± one standard deviation.

Site	Bulk density (g cm^{-3})	Organic Matter (%)	Sand (%)	Silt (%)	Clay (%)
1	0.122 ± 0.1	24.5 ± 12.41	9.8 ± 7.46	73.5 ± 5.5	18.4 ± 4.56
2	0.123 ± 0.13	29.3 ± 14.77	10.1 ± 6.97	71.6 ± 4.35	18.4 ± 5.32
3	0.265 ± 0.09	17.5 ± 6	8.3 ± 8.3	71.3 ± 5.17	20.4 ± 4.96
4	0.302 ± 0.08	16.1 ± 5.43	6.4 ± 6.74	70.8 ± 4.14	22.8 ± 5.46
5	0.276 ± 0.08	15.5 ± 3.94	12.7 ± 11.91	68.5 ± 8.63	18.8 ± 3.71
6	0.34 ± 0.05	17 ± 4.22	3.7 ± 3.32	72.1 ± 2.88	24.2 ± 4.93
7	0.284 ± 0.06	21 ± 6.79	3.9 ± 3.99	72 ± 2.18	24.2 ± 4.12
8	0.155 ± 0.05	34.6 ± 7.71	6.3 ± 4.14	72.6 ± 3.64	21.1 ± 3.94
9	0.112 ± 0.08	29.5 ± 12.1	6.2 ± 7.12	21.5 ± 4.67	72.3 ± 4.89
All	0.3583 ± 0.12	22.8 ± 11.02	6.8 ± 7.15	71.6 ± 4.81	21.5 ± 4.94

Table 3-2. The summary of depth integrated radioisotope inventory for excess lead ($^{210}Pb_{xs}$) and cesium (^{137}Cs), including total standard error and intervals included in the calculation. Values with a plus ($^{+}$) indicate higher than the expected regional value (if deposition is from atmosphere alone); values with a minus ($^{-}$) are lower than expected. Total compaction is also noted.

Site	Interval (cm)	$^{210}Pb_{xs}$ Inventory* (dpm cm^{-2})	Interval (cm)	^{137}Cs Inventory 1950-1964** (dpm cm^{-2})	Compaction %
1	0-40	38.07 ± 1.09	22-30	4.58 ± 0.32	15
2	0-28	16.85 ± 0.52^{-}	14-24	7.96 ± 0.43^{+}	28
3	0-36	24.66 ± 0.84	22-32	3.46 ± 0.40	34
4	0-44	40.04 ± 1.45	30-42	6.75 ± 0.57^{+}	34
5	0-40	47.97 ± 1.48^{+}	34-42	3.04 ± 0.39	28
6	0-28	28.09 ± 0.83	26-34	2.84 ± 0.29^{-}	29
7	0-42	24.36 ± 1.05	18-30	4.18 ± 0.35	10
8	0-40	23.53 ± 0.62	14-30	5.30 ± 0.52	21
9	0-40	33.15 ± 0.85	22-32	8.08 ± 0.21^{+}	3

* Ideal $^{210}Pb_{xs}$ inventory is approximately 33 ± 8 dpm cm^{-2} for Galveston, TX (Baskaran, 2011; Baskaran et al., 1993).

** Ideal 137Cs inventory for coastal Louisiana is approximately 4.3 to 4.8 ± 1.1 dpm cm^{-2} inventory from 1950 to 1965 (lower tail) based on atmospheric ^{20}Sr calculations by Milan et al. (1995) and corrected for decay (Appendix B).

Table 3-3. Calculations of average sedimentation rate (cm yr^{-1}) for coastal marsh sites, with and without taking into account compaction, by applying the Constant Flux : Constant Sedimentation (CF:CS) and Constant Rate of Supply (CRS) models to $^{210}Pb_{xs}$ data. Sedimentation rates are also calculated from ^{137}Cs, assuming the peak of ^{137}Cs at depth was equivalent to the year 1964. Relative mean sea-level rise rates are provided for comparison.

	CF:CS Accretion[a] (cm yr^{-1})		CRS Accretion[b] (cm yr^{-1} ± SD)		^{137}Cs Peak[c] (cm yr^{-1})	
Site	w/o comp	w/comp	w/o comp	w/comp	w/o comp	w/comp
1	0.45	0.51	0.43 ± 0.19	0.49 ± 0.19	0.51	0.59
2	0.27	0.34	0.21 ± 0.03	0.26 ± 0.03	0.33	0.39
3	0.57	0.73	0.43 ± 0.12	0.55 ± 0.12	0.51	0.61
4	0.80	1.01	0.56 ± 0.18	0.71 ± 0.18	0.69	0.82
5	1.50	1.84	0.83 ± 0.35	1.03 ± 0.35	0.78	0.90
6	0.57	0.71	0.40 ± 0.13	0.50 ± 0.13	0.60	0.69
7	0.40	0.50	0.37 ± 0.05	0.46 ± 0.05	0.42	0.49
8	0.33	0.39	0.31 ± 0.06	0.37 ± 0.06	0.38	0.42
9	0.43	0.44	0.50 ± 0.31	0.51 ± 0.31	0.51	0.52
Relative mean sea-level rise[d] :						
Eugene Island, LA (1939-1974)					0.96 ± 0.12 cm yr^{-1}	
Grand Isle, LA (1947-2006)					0.92 ± 0.06 cm yr^{-1}	

[a]Calculated from slope of least squares regression through plot of ln($^{210}Pb_{xs}$) against depth. Total compaction is integrated equally throughout the entire depth.
[b]Mean ± SD. Total compaction is integrated equally throughout the entire depth.
[c]The two values are calculated from the 1964 peak (depth in cm / 45 years). Total compaction is assumed to be above the 1964 peak.
[d]From National Oceanic and Atmospheric Administration's (NOAA) Sea Levels Online (http://tidesandcurrents.noaa.gov/sltrends/sltrends.shtml, accessed on 9/1/2012)

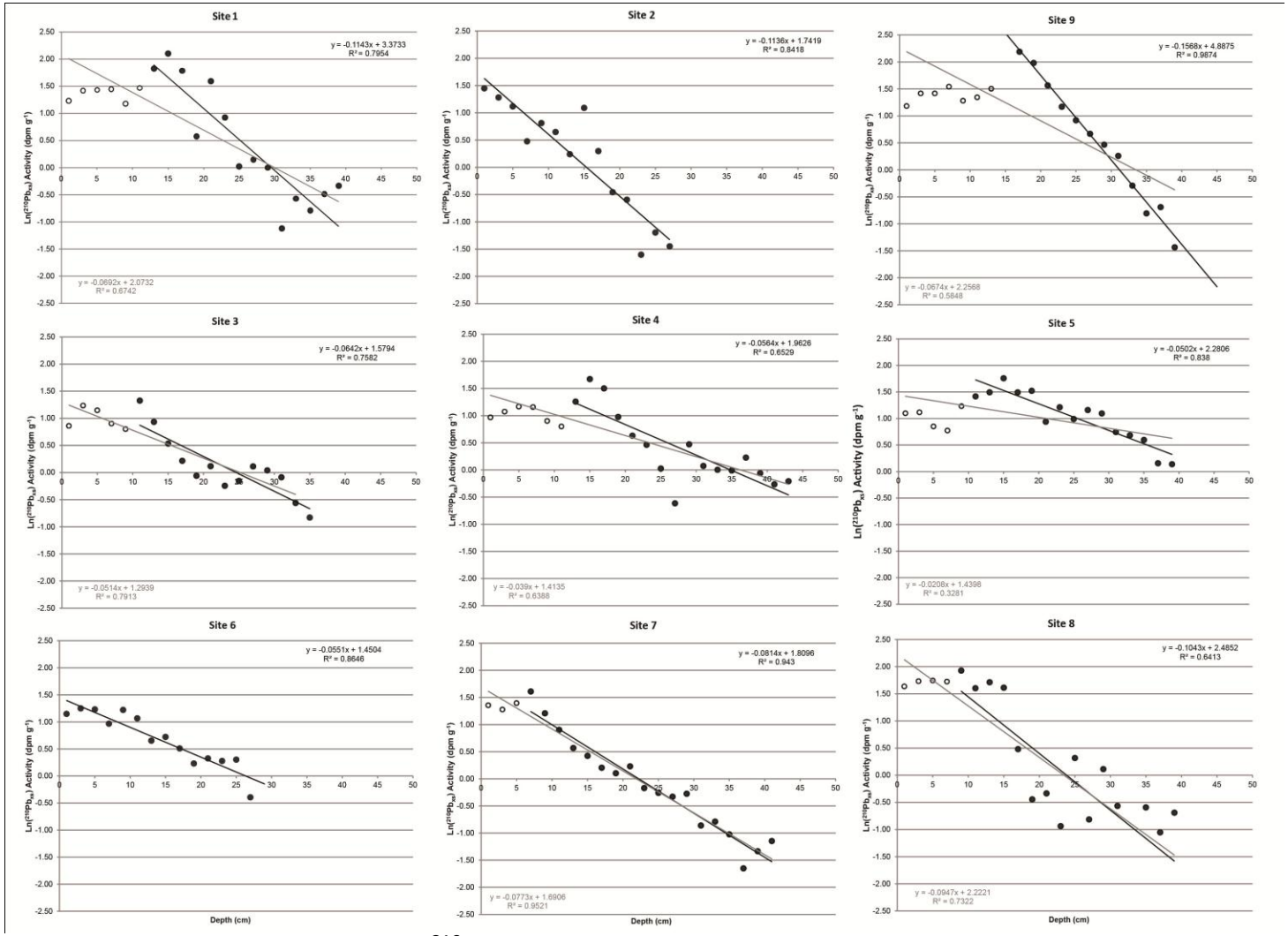

Figure 3-1. Plots of natural log of $^{210}Pb_{xs}$ versus linear depth are applied to estimate accumulation rates for each sediment core following the Constant Flux : Constant Sedimentation (CF:CS) model. Two linear trend lines, equations, and coefficient of determination (R^2) are given. The first regression (grey) includes all data points; the second (black) removes data from uppermost zone where indications of mixing or storm deposition is evident (white points).

Table 3-4. Chronology estimates for sediment cores from sites 1 and 2 using two ^{210}Pb age models. Intervals with peak ^{137}Cs (1964) and first occurrence (1950) are also indicated. Grayed intervals indicate possible storm sedimentation.

Site 1			
Depth (cm)	CF:CS[a] Date (yr ± 95% CI)	CRS[b] Date (yr ± SD)	^{137}Cs Date (yr)
0	2009 ± 0.00	2009 ± 1.56	2009
2	2005 ± 0.63	2007 ± 1.55	
4	2002 ± 1.27	2004 ± 1.56	
6	1998 ± 1.90	2001 ± 1.58	
8	1994 ± 2.54	1996 ± 1.60	
10	1990 ± 3.17	1993 ± 1.61	
12	1986 ± 3.81	1986 ± 1.63	
14	1982 ± 4.44	1978 ± 1.68	2005
16	1978 ± 5.07	1967 ± 1.82	1996
18	1974 ± 5.71	1956 ± 2.04	1988
20	1971 ± 6.34	1954 ± 2.03	1980
22	**1967 ± 6.98**	1940 ± 2.44	**1964**
24	1963 ± 7.61	1928 ± 2.94	1959
26	1959 ± 8.24	1918 ± 3.22	1957
28	**1955 ± 8.88**	1912 ± 3.45	**1950**
30	1951 ± 9.51	1908 ± 3.62	
32	1947 ± 10.15	1905 ± 3.44	
34	1944 ± 10.78	1896 ± 3.40	
36	1940 ± 11.42	1886 ± 3.06	

Site 2			
Depth (cm)	CF:CS[a] Date (yr ± 95% CI)	CRS[b] Date (yr ± SD)	^{137}Cs Date (yr)
0	2009 ± 0.00	2009 ± 3.02	2009
2	2003 ± 0.80	2004 ± 3.17	
4	1997 ± 1.59	1997 ± 3.40	
6	1990 ± 2.39	1988 ± 3.81	
8	1984 ± 3.18	1985 ± 3.95	2005
10	1978 ± 3.98	1981 ± 4.12	1991
12	1971 ± 4.77	1978 ± 4.27	1977
14	**1965 ± 5.57**	**1976 ± 4.36**	**1964**
16	1959 ± 6.36	1965 ± 5.29	1960
18	1952 ± 7.16	1947 ± 7.25	1957
20	1946 ± 7.95	1932 ± 8.80	1953
22	**1940 ± 8.75**	1921 ± 10.36	**1950**
24	1933 ± 9.54	1914 ± 9.79	

[a]Constant Flux : Constant Sedimentation (CF:CS) calculated from slope of best-fit regression through plot of ln(^{210}Pb$_{xs}$) vs depth. Total compaction is integrated equally throughout the entire depth. Error is estimated from 95% confidence interval for the regression line.
[b]Constant Rate of Supply (CRS): Mean ± SD. Total compaction is integrated equally throughout the entire depth.

Table 3-5. Chronology estimates for sediment cores from sites 3 and 4 using two ^{210}Pb age models. Intervals with peak ^{137}Cs (1964) and first occurrence (1950) are also indicated. Grayed intervals indicate possible storm sedimentation.

Site 3			
Depth (cm)	CF:CS[a] Date (yr ± 95% CI)	CRS[b] Date (yr ± SD)	^{137}Cs Date (yr)
0	2009 ± 0.00	2009 ± 2.64	2009
2	2006 ± 0.34	2008 ± 2.65	
4	2003 ± 0.68	2006 ± 2.69	
6	2000 ± 1.03	2004 ± 2.75	
8	1997 ± 1.37	2000 ± 2.82	
10	1994 ± 1.71	1997 ± 2.90	2005
12	1991 ± 2.05	1992 ± 3.06	1997
14	1988 ± 2.39	1989 ± 3.18	1991
16	1985 ± 2.73	1986 ± 3.23	1984
18	1982 ± 3.08	1984 ± 3.28	1977
20	1979 ± 3.42	1981 ± 3.30	1971
22	1976 ± 3.76	1977 ± 3.38	**1964**
24	1973 ± 4.10	1974 ± 3.38	1960
26	1970 ± 4.44	1969 ± 3.39	1957
28	1967 ± 4.78	1961 ± 3.59	1953
30	1964 ± 5.13	**1949 ± 3.92**	**1950**
32	1961 ± 5.47	1930 ± 4.67	
34	1958 ± 5.81	1903 ± 5.23	

[a]Constant Flux : Constant Sedimentation (CF:CS) calculated from slope of best-fit regression through plot of ln(^{210}Pb$_{xs}$) vs depth. Error is estimated from 95% confidence interval.
[b]Constant Rate of Supply (CRS): Mean ± SD. Total compaction is integrated equally throughout the entire depth.

Site 4			
Depth (cm)	CF:CS[a] Date (yr ± 95% CI)	CRS[b] Date (yr ± SD)	^{137}Cs Date (yr)
0	2009 ± 0.00	2009 ± 2.99	2009
2	2007 ± 0.36	2009 ± 3.00	
4	2005 ± 0.72	2008 ± 3.01	
6	2003 ± 1.08	2006 ± 3.04	
8	2001 ± 1.44	2005 ± 3.08	
10	1999 ± 1.80	2003 ± 3.11	
12	1997 ± 2.15	2001 ± 3.13	2005
14	1994 ± 2.51	1997 ± 3.25	2000
16	1992 ± 2.87	1993 ± 3.42	1995
18	1990 ± 3.23	1989 ± 3.59	1991
20	1988 ± 3.59	1986 ± 3.71	1986
22	1986 ± 3.95	1983 ± 3.80	1982
24	1984 ± 4.31	1980 ± 3.88	1977
26	1982 ± 4.67	1977 ± 3.89	1973
28	1980 ± 5.03	1975 ± 3.79	1968
30	1977 ± 5.39	**1970 ± 3.97**	**1964**
32	1975 ± 5.74	1965 ± 4.03	1963
34	1973 ± 6.10	1959 ± 4.01	1961
36	1971 ± 6.46	1951 ± 4.03	1960
38	1969 ± 6.82	1940 ± 4.36	1958
40	1967 ± 7.18	1927 ± 4.61	**1950**
42	1965 ± 7.54	1908 ± 4.48	

Table 3-6. Chronology estimates for sediment core from site 5 using two ^{210}Pb age models. Intervals with peak ^{137}Cs (1964) and first occurrence (1950) are also indicated. Grayed intervals indicate possible storm sedimentation.

Site 5				Site 5 – removing surface hurricane deposit			
Depth (cm)	CF:CS[a] Date (yr ± 95% CI)	CRS[b] Date (yr ± SD)	^{137}Cs Date (yr)	Depth (cm)	CF:CS[a] Date (yr ± 95% CI)	CRS[b] Date (yr ± SD)	^{137}Cs Date (yr)
0	2009 ± 0.00	2009 ± 1.61		0			2009
2	2008 ± 0.72	2009 ± 1.61		2			
4	2007 ± 1.11	2008 ± 1.61		4			
6	2006 ± 1.50	2008 ± 1.61		6			
8	2004 ± 1.90	2007 ± 1.62	2004	8	2004 ± 0.00	2005 ± 1.62	2004
10	2003 ± 2.29	2006 ± 1.63	2001	10	2002 ± 0.37	2004 ± 1.63	2001
12	2002 ± 2.68	2004 ± 1.64	1998	12	1999 ± 0.73	2003 ± 1.64	1998
14	2001 ± 3.07	2003 ± 1.66	1995	14	1997 ± 1.10	2001 ± 1.65	1995
16	2000 ± 3.46	2000 ± 1.69	1992	16	1994 ± 1.47	1999 ± 1.68	1992
18	1999 ± 3.85	1998 ± 1.72	1989	18	1992 ± 1.83	1996 ± 1.71	1989
20	1997 ± 4.25	1994 ± 1.75	1986	20	1989 ± 2.20	1993 ± 1.75	1986
22	1996 ± 4.64	1991 ± 1.77	1982	22	1987 ± 2.56	1990 ± 1.76	1982
24	1995 ± 5.03	1987 ± 1.81	1979	24	1985 ± 2.93	1986 ± 1.80	1979
26	1994 ± 5.42	1983 ± 1.85	1976	26	1982 ± 3.30	1981 ± 1.83	1976
28	1993 ± 5.81	1976 ± 1.93	1973	28	1980 ± 3.66	1974 ± 1.90	1973
30	1992 ± 6.20	1966 ± 2.00	1970	30	1977 ± 4.03	1965 ± 1.97	1970
32	1990 ± 6.60	1957 ± 2.07	1967	32	1975 ± 4.40	1956 ± 2.04	1967
34	1989 ± 6.99	1946 ± 2.18	**1964**	34	1972 ± 4.76	1944 ± 2.11	**1964**
36	1988 ± 7.38	1929 ± 2.26	1959	36	1970 ± 5.13	1928 ± 2.26	1959
38	1987 ± 7.77	1908 ± 2.28	1955	38	1967 ± 5.49	1907 ± 2.28	1955
40			**1950**	40			**1950**

[a]Constant Flux : Constant Sedimentation (CF:CS) calculated from slope of best-fit regression through plot of ln(^{210}Pb$_{xs}$) vs depth. Total compaction is integrated equally throughout the entire depth. Error is estimated from 95% confidence interval for the regression line.
[b]Constant Rate of Supply (CRS): Mean ± SD. Total compaction is integrated equally throughout the entire depth.

Table 3-7. Chronology estimates for sediment cores from sites 6 and 7 using two ^{210}Pb age models. Intervals with peak ^{137}Cs (1964) and first occurrence (1950) are also indicated. Grayed intervals indicate possible storm sedimentation.

Site 6			
Depth (cm)	CF:CS[a] Date (yr ± 95% CI)	CRS[b] Date (yr ± SD)	^{137}Cs Date (yr)
0	2009 ± 0.00	2009 ± 2.12	2009
2	2006 ± 0.35	2008 ± 2.05	
4	2003 ± 0.71	2006 ± 1.95	
6	2000 ± 1.06	2002 ± 1.82	
8	1997 ± 1.42	1998 ± 1.67	2005
10	1994 ± 1.77	1994 ± 1.54	2000
12	1991 ± 2.12	1990 ± 1.40	1995
14	1988 ± 2.48	1986 ± 1.31	1991
16	1985 ± 2.83	1982 ± 1.19	1986
18	1981 ± 3.18	1977 ± 1.06	1982
20	1978 ± 3.54	1972 ± 0.92	1977
22	1975 ± 3.89	1961 ± 0.70	1973
24	1972 ± 4.25	1948 ± 0.47	1968
26	**1969 ± 4.60**	1914 ± 0.22	**1964**
28	1966 ± 4.95		1959
30	1963 ± 5.31		**1950**

Site 7			
Depth (cm)	CF:CS[a] Date (yr ± 95% CI)	CRS[b] Date (yr ± SD)	^{137}Cs Date (yr)
0	2009 ± 0	2009 ± 2.3	2009
2	2004 ± 0.26	2005 ± 2.37	
4	1999 ± 0.51	2001 ± 2.45	
6	1994 ± 0.77	1995 ± 2.58	2005
8	1989 ± 1.02	1988 ± 2.77	1997
10	1985 ± 1.28	1983 ± 2.94	1991
12	1980 ± 1.53	1978 ± 3.11	1984
14	1975 ± 1.79	1974 ± 3.26	1977
16	1970 ± 2.04	1969 ± 3.44	1971
18	**1965 ± 2.3**	**1964 ± 3.6**	**1964**
20	1960 ± 2.55	1960 ± 3.75	1960
22	1955 ± 2.81	1954 ± 4.1	1957
24	**1950 ± 3.06**	**1948 ± 4.34**	**1950**
26	1945 ± 3.32	1942 ± 4.65	
28	1940 ± 3.57	1933 ± 5.11	
30	1935 ± 3.83	1921 ± 6.09	
32	1930 ± 4.08	1912 ± 6.61	
34	1925 ± 4.34	1900 ± 8.01	
36	1920 ± 4.59	1886 ± 10.08	
38	1915 ± 4.85	1878 ± 10.58	
40	1910 ± 5.1	1860 ± 14.28	

[a]Constant Flux : Constant Sedimentation (CF:CS) calculated from slope of best-fit regression through plot of ln($^{210}Pb_{xs}$) vs depth. Total compaction is integrated equally throughout the entire depth. Error is estimated from 95% confidence interval for the regression line.
[b]Constant Rate of Supply (CRS): Mean ± SD. Total compaction is integrated equally throughout the entire depth.

Table 3-8. Chronology estimates for sediment cores from sites 8 and 9 using two ^{210}Pb age models. Intervals with peak ^{137}Cs (1964) and first occurrence (1950) are also indicated. Grayed intervals indicate possible storm sedimentation.

Site 8				Site 9			
Depth (cm)	CF:CS[a] Date (yr ± 95% CI)	CRS[b] Date (yr ± SD)	^{137}Cs Date (yr)	Depth (cm)	CF:CS[a] Date (yr ± 95% CI)	CRS[b] Date (yr ± SD)	^{137}Cs Date (yr)
0	2009 ± 0.00	2009 ± 2.14	2009	0	2009 ± 0.00	2009 ± 1.70	
2	2004 ± 0.78	2007 ± 2.19		2	2005 ± 1.19	2008 ± 1.70	
4	1998 ± 1.57	2004 ± 2.26		4	2000 ± 2.04	2005 ± 1.71	
6	1993 ± 2.35	2001 ± 2.37		6	1996 ± 2.90	2001 ± 1.73	
8	1987 ± 3.14	1997 ± 2.52		8	1992 ± 3.75	1997 ± 1.77	
10	1982 ± 3.92	1991 ± 2.78		10	1987 ± 4.61	1992 ± 1.80	
12	1976 ± 4.71	1985 ± 3.05		12	1983 ± 5.47	1987 ± 1.85	
14	1971 ± 5.49	1976 ± 3.63		14	1979 ± 6.32	1981 ± 1.90	2005
16	**1965 ± 6.27**	**1964 ± 4.65**	**1964?**	16	1974 ± 7.18	1974 ± 2.06	1994
18	1960 ± 7.06	1959 ± 5.04		18	1970 ± 8.03	1967 ± 2.23	1984
20	1954 ± 7.84	1957 ± 5.00		20	1966 ± 8.89	1961 ± 2.44	1974
22	1949 ± 8.63	1954 ± 5.07		22	**1962 ± 9.75**	1953 ± 2.70	**1964**
24	1943 ± 9.41	1953 ± 4.89		24	1957 ± 10.60	1946 ± 2.95	1961
26	1938 ± 10.20	1945 ± 5.57		26	1953 ± 11.46	1936 ± 3.40	1958
28	1932 ± 10.98	1941 ± 5.32		28	1949 ± 12.31	1923 ± 4.12	1956
30	1927 ± 11.77	1929 ± 6.11	**1950?**	30	1944 ± 13.17	1911 ± 4.88	1953
32	1921 ± 12.55	1922 ± 6.34		32	**1940 ± 14.03**	1899 ± 5.97	**1950**
34	1916 ± 13.33	1921 ± 5.25		34	1936 ± 14.88	1882 ± 7.19	
36	1910 ± 14.12	1910 ± 5.32		36	1931 ± 15.74	1862 ± 7.71	
38	1905 ± 14.90	1894 ± 4.63		38	1927 ± 16.59	1821 ± 12.02	

[a]Constant Flux : Constant Sedimentation (CF:CS) calculated from slope of best-fit regression through plot of ln(^{210}Pb$_{xs}$) vs depth. Total compaction is integrated equally throughout the entire depth. Error is estimated from 95% confidence interval for the regression line.
[b]Constant Rate of Supply (CRS): Mean ± SD. Total compaction is integrated equally throughout the entire depth.

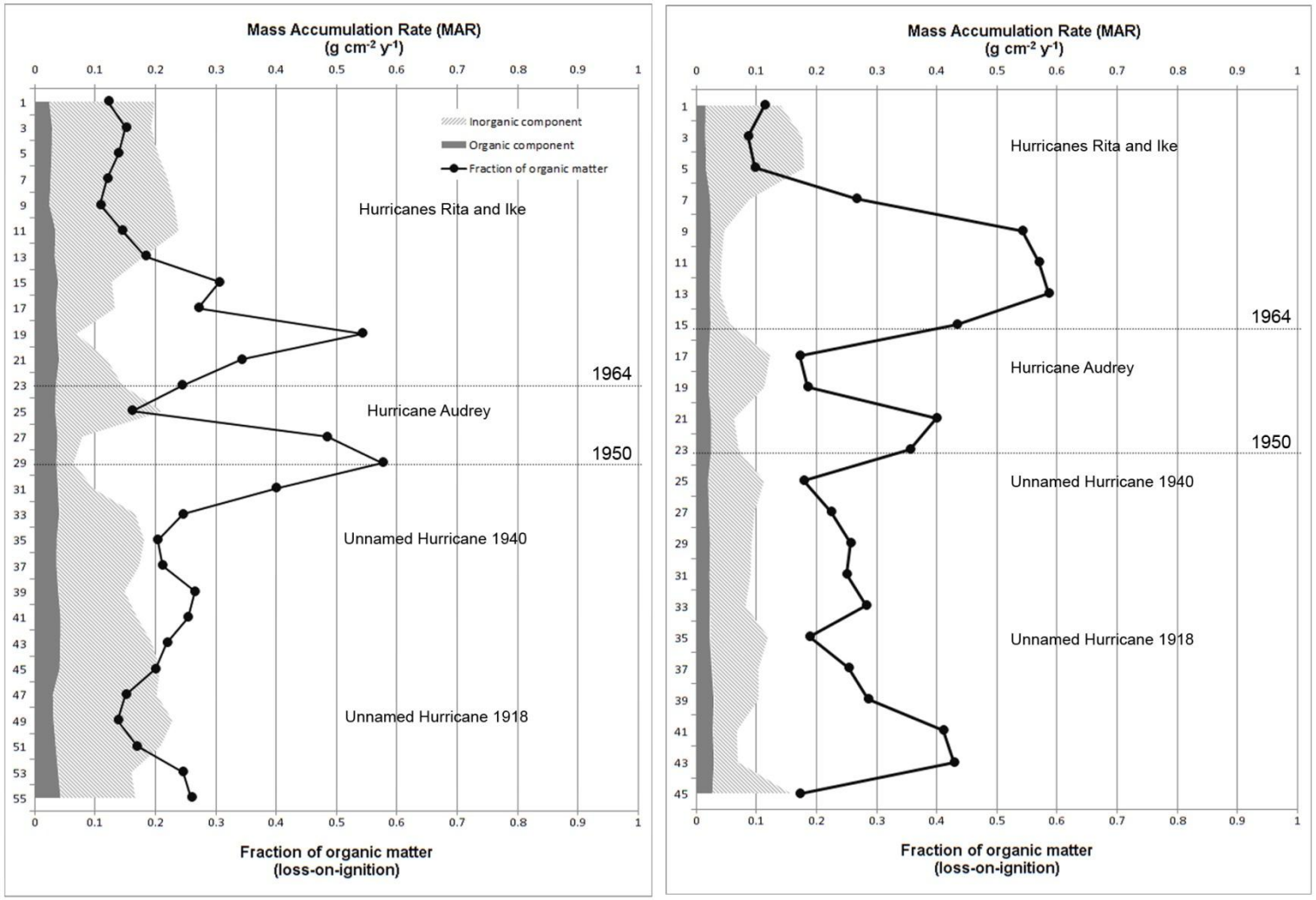

Figure 3-2. Organic matter fraction (f_{om}; black line) and mass accumulation rates (MAR) for both organic accumulation (orgMAR; dark gray) and mineral deposition rate (minMAR; light gray) data. Vertical scale is present as a linear distance at depth from surface (cm). A) Depth profile data for Site 1. B) Depth profile data for site 2. C) Depth profile data for site 3. D) Depth profile data for site 4. E) Depth profile data for site 5. F) Depth profile data for site 6. G) Depth profile data for site 7. H) Depth profile data for site 8. I) Depth profile data for site 9.

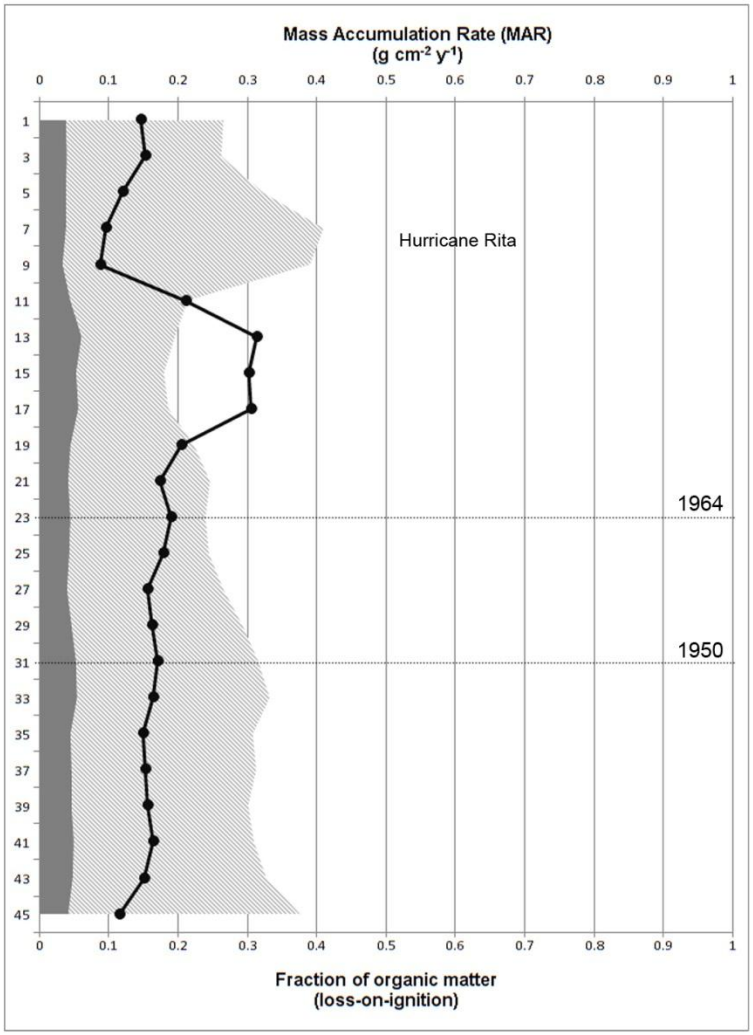

C

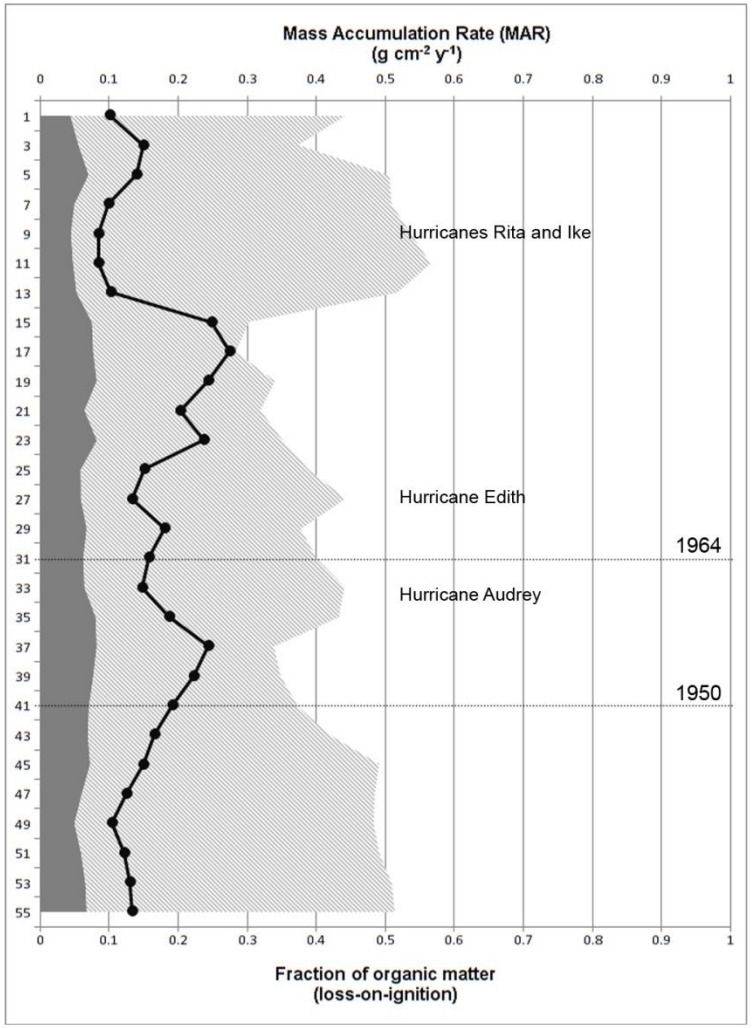

D

Figure 3-2. Continued.

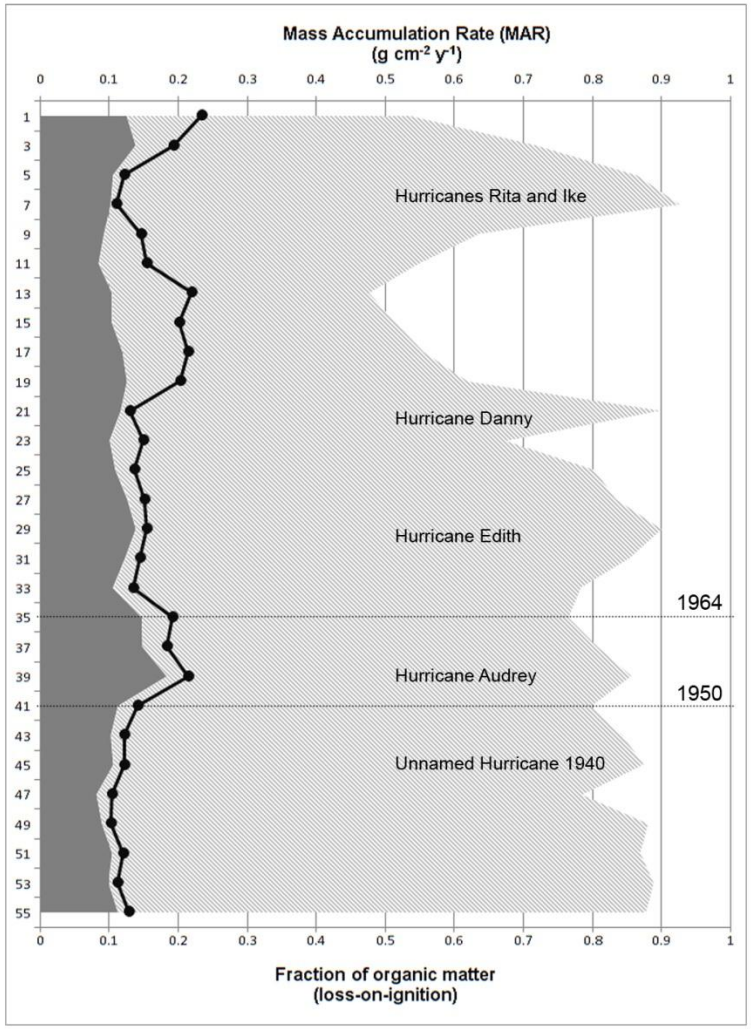

E

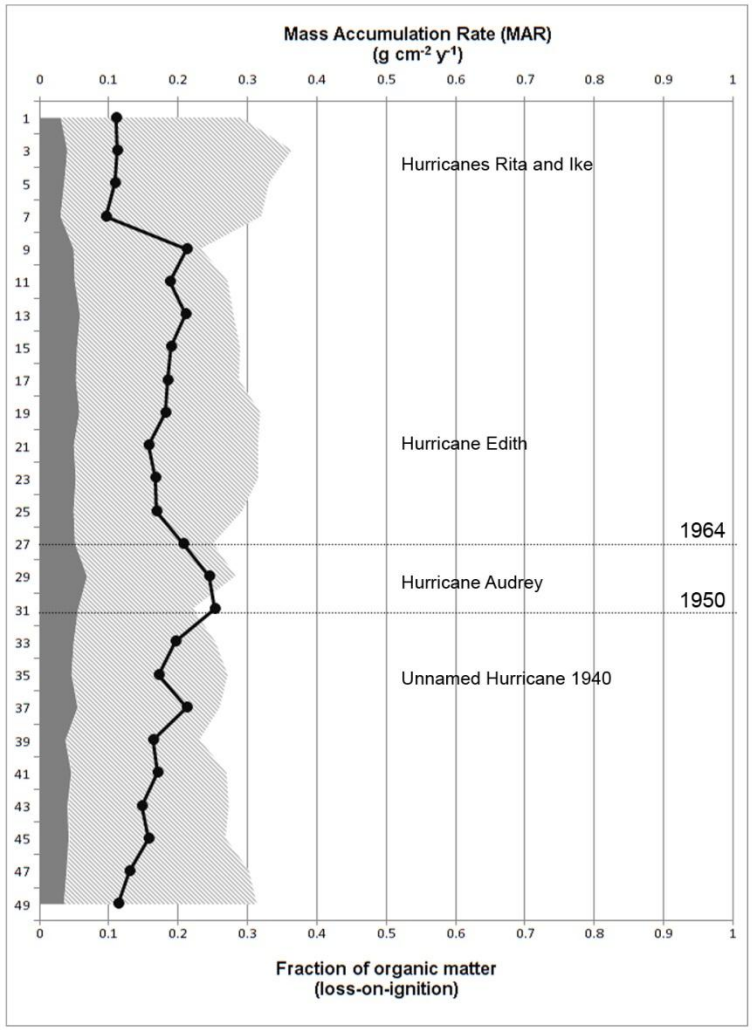

F

Figure 3-2. Continued.

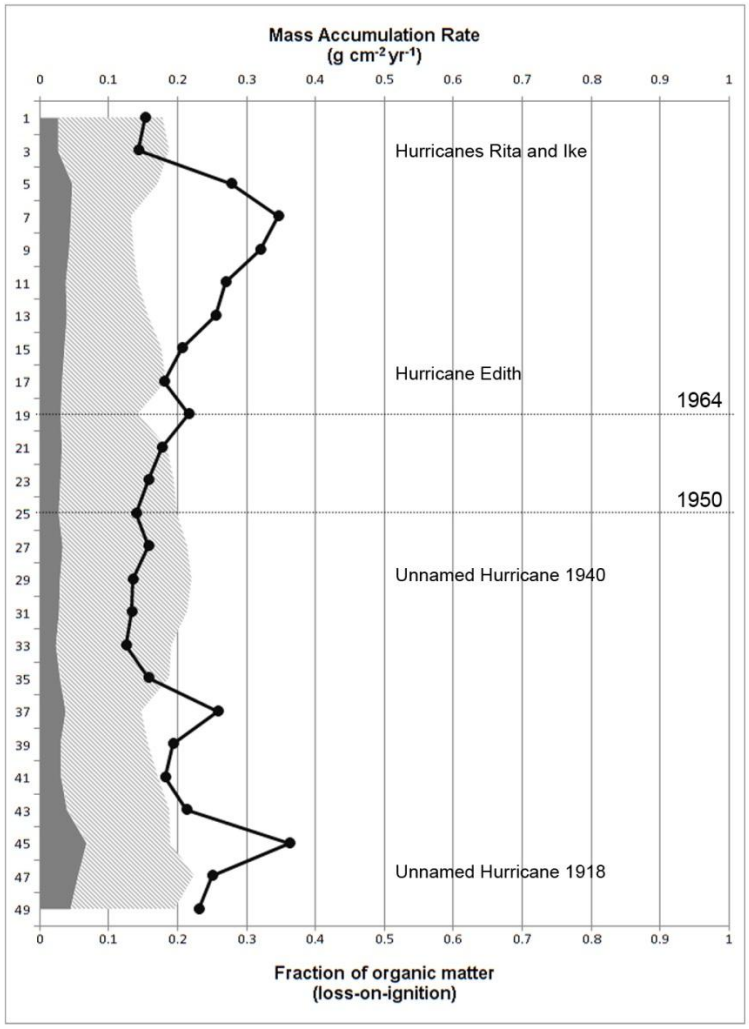

G

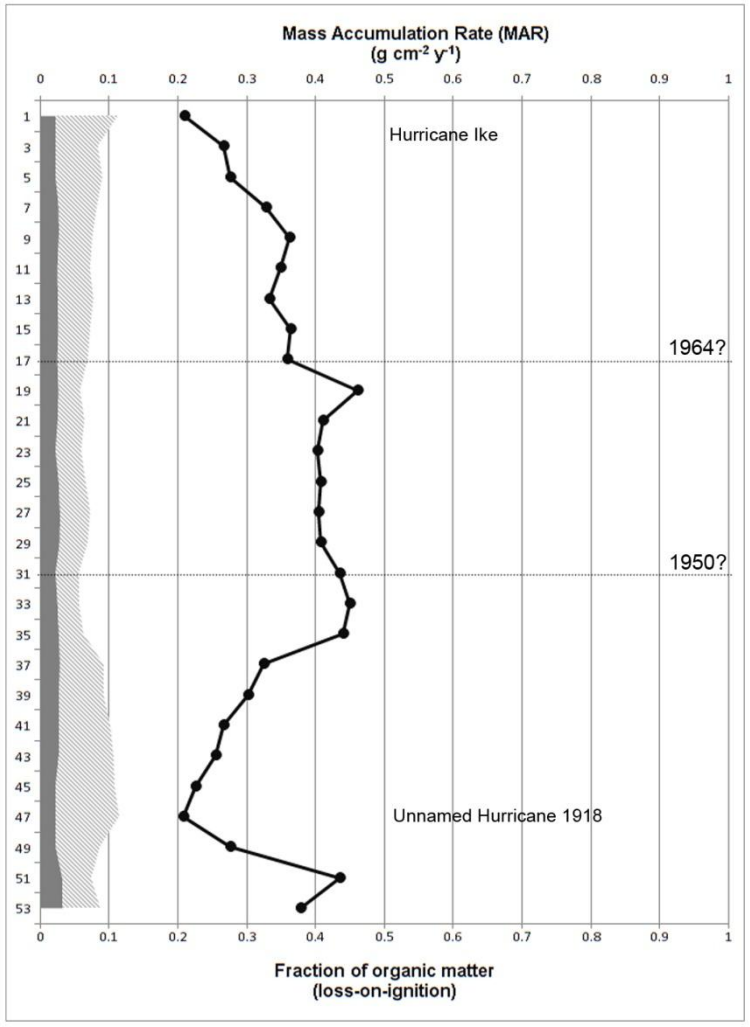

H

Figure 3-2. Continued.

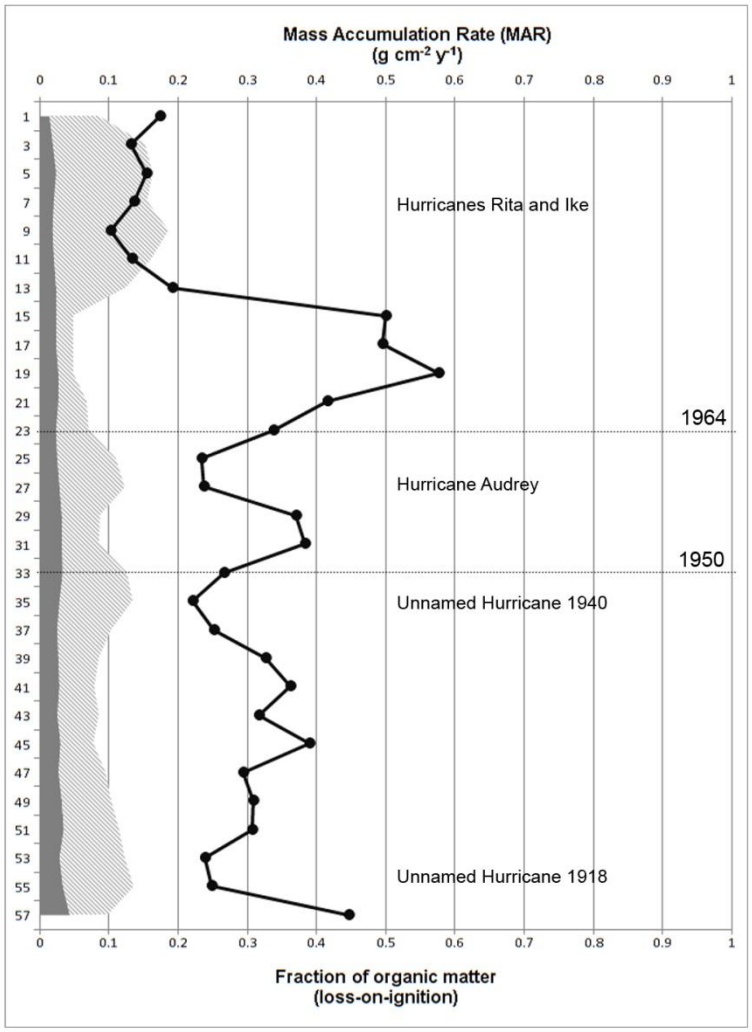

I

Figure 3-2. Continued.

CHAPTER 4
DIATOM ASSEMBLAGES OF THE CHENIER PLAIN, LOUISIANA: DEVELOPING DIATOM-BASED INFERENCES OF ENVIRONMENTAL CHANGE

Background

Diatoms are an excellent indicator of environmental conditions because they are sensitive to the water chemistry in which they live and respond rapidly to change (Battarbee, 1986). They are often used as a proxy for environmental change because they are influenced by environmental processes in predictable ways and their siliceous frustule is generally well-preserved in the sedimentary record (Sherrod, 1999). In coastal marshes, diatoms have been used to reconstruct salinity (Fritz et al., 1991; Parsons et al., 1999a; Sherrod, 1999; Wachnicka et al., 2010), relative sea level (Gehrels et al., 2001; Horton et al., 2006; Sherrod, 1999; Szkornik et al., 2006; Zong, 1997), and extreme events, such as hurricanes or tsunamis (Hayward et al., 2004; Hemphill-Haley, 1995; Parsons, 1998; Zong et al., 2003). Reconstructions using diatom microfossils are valuable because they provide a record of coastal change that goes beyond more recent instrumental records; this is particularly true for sea level histories, since much of the modern record is only several decades in length and long-term trends may not be evident.

The successful application of environmental reconstruction using diatoms requires knowledge of the relationships between diatom taxa and environmental parameters. The influence of salinity on marine-littoral diatom species is widely accepted (Palmer and Abbott, 1986) and many early diatomists took to classifying species into halophilic groups (e.g. Kolbe, 1927; Patrick and Reimer, 1966a, b; van der Werff and Huls, 1957-1974; Van Heurck, 1896). Early diatom reconstructions involved the determinations of sea-level transgressions/regressions based on the proportions of

sensitive fresh, brackish, and marine species (Palmer and Abbott, 1986). Due to the expansion of microcomputers and statistical programs, a more quantitative process was developed using multivariate statistics that examines diatom composition in surficial sediments, which represent recent sediment deposition, against measured environmental variables. Gradient analysis provides the statistical tools for examining species response to measured environmental variables and determine the strength of the relationship (Legendre and Legendre, 1998). For the variables that show strong relationships to species composition, transfer functions provide the inference of environmental values from fossil samples (Sachs et al., 1977). A transfer function is a multivariate technique where modern assemblages and their environmental preferences (modern analogue) are correlated with fossil assemblages to reconstruct the past environment or climate.

The appeal of diatoms for sea-level reconstructions is due to their sensitivity to water parameters, such as salinity and flooding duration, which are influenced by marsh height in relation to the tidal frame, as well as freshwater discharge to the coast. The work of many authors indicates a strong vertical zonation of diatom species distribution, and diatoms have aided in the reconstruction of sea-level histories for numerous locations throughout the world (Gehrels et al., 2001; Hayward et al., 2004; Horton et al., 2006; Horton et al., 2007; Patterson et al., 2000; Shennan et al., 1995; Szkornik et al., 2006; Zong, 1997; Zong and Tooley, 1996). Studies of diatoms and their relation to elevation or tidal range for the coastal wetlands of the northern Gulf of Mexico have not yet been conducted. Therefore, diatom distributions for the coastal wetlands of the Chenier plain, Louisiana were examined with regards to their distribution in relation to

tidal frame, vegetation, and sedimentary characteristics. In this study, tidal frame for each sample site was identified by measuring marsh surface elevation and average water level height in relation to a vertical datum (North American Vertical Datum 1988).

Knowledge of sea-level history is particularly important in coastal areas like Louisiana, where the rapid deterioration of coastal wetlands has been attributed to decreased marsh-elevation and salinization (Boesch et al., 1994). Marsh elevation is influenced by many factors including subsidence and vertical accretion. Vertical accretion is influenced by inundation frequency and sedimentation. Theoretically, the process of vertical accretion is a negative feedback loop, where accretion of sediment causes an increase in elevation; an increase in elevation causes a reduction in flood frequency; and reduction in flood frequency reduces sedimentation (Pethick, 1981). Vegetation also influences vertical accretion through trapping of suspended sediments (Boorman et al., 1998) and production and trapping of organic matter (Nyman et al., 1990). Over time, if vertical accretion is less than sea level rise and subsidence, flood frequency can increase above the plant tolerance, causing vegetation dieback and marsh collapse (DeLaune et al., 1994).

The primary goal of this study was to determine if the diatom species assemblage was correlated with the sea-level parameters, elevation and water level, to determine if diatom microfossils can be used as a paleo-indicator of sea level. It was also desirable to test the correlation of these parameters independent of salinity, since salinity is a well-accepted predictor of diatom species distribution. Previous work on this topic often collected samples along transects placed along an elevation gradient. Samples collected in this method could be subject to spatial autocorrelation due to their

close proximity (Telford and Birks, 2005; Telford et al., 2004) and collinearity with salinity, a known predictor of diatom distributions. Spatial autocorrelation is the spatial dependence of an organism to the underlying environmental condition that is spatially structured or due to community or demographic processes (e.g. dispersal) (Legendre, 1993). Using cross-validation, the predictive power of the transfer function can be over-optimistic and lead to unrealistic estimates of reconstruction error if spatial autocorrelation is present in the data set (Telford and Birks, 2005). Also, at a local level, elevation and water level may be correlated with salinity since tidal-flushing and freshwater flow parameters tend to vary with elevation (i.e. higher elevations receive more freshwater runoff and less tidal flushing, and vice versa). However, at a regional scale, sites with similar elevation from widely different locations are more likely to vary in their salinity fluctuations because of physiographic differences in freshwater and tidal flooding sources. Therefore, at the regional scale, it may be possible to disentangle tidal influences from salinity by sampling sites with similar elevations, but differing salinity. Salinity, water level, and marsh flooding estimates are likely to reflect the complex interaction of fresh and tidal fluctuations.

Samples sites for the modern calibration data were located randomly over a large geographic area (approximately 5000 km^2) creating a regional training data set (also called a calibration data set). Sites were first stratified by salinity and sites were randomly selected from each stratum. This sample design was preferred for four reasons: 1) it reduces the chance of spatial autocorrelation, a potential statistical problem for samples collected along transects (Telford and Birks, 2005), 2) it was desirable to separate the effects of salinity, a known predictor of diatom species, and

the sea-level parameters of interest, elevation and water level, 3) a transfer function developed from a broad regional training provides a more realistic analogue for fossil data (Gehrels et al., 2001) and can have greater applicability to studies throughout the coastal plain.

Regional Setting

The Louisiana coastal zone can be divided into two basic geomorphic zones: the Mississippi delta plain on the southeast coast and the Chenier plain of the southwest with the dividing line located near Vermillion Bay (29°43'11" N, 91°58'34" W). The Chenier plain extends from Vermillion Bay to the Texas state border and includes over 6,000 km^2 of coastal marshes. It was formed by the deposits of fine-grained sediments of the Mississippi River during the Middle to Late Holocene. A series of regressive-transgressive phases created relict beach ridges (called 'cheniers') within a 30-km wide coastal plain of low-energy fresh, brackish, and saline marshes (McBride et al., 2007). The cheniers act as barriers, reducing tidal flow to some areas of the marsh. The sediments are largely fine-grained silts and clays, with large amounts of organics and peat. Vegetation follows a general north-south salinity gradient of saline to brackish to fresh marsh. Visser et al. (2000) identified seven marsh types within the three salinity zones, with half of the marsh types being classified as oligohaline. The marsh types include: fresh maidencane, fresh bulltongue, oligohaline bullwhip, oligohaline paspalum, oligohaline wiregrass, mesohaline wiregrass, and mesohaline mixture. Although vegetation species cover is more commonly used to classify marsh types, salinity of fresh marsh is less than 1‰, oligohaline is 1 to 5‰, and mesohaline is 5 to 23‰. The marshes of the Chenier plain are not experiencing as high wetland loss as the Mississippi delta plain (Barras et al., 2003; Barras et al., 1994; Britsch and Dunbar,

1993), however these microtidal marshes receive limited sedimentation and wetland loss rates are increasing, mostly due to subsidence, erosion, and human alterations to hydrology.

Methods

All samples were collected from a network of permanent wetland monitoring stations located throughout coastal Louisiana called the Coastwide Reference and Monitoring Stations (CRMS) (Folse et al., 2008, revised 2012; Steyer, 2010). CRMS was designed to monitor coastal habitats in Louisiana and evaluate the effectiveness of wetland restoration strategies. The stations are maintained as a joint partnership by the U.S. Geological Survey (USGS) and Louisiana Department of Natural Resources (LDNR). The CRMS design implements a multiple reference approach by collecting systematic data on hydrology, vegetation, and sediments. Three hundred sites were randomly selected from a gridwork of over six thousand locations evenly distributed across the entire coast (Chabreck and Linscombe, 1997); 108 of these sites are located in the Chenier plain. The sites were selected by using vegetation type as allocation strata to ensure that all major vegetation types were represented (Steyer et al., 2003). For this initial study, 46 of the 108 sites from the Chenier plain were selected for diatom analyses by stratifying the sites into five groups by elevation and randomly selecting 10 sites from each elevation group (4 sites were dropped due to difficulty in sampling or extremely low diatom counts). The goal was to have the range of salinity and elevation gradients present within the region (Figure 4-1). Elevation for all CRMS located in the Chenier plain was plotted, grouped into three equal elevation classes, and sites randomly selected from each class. Sites were classified into salinity-vegetation classes as described by Visser et al. (2000) using CRMS salinity and vegetation transect data to

verify that stations from all classes were included (see Regional Setting for description of classes). If sampling a selected station was not possible (such as due to restricted access during hunting season) another site with similar classification was supplemented whenever possible.

At each site, sediment samples provided the present-day record of diatom assemblage. One sample was collected at each site during the winter of 2010 (October 2009 through February 2010) by pushing a 10-cm diameter polyvinyl carbonate cylinder into the sediment and removing the top 0-2 cm surface by extrusion. There was no attempt to separate autochothonous and allochthonous diatoms, and the assemblage also contains diatoms living at the time of sample collection. However, the samples would accurately correspond to diatom assemblages found deeper within the sediment for paleo-reconstructions providing a sufficient analogue and diatoms show a high degree of site fidelity (Hassan et al., 2008). All samples were stored in leak-proof containers, treated with isopropyl alcohol and placed on ice immediately to preserve the sample and reduce the chance of bacteria growth during transport, and remained refrigerated until processed in the lab.

Diatom Analysis

Samples were processed using standard techniques to obtain density estimates of diatom species (Battarbee, 1986; Patrick and Reimer, 1966a). Sediment was homogenized; 0.5 ml was placed in a 1000 mL beaker and digested using 30% hydrogen peroxide. Since wetland samples contained a significant amount of organics, a very small addition of potassium dichromate was added to increase digestion (van der Werff, 1956). Undigested organics (large roots or stems) were removed using a 1-mm sieve. Due to the high concentration of fine-grained sediments that could impede diatom

counting, fine-grained sediments were removed by adding a sodium hexametaphosphate solution to disperse and deflocculate clays, followed by repeated washing of distilled water until the supernatant was clear (Hinchey and Green, 1994). A known volume of the cleaned diatom solution was placed into settling trays containing four slide cover slips and allowed to evaporate (Battarbee, 1973). Cover slips were mounted to slides using Zrax, a high refractive index (R.I. ~ 1.7+) mounting medium. A minimum of 300 diatoms were counted under 1000x magnification using a Nikon Optiphot light microscope. For two sites, diatom densities were extremely low and the entire slide was counted.

Environmental Variables

Data for hydrology, elevation, vertical accretion, and vegetation characteristics were summarized from the CRMS database (Steyer, 2010). Highly-accurate estimates of marsh elevation were obtained for each site using a Trimble 5700 RTK base station and Trimble 5800 rover unit. The RTK base station was placed over secondary monuments to transmit real-time corrections to the rover unit. Data were downloaded and processed using Timble Geomatics Office software. At each site, salinity and water level data were measured at 15-minute increments using a data sonde (i.e. InSitu Aquatroll 200; data sonde models vary by site, but must meet defined data standards; Folse et al., 2008, revised 2012). Hydrologic data were summarized for mean, standard deviation, minimum and maximum values.

Water level gauges were vertically surveyed relative to the top of a rod-surface elevation table (RSET) to NAVD88 (Cahoon et al., 2002). Water level was measured as the height of the water relative to North America Vertical Datum 1988 (NAVD88). The RSET makes it possible to partition change in sediment elevation over shallower and

deeper depths of the sediment profile. RSET data were used to estimate change in sediment elevation by calculating the linear slope of multiple sequential elevation measurements. Vertical accretion was determined from repeated measurements of feldspar marker horizons (Cahoon and Turner, 1989; DeLaune et al., 1983), which measures actual sediment deposited on the marsh surface. When feldspar markers are combined with RSET data, the relative component of marsh change attributable to vertical accretion versus compaction or subsidence can be determined.

Vegetation data were compiled by estimating species cover for ten 4-m^2 quadrats located along a 288-meter vegetation transect (Cretini et al., 2011; Folse et al., 2008, revised 2012). Data were summarized as total vegetation cover and primary species cover.

Sediment samples collected at each site were analyzed in the lab for grain-size, bulk density, and organic carbon. Bulk density was measured using the dried weight of a known wet volume (30 cm^3). Total organic carbon was determined by loss-on-ignition (LOI) (Dean, 1974; Moore and Reynolds, 1989). Grain size attributes were obtained using a Beckman Coulter *LS 200* particle-size analyzer. The Coulter uses laser diffraction to measure the size distribution of sedimentary particles between 0.4 - 2000 µm. Three subsamples were measured at minimum three times for a total of nine or more estimates (additional estimates were made if plotted distributions varied significantly from each other). Sediment size distribution were summarized into grain size constituents (mean grain size, standard deviation, percent clay, percent silt, and percent sand) using the Folk and Ward method (Folk, 1974) by the program GRADISTAT (Version 8; Blott and Pye, 2001).

Statistical Analyses

The relationship between diatom species assemblages and environmental constraints was explored using both direct and indirect gradient analysis techniques. Statistical analyses generally follow procedures described by ter Braak (1995a, b), Legendre and Legendre (1998), and Borcard et al. (2011) and were undertaken using the package “vegan” in R (Oksanen, 2011b). Environmental variables were first examined for multicollinearity using Pearson correlation coefficients with asymptotic *p*-values. Collinearity is common with ecological data and, although it may not produce a problem for ordination analyses, it can hinder the interpretation of results because it is difficult to ascertain the independent effects of each variable. In addition, variance inflation is a diagnostic tool to identify useless constraints; therefore, variance inflation factors (VIF) were calculated to determine if variables included in the final models were not unduly influenced by collinearity.

Ordination statistics can be applied to multivariate environmental data in order to examine the relationships of ecological communities to environmental parameters. They are commonly divided into two categories: indirect and direct gradient analysis. Indirect gradient analysis (also called an unconstrained ordination) uses only the species data, displaying gradients between species regardless of the measured environmental data. The ordination axes can be considered hypothetical environmental variables. Direct gradient analysis (also called a constrained ordination) utilizes environmental data in addition to the species data, permitting the test of a null hypothesis that species composition is unrelated to the measured variables. Vectors of environmental variables can be fitted onto an unconstrained ordination. The result is similar to a constrained ordination; however, since species data are not directly related to the environmental

variables, the expressed gradients are not limited to the measured variables. Performing indirect gradient analysis prior to direct analyses can improve the interpretation of results since it is possible that the most important gradients are not measured.

Two indirect gradient analysis methods were examined for species relationships to environmental gradients: Principal Components Analysis (PCA) and Multidimensional Scaling (MDS). PCA is an eigenvalue-based method where the maximum variance is projected along principle axes. The eigenvalue is a measure of the amount of variation along an axis and the rank of the axis; the eigenvectors are the sample scores. The eigenvector with the highest eigenvalue is the indicator of greatest variation and the principle component. The result demonstrates the relationship of species and sites projected along their most influential gradients. MDS is a distance-based ordination technique that uses a distance metric with the purpose of providing a visual representation of the similarities or differences among a set of samples (Shepard, 1962). While highly sensitive to the chosen distance metric, it is well-published with ecological data and regarded as a useful tool for examining site or species similarities or dissimilarities. MDS with two dimensions was performed using the Bray-Curtis dissimilarity index (Bray and Curtis, 1957). The Bray-Curtis index is useful in detecting underlying ecological gradients (Faith et al., 1987). MDS produces a plot that is useful for examining species and site similarities and differences. Sites or species that are more similar will be closer together, whereas sites and species that are dissimilar will be further apart. The exact distances are more arbitrary, but the proximity or general “clumping” is meaningful.

Two direct gradient analysis techniques were employed: Redundancy Analysis (RDA) and Canonical Correspondence Analysis (CCA). Both are examples of canonical ordination which explores the relationships between two matrices: a response matrix (species data) and an explanatory matrix (environmental data). RDA is a constrained form of PCA; CCA is a constrained form of Correspondence Analysis (CA). Each technique has its own advantages and possible disadvantages; however, the subject of when it is best to use one over the other has not been settled. CCA is most appropriate for unimodal species responses and "long gradients" (i.e. species are sampled along their entire ecological range). However, these two conditions are difficult to test formally and the latter "rule" has not been rigorously tested or statistically justified (Oksanen, 2011a). However, "gradient length" (which is more a measure of species turnover than a measure of the sampled gradient) can be examined through a detrended correspondence analysis (DCA) (Hill and Gauch, 1980; Stevenson et al., 1996). Since RDA is a linear method, variance partitioning is possible and the interpretation of eigenvalues is more straightforward since the variance is a true variance, whereas in CCA the "variance" is derived from Chi-square and is termed "inertia". In addition, CCA focuses on species relative abundance and will therefore not detect a gradient along which all species are positively correlated with environmental variables (ter Braak and Šmilauer, 1998). For these reasons, it is prudent to examine and draw conclusions after performing both ordination methods.

RDA measures the influence of environmental variables on the variance of species assemblage data (Legendre and Anderson, 1999). Since RDA is sensitive to zero values, diatom data were Hellinger transformed, which minimizes the effect of zero

values common to abundance data (Legendre and Gallagher, 2001). Using partial RDA (pRDA) and variance partitioning, we can advance our understanding of the influence of each environmental variable (such as, water level), taking into account the influence of other variables (salinity, bulk density, and LOI) (Borcard et al., 2011; ter Braak and Šmilauer, 1998). In essence, pRDA removes the effect of the conditioning variables providing information on the independent effects of the chosen explanatory variable. The null value that no relationship exists between matrices and species patterns was conducted using Monte Carlo permutation tests with 1000 random permutations. The Monte Carlo test indicates whether the observed ordination is stronger than expected due to chance (Barnard, 1963; Besag and Diggle, 1977). Reported R^2 values for RDA were adjusted using Ezekiel's formula, since R^2 is influenced by the number of variables (Ezekiel, 1941). There is no adjusted R^2 in CCA, therefore unadjusted values were reported. Stepwise model building using forward selection was used to identify the most parsimonious model and identify significant environmental variables for further analysis in reduced models.

Bi-plots of RDA results provide graphical illustrations of species-environment and sample-environment relationships. In the species–environment bi-plot, the position of species projected perpendicular to the environmental arrows approximate their weighted average optima along each environmental parameter and the location on the bi-plot demonstrates the variables with the greatest influence on their variation. The position of samples shows not only their relationship to the environmental variables, but also to the species, where more closely positioned species are likely to have greater

density within the sample. The angles between the environmental variables and species reflect their correlation.

Spatial autocorrelation is a common problem for microfossil-sea-level studies, particularly where samples are collected along transects, because statistical tests like regression analyses assume independent measures of abundance, or that each new observations brings with it one full degree of freedom. However, if individuals of one site are found in the other site due to proximity, either due to species moving between sites or the influence of an underlying habitat variable, abundance measurements are spatially dependent. Spatial autocorrelation can result in overly optimistic estimates and inappropriate model choice (Legendre and Fortin, 1989; Telford and Birks, 2005). A multi-scale ordination (MSO) was conducted to test for spatial autocorrelation (Wagner, 2004). MSO partitions ordination results into distance classes and uses a variogram to check assumptions of stationarity and independence of residuals.

Results

Most sites were characterized as oligohaline (N = 27), with fewer mesohaline (N= 10) and fresh (N = 9) sites. Summary of site environmental characteristics is in Table 4-1. Elevation range was over 0.5 meter (-0.06 to 0.58 m NAVD88). Distance between sample sites ranged from 0.8 and 161 km (the closest and furthest pair-wise distance, respectively) and averaged 56 km. The sampled region covered an area of over 6,000 km^2.

Diatom assemblages

A total of 173 diatom taxa were identified from 46 surface sediment samples. Over 16,000 valves were counted. Total number of taxa per sample ranged from 22 to 70 species. Average diatom valve density was approximately 40,000 valves per gram of

sediment; however the range of valve density was very large, from 400 to over 300,000 valves per gram of sediment.

The diatom abundance was dominated by *Cyclotella meneghiniana*, *Nitzschia obtusa*, *Navicula tripunctata*, *Tryblionella granulata*, *Caloneis formosa,*and *Bacillaria paradoxa*, representing 32% of the total assemblage. *C. meneghiniana* was the only species found in all 47 samples and accounted for 7% of all counts. Twenty-seven species had a maximum abundance of less than 1%, however half of the total species were found in 10 or more sites.

Statistical Analysis

Pearson correlation coefficients are given in Table 4-2. Water level and elevation are positively correlated. In addition, a condition of multi-collinearity between salinity, bulk density, and LOI was identified. Variation inflation factors for the variables are low and do not suggest significant correlation (Table 4-3).

A two-dimensional MDS ordination plot is found in Figure 4-2. CRMS 1650, 1277, 565, 574 and 535 appear to be similar with indicator species in the genera *Eunotia*, *Pinnularia*, *Fustulia*, and *Gomphonema*. Plots of environmental variables reveal these sites are characterized by low salinity and low bulk density. The distinction between the remaining sites is less clear, however CRMS 564, 580, 589, 609, 610, 680, 685, and 1858 are more similar. These sites are characterized by high bulk density and moderate to high salinity values. The remaining sites have moderate to low bulk density values and moderate to high salinity.

A summary of PCA results can be found in Table 4-4. Several species show a strong response to the environmental gradients represented by axis 1, 2, and 3; these axes together account for 39% of the variation. As shown in Figure 4-3, environmental

gradients seem to influence species abundance. Numerous species have a strong correlation to gradients reflected by the axes. Species with high negative scores on axis 1 are largely freshwater species including *Nitzschia obtusa, N. nana*, *Eunotia minor*, *E. flexuosa* and *E. monodon*. Highly positive correlations are largely marine species, such as *Tryblionella granulata*, *Actinotypchus senarius*, several *Thalassiosira* species, and *Caloneis formosa*, supporting the indication by the PCA that axis 1 is strongly influenced by a salinity gradient. Water level and elevation are most strongly fitted to axis 2, suggesting species influence by a secondary environmental gradient. High positive scores for species along axis 2 include those for *Navicula tripuncta, Baccilaria paradoxa, Caloneis formsa*, and *Amphora coffeaeformis*. Species with a high negative score strongly associated with axis 2 include a mix of fresh and marine species, benthic and planktonic forms: *Eunotia minor, E. flexuosa, Coscinodiscus* spp., *Tryblionella granulata*, and *Actinoptychus senarius.*

RDA results clarified the influence of the measured variables (Table 4-5). The first axis explains 14% of the total variation in the diatom species data. Taken together, the first two axes explain about 20% of the total variation in the diatom data, and over 60% of the species-environment relationship. Monte Carlo permutations demonstrate the observed ordination is stronger than expected due to chance and is significant ($p < 0.005$). The eigenvalues for the first three axes are also significant, however the third axis is less significant (*p*-value = 0.015). Monte Carlo permutation tests on the full model identify the variables salinity, LOI, bulk density, and elevation as significant. Three variables were contributed significantly to the RDA first component: LOI ($r = -0.83$, p-value = 0.03), bulk density ($r = 0.78$, p-value = 0.01), and salinity ($r = 0.77$, p-value =

0.01). Elevation (r = -0.50, p-value = 0.03) was the only significant variable aligned with the RDA second component.

Forward step-wise selection procedure identified the term water level (which is correlated with elevation) in addition to salinity, bulk density, and LOI, as providing the most parsimonious model. Ezekiel's adjusted R^2 is influenced by the number of variables, so by removing extraneous variables, the adjusted constrained variation increases to 16%; and the first two axes explain over 80% of the total variation that could be explained by the measured environmental variables.

Partial RDA revealed that salinity has the greatest influence on diatom species variance, followed by water level, LOI, and bulk density (R_{adj} = 0.044, 0.017, 0.016, 0.015, respectively). Less than 2% of the species variance is explained by water level; however, there is minimal overlap (less than half a percent) with the other three variables. The influence of water level on diatom species variance is independent of the effects of salinity, bulk density, and LOI, whereas these three variables overlap in their influence on diatom species.

Bi-plots of RDA results are found in Figure 4-4. In order to simplify the diagram, environmental variables in the bi-plots were reduced to include only the most parsimonious model as identified by forward selection procedures. Salinity and bulk density align closely with RDA axis 1. Axis 2 is most strongly represented by salinity and water level. Diatom species closely aligned with positive water level were planktonic forms in the genera *Actinoptychus*, *Cyclotella*, *Coscinodiscus*, *Thalassiosira*, and *Schionodiscus*. Genera strongly associated with negative water level include *Amphora*,

Caloneis, *Mastogloia*, and *Tryblionella*. It is also clear from the species bi-plot that many diatom species are not linked strongly toward the measured environmental variables.

CCA results were similar to RDA (Table 4-7). The unadjusted explained inertia is 34%. The first three canonical axes are significant. LOI, salinity, and bulk density are explained by axis 1. For axis 2, water level and elevation are the strongest components. Salinity, LOI and elevation explain the greatest proportion of inertia for axis 3. LOI, salinity, water level, and bulk density gave the most parsimonious model by the automatic stepwise procedure. The reduced model explains 21% of the total inertia, however this number is unadjusted and would therefore be higher if a method existed for its adjustment (Borcard et al., 2011). Axis 1 explains 59% of the total inertia of the measured variables, and axis 2 accounts for another 25%.

Bi-plots of CCA results provide additional information regarding species, samples and their environmental constraints (Figure 4-5). A bi-plot of samples and environmental constraints shows three well-defined groups, one linked to high salinity and low water level (CRMS 1738, 644, 614), a second group linked to high salinity and high water level (CRMS 1858, 589, 610, 685, 680), and a third linked to high organic matter (high LOI, low salinity) and high water level (CRMS 574, 1277, 565). The analyzed group of sites appears to be missing locations that have low salinity and low water levels. A large number of species are not strongly influenced by the measured parameters; however several species do exhibit strong affinities for certain environments. Diatom species that appear linked to the low salinity, high water level include *Brachysira vitrea, Pinnularia stomataphora*, *Stauroneis pachycephala*. Numerous high salinity, high water level species can be identified, including *Hyalodiscus* sp., *Frustulia weinholdii*, *Suriella*

gemmata, and several *Navicula* species. Species linked to high salinity and low water levels include *Petroneis marina*, several species of *Nitzschia*, and *Mastogloia braunii*.

Multiscale ordination (MSO) plot can be seen in Figure 4-6. Species-environment correlations do not vary with scale (the explained plus residual values remain within the confidence interval envelope) and samples closer than 3 km (distance interval 1) have a significant spatial autocorrelation. It should be noted that since samples were collected over a large geographic area, few sites were closer than 3 km, therefore this distance interval (0 to 3 km) had fewer representatives (14 of a total 1035 pair-wise combinations) compared to other distance classes.

Discussion

Diatom reconstructions of salinity are possible using diatom species data obtained from randomly distributed samples collected over a large geographic area. Salinity, bulk density, LOI, water level were identified by both gradient analysis techniques as significant and providing the most parsimonious model. Elevation was also found to be significant, but was removed during the forward selection procedure, likely due to its high correlation with water level. Water level was an absolute measurement, in that it was calculated based on average water level height in reference to a vertical datum and not relative to the marsh surface. Interestingly, the water level and elevation correlation was positive, indicating higher marsh elevations with higher mean water level. Several high elevation, high water-level sites were located near the Gulf of Mexico and were also high in salinity, likely due to regular inundation of tides and high mineral sedimentation rates. The three variables salinity, bulk density, and LOI were also significantly correlated (high salinity = high bulk density = low LOI), making it difficult to separate the effects of any one variable. Variance partitioning shows that a

very strong overlap exists between LOI, bulk density, and salinity. This is not altogether surprising given the influence of salinity on vegetation growth (Mendelssohn and Morris, 2002), and the influence of vegetation on both sedimentation (Stumpf, 1983) and organic matter production in soils (Nyman et al., 1990; Nyman et al., 1993). On the other hand, water level was largely independent of the other three variables. The significant independent tests of water level and elevation suggests it is possible to develop a statistically significant diatom-based transfer function for sea-level reconstructions. However, due to the high number of species which were not influenced by water level or salinity and the minimal representation of sites at low water-levels, additional samples sites would be required.

The correlation between diatom assemblage and water level was not as strong as reported in similar transect-based studies. However, none of these studies tested for spatial autocorrelation. Spatial autocorrelation is a potential problem for training data collected along transects because ordination procedures assume independence. These analyses indicate that samples obtained from distances less than 3 km may have spatially autocorrelated residuals, which would be a problem for transect-based methods using cross-validation to evaluate models and estimate reconstruction error since estimates would be over-optimistic. Since very few samples in this study were collected closer than 3 km, the study design does not allow the test of shorter distances and the actual sample distance where spatial autocorrelation is a problem may be shorter. In addition to the MSO method used here (Wagner, 2004), Telford and Birks (2005) proposed a method to investigate the influence of spatial autocorrelation. The process involves deleting samples at random to test the influence on R^2 during cross

validation versus deleting samples based on their geographic distance or environmental similarity. The MSO procedure performed in this study provides a similar indication of spatial autocorrelation, so this additional analysis was not conducted. Horton and Sawai (2010) performed this test on surface sediment samples collected from an estuary in China. Results indicate a divergence in R^2 values for distances greater than 20 km. Spatial autocorrelation of diatom data in an estuary is likely very different than in a salt marsh because of differences in the spatial structure. The response of diatoms to the spatial extent of ecological processes may be important to determining the underlying species-environmental relationships (de Knegt et al., 2009). The ecological scale of diatom communities is an important consideration and deserves some much needed attention. Although spatial autocorrelation in transfer functions is seen as problematic, the implied structure of the residuals might provide information about processes not captured by the current model. Additional samples with varying spatial distances, located at closer distances than the current sampling scheme, would be required to isolate the effect of spatial scale on species-environment relationships.

Training data collected using randomly located sample sites may be preferred for future sea-level paleoenvironmental analyses. However, these analyses may require a larger sample size than was used here in order to take full advantage of regional species diversity. The species-environment ordination plots show a large number of species clumped toward the center of the diagram, indicating a significant number of species that either: 1) were not influenced by the measured environmental variables (species are indifferent to the measured environmental variables), or 2) were not sampled enough in the current design to distinguish the full extent of their environmental

tolerances. Since over half of the diatom species were found in 10 or more samples, there appears to be a consistent regional flora, but there are also a number of species that are locally specific. This premise is consistent with the general observation that, despite the large diversity in diatom species, there is some consistency in marine-littoral diatom species throughout the world; however, geographically limited species are also present (Witkowski et al., 2000). Ordination plots of samples indicate that sites representing low water level and high salinity may be lacking in the current design. Regional sampling schemes may require more sampling than transect-based studies in order to cover the full gradient of environmental parameters and include enough samples to identify species tolerances.

Despite the limitations, diatom-based reconstructions from a regional training set can provide a powerful tool for examining sea-level change because diatom species respond to salinity and an increase in salinity may be an identifying characteristic of sea-level rise. Salinity influences numerous aspects of coastal marsh ecology which in turn influence marsh elevation. Paleo-reconstructions that examine wetland salinity can provide significant clues on the impacts of sea-level rise, as well as other climate and anthropogenic events. Comparing the results of reconstructions for marsh locations that have recently submerged to sites that are stable may shed light on the mechanism of wetland submergence. In addition, this study demonstrates that diatom species are also influenced by water level.

Though this data set does not provide enough sample variation to adequately reflect the full tolerance of diatom species, it does indicate that planktonic forms are indicative of high water levels. Additional samples from low water-level and high salinity

marsh locations will likely provide a more robust analogue for variations in water level and salinity. The transfer function technique takes the knowledge provided by studies on modern distributions and species preferences and translates that into quantitative estimates of environmental variables from fossil species data. A transfer function created from a regional calibration data set will increase its applicability to more locations by ensuring that species within the fossil data set is well represented in the calibration data set. The transfer function can then be more widely applicable to sites throughout the Chenier plain in providing reconstructions of past sea level.

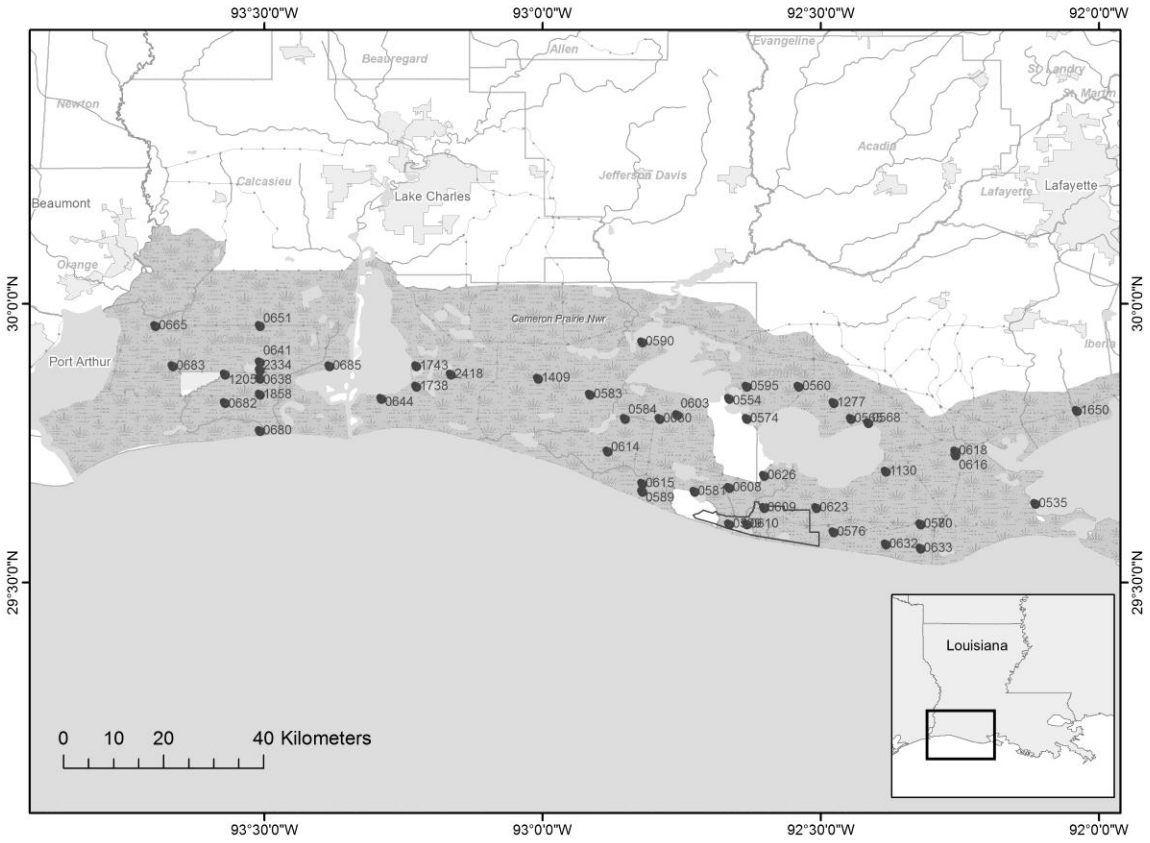

Figure 4-1. Locations of sediment samples collected in the coastal marsh of southwest Louisiana.

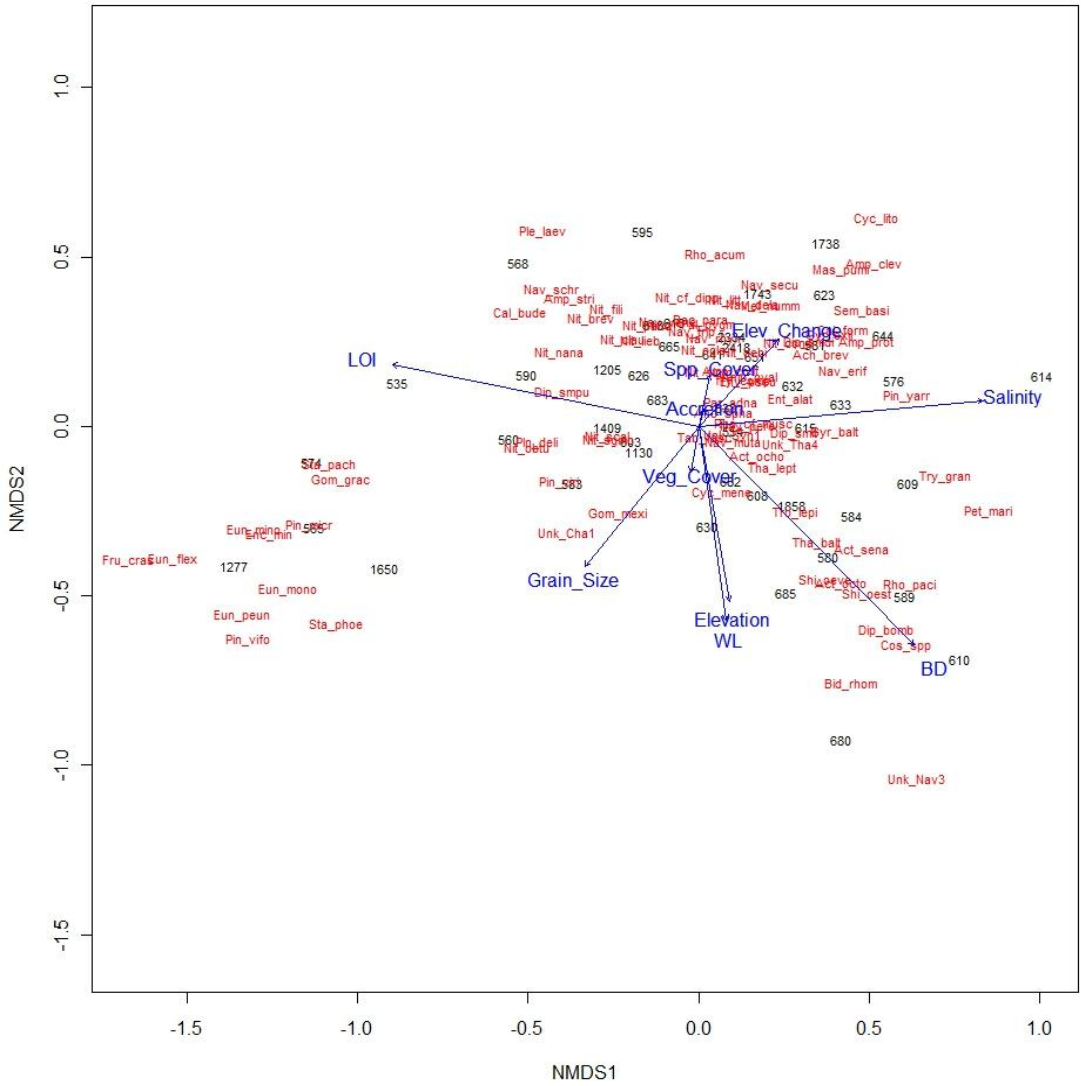

Figure 4-2. Multidimensional scaling (MDS) plot of diatom species assemblage data using the Bray-Curtis dissimilarity measure (Bray and Curtis, 1957). Environmental variables are fitted to the ordination axis to reveal their corrresponding relationship to sites and species (Appendix).

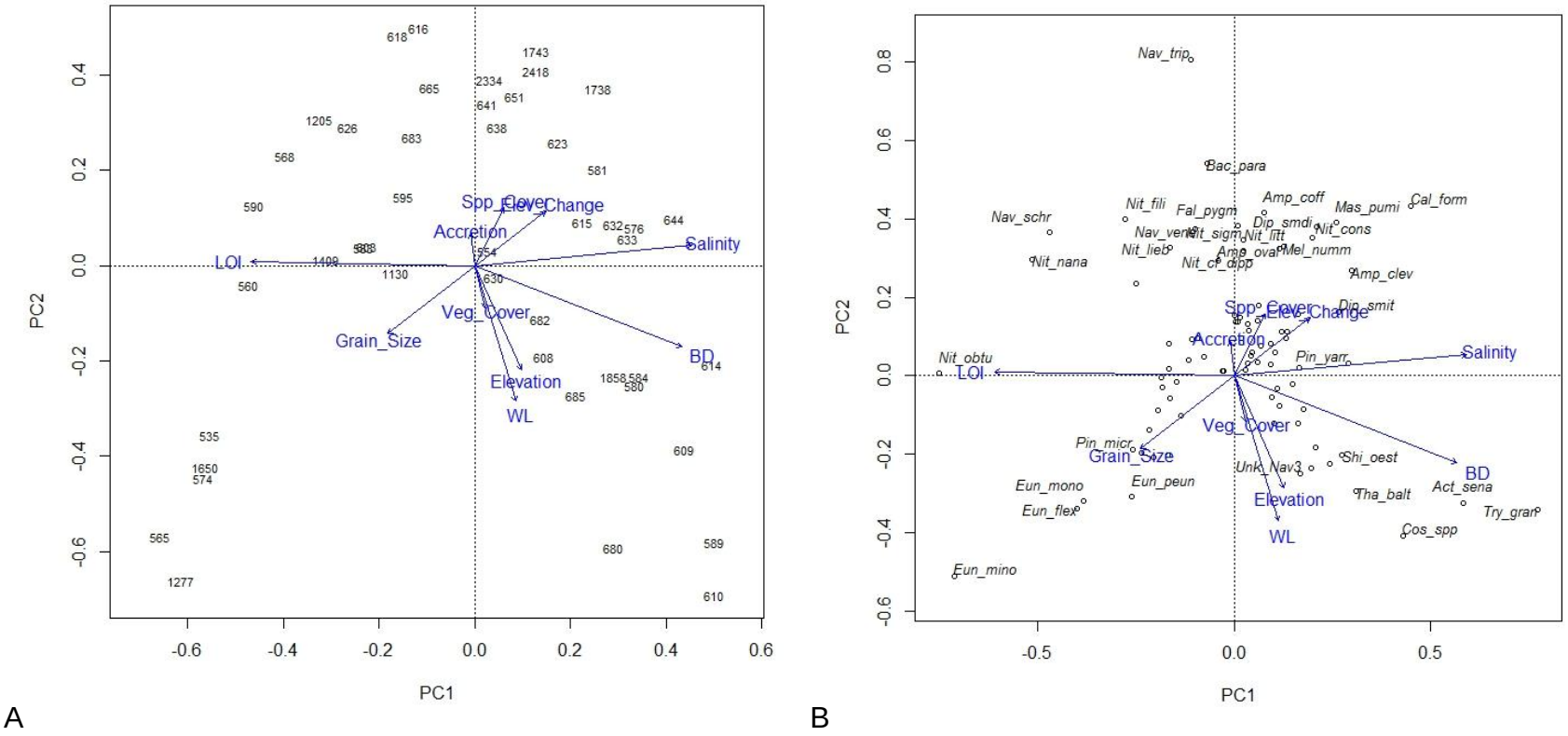

A B

Figure 4-3. PCA results of Hellinger-transformed diatom assemblage. Environmental variables are fitted to the ordination axis to reveal their corrresponding relationship to sites and species. Environmental variables for both figures include loss-on-ignition (LOI), total vegetation cover (Veg_Cover), primary species cover (Spp_Cov), salinity, elevation change (Elev_Change), vertical accretion (Accretion), bulk density (BD), elevation, water level (WL), and grain size (Grain_Size). A) Correlation bi-plot and sample scores: the eigenvectors are scaled to square root of their eigenvalue. B) Distance bi-plot and species scores: the eigenvectors are scaled to unit length.

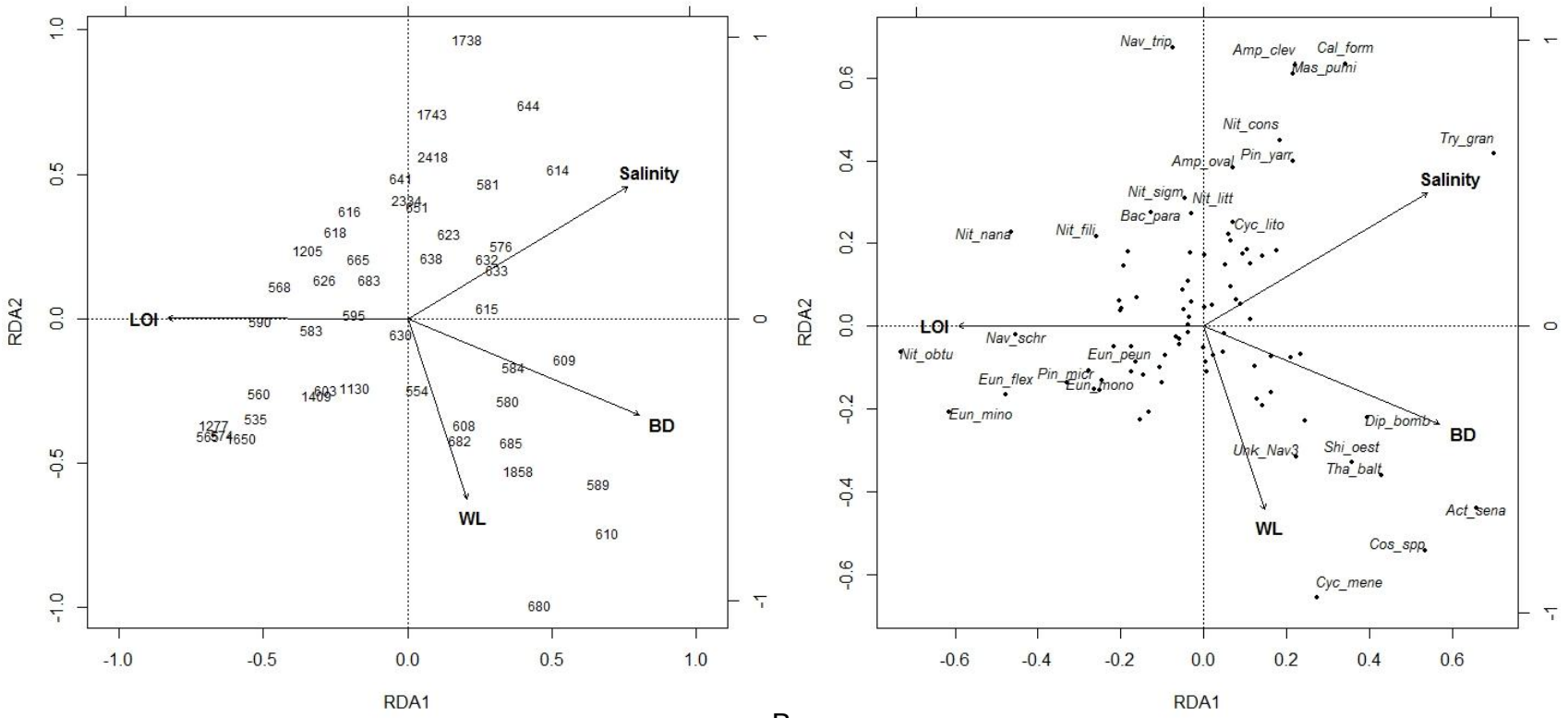

A B

Figure 4-4. RDA bi-plots of Hellinger-transformed diatom abundance data constrained by the forward-selected environmental variables water level (WL), salinity, bulk density (BD) and loss-on-ignition (LOI). A) Correlation bi-plot and sample scores: the eigenvectors are scaled to square root of their eigenvalue. B) Distance bi-plot and species scores: the eigenvectors are scaled to unit length.

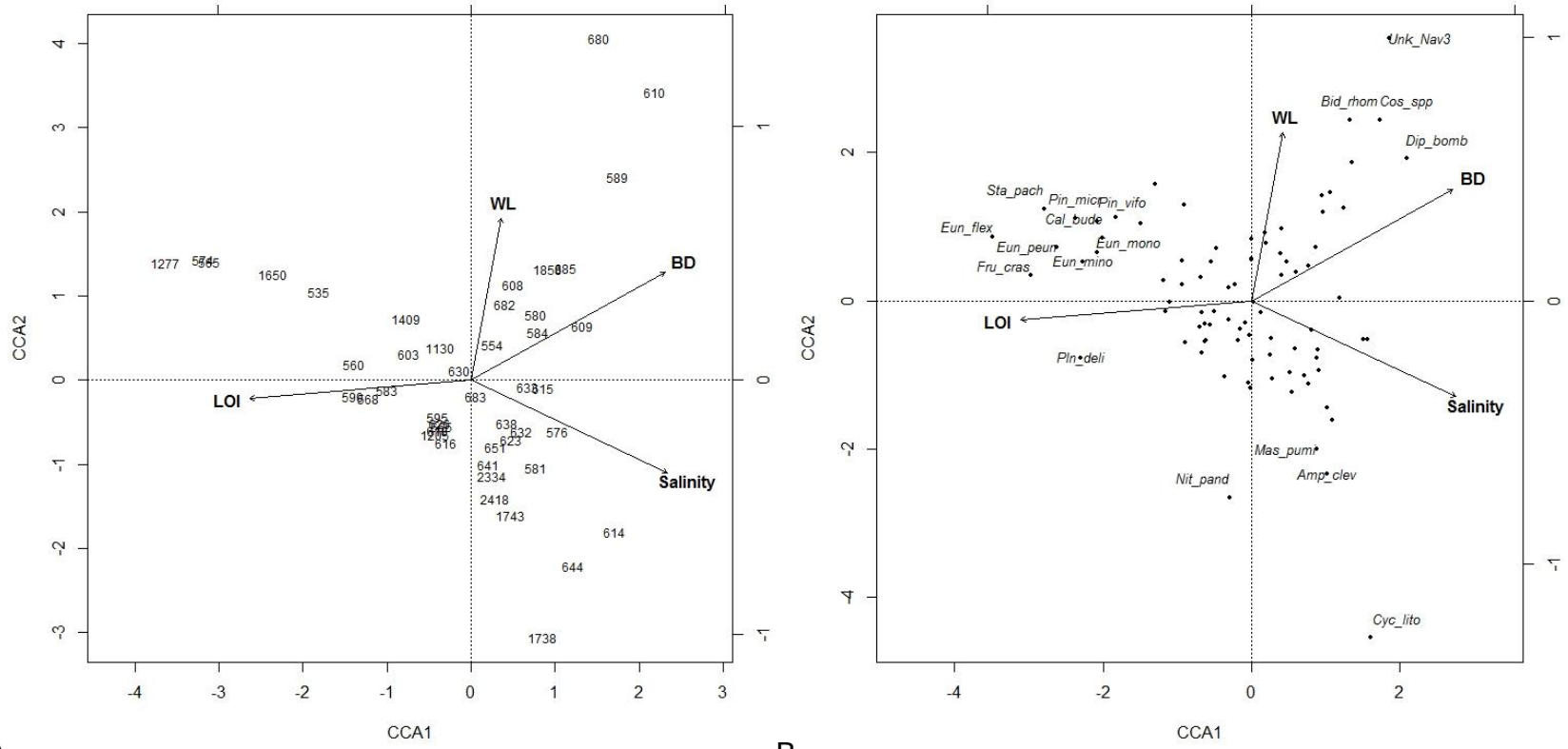

A B

Figure 4-5. CCA bi-plot of the diatom abundance data constrained by the forward-selected environmental variables water level (WL), salinity, bulk density (BD) and loss-on-ignition (LOI). A) Correlation bi-plot and sample scores: the eigenvectors are scaled to square root of their eigenvalue. B) Distance bi-plot and species scores: the eigenvectors are scaled to unit length.

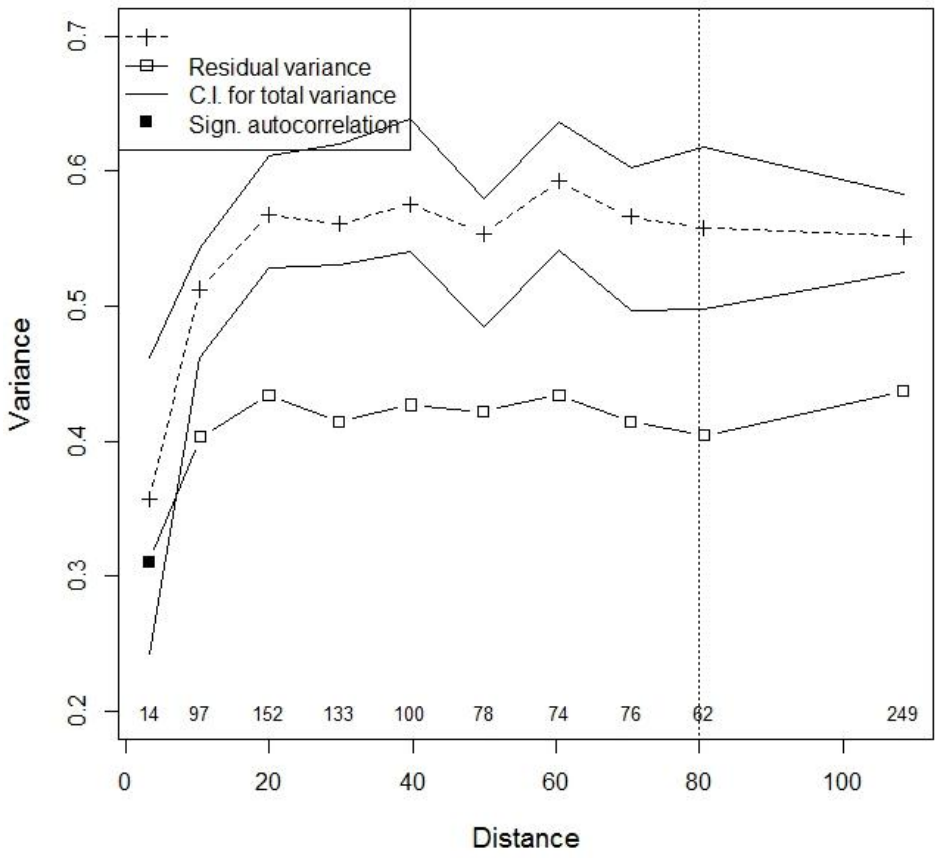

Figure 4-6. Results from multi-scale ordination (MSO) demonstrate a significant spatial autocorrelation in the first distance interval at approximately 3 km (black square). Distance along the horizontal access is in kilometers (km). Number above the horizontal access display the number of site-pairs in the distance class.

Table 4-1. Descriptive statistics for environmental variables measured at 46 sampling sites.

Variable	Mean	Std. Dev.	Minimum	Maximum
Elevation (m NAVD88)	0.31	0.14	-0.06	0.58
Salinity (‰)	7.39	5.41	0.30	22.84
Water Level (m NAVD88)	0.36	0.11	0.06	0.56
Bulk density (g cm^{-3})	0.27	0.13	0.07	0.64
Loss-on-ignition (%)	33.16	16.83	10.34	88.53
Accretion (cm yr^{-1})	0.47	0.89	-0.78	4.54
Elevation change (cm yr^{-1})	-0.06	0.91	-2.32	2.38
Mean grain size (phi)	9.59	5.67	4.53	30.78
Vegetation cover (%)	60.5	11.68	36.2	84.3

Table 4-2. Pearson correlation coefficients and results of significance tests between environmental variables for samples collected in the Chenier plain of Louisiana. Pearson coefficients are on the top-right (white) and p-values of significance tests are on the lower-left (grey) portion of the table matrix. Correlation coefficients and p-values significant at the 0.005 level are in bold.

	Elev	WL	Salinity	BD	LOI	Veg	Spp	Acc	Sed	Grain
Elev		**0.78**	0.13	0.07	0.00	0.23	0.02	-.33	0.10	0.24
WL	**0.000**		-0.04	0.06	0.06	0.03	-0.11	-0.28	0.02	0.17
Salinity	0.389	0.785		**0.46**	**-0.46**	0.26	0.30	-0.12	0.13	-0.19
BD	0.659	0.696	**0.001**		**-0.81**	0.13	0.01	0.03	0.05	-0.07
LOI	0.995	0.712	**0.001**	**0.000**		-0.16	0.07	-0.02	-0.07	0.35
Veg	0.122	0.848	0.082	0.380	0.281		0.36	-0.23	-0.13	-0.05
Spp	0.921	0.479	0.043	0.940	0.621	0.015		-0.24	0.03	-0.11
Acc	0.026	0.057	0.424	0.848	0.332	0.127	0.107		0.09	-0.08
Sed	0.516	0.883	0.371	0.755	0.651	0.388	0.838	0.530		0.01
Grain	0.102	0.246	0.211	0.627	0.018	0.723	0.471	0.592	0.949	

Elev = elevation (m NAVD88); WL = water level (m NAVD88); BD = bulk density (g cm^{-3}); LOI = loss-on-ignition (%); Veg = total vegetation percent cover (%); Spp = primary species percent cover (%); Acc = vertical accretion (cm yr^{-1}); Sed = sediment elevation change (cm yr^{-1}); Grain = mean grain size (phi).

Table 4-3. Variance inflation factors (VIF) for environmental variables included in constrained ordination analyses.

Elev	WL	Salinity	BD	LOI	Veg	Spp	Acc	Sed	Grain
3.605	3.226	1.602	3.879	4.483	1.398	1.443	1.279	1.101	1.516

Elev = elevation (m NAVD88); WL = water level (m NAVD88), BD = bulk density (g cm^{-3}), LOI = loss on ignition (%), Veg = total vegetation cover (%), Spp = dominant species cover (%), Acc = vertical accretion (cm yr^{-1}), and Grain = mean grain size (phi).

Table 4-4. Results of principle components analysis (PCA) of diatom assemblage data for Louisana coastal marsh samples. Total inertia is 0.56.

	Axis			
	1	2	3	4
Eigenvalue	0.01	0.07	0.05	0.03
Proportion explained	0.18	0.13	0.09	0.06
Cumulative proportion explained	0.18	0.31	0.39	0.45

Table 4-5. Results of redundancy analysis (RDA) on diatom species assemblage constrained to select environmental variables.

	Axis			
Parameter	1**	2**	3*	4
Eigenvalues	0.142	0.072	0.034	0.022
Species-environment correlation	0.901	0.823	0.687	0.779
Cumulative percentage variance				
of species data	14.2	21.3	24.7	26.9
of species-environment relation	40.5	61.1	70.7	77.1
p-value	0.005	0.005	0.015	0.230
Bi-plot scores for environmental variables				
Elevation*	0.189	-0.500	-0.229	0.321
Water level	0.169	-0.635	-0.251	0.143
Salinity**	0.774	0.337	-0.427	0.018
Bulk density**	0.781	-0.408	0.074	-0.148
LOI*	-0.831	0.090	-0.359	0.081
Total vegetation cover	0.045	-0.152	-0.035	0.068
Species cover	0.093	0.284	-0.097	0.319
Vertical accretion	-0.016	0.081	0.205	0.104
Elevation change	0.249	0.132	0.448	-0.100
Grain size	-0.305	-0.285	-0.318	-0.601

Monte Carlo permutation tests to assess the significance of axes and constraints indicate: *p-value < 0.05 and **p-value < 0.01

Table 4-6. Results of canonical correspondence analysis (CCA) on diatom species assemblage constrained to select environmental variables

	Axis 1**	2**	3*	4
Eigenvalues	0.279	0.119	0.066	0.054
Species-environment correlation	0.876	0.837	0.890	0.661
Cumulative percentage variance				
of species data	13.6	19.4	22.6	25.3
of species-environment relation	39.8	56.9	66.3	74
p-value	0.005	0.005	0.025	0.076
Bi-plot scores for environmental variables				
Elevation*	0.151	0.507	0.023	-0.277
Water level	0.079	0.622	-0.110	-0.166
Salinity**	0.753	-0.226	-0.157	-0.463
Bulk density**	0.708	0.496	-0.047	0.075
LOI**	-0.830	-0.189	-0.111	-0.264
Total vegetation cover	0.018	0.187	0.136	-0.017
Species cover	0.111	-0.260	-0.067	0.142
Vertical accretion	0.009	-0.095	0.108	0.218
Elevation change	0.244	-0.142	-0.242	0.406
Grain size**	-0.384	0.281	-0.769	-0.151

Monte Carlo permutation tests to assess the significance of axes and constraints indicate: *p-value < 0.05 and **p-value < 0.01

CHAPTER 5
DIATOM-INFERRED SALINITY RECONSTRUCTION FOR COASTAL MARSH IN LOUISIANA'S CHENIER PLAIN

Background

Louisiana is experiencing significantly high rates of wetland loss (Barras et al., 2003; Britsch and Dunbar, 1993; Britsch and Kemp, 1990; Day et al., 1999; Dunbar et al., 1990; Dunbar et al., 1992). Wetland loss has been attributed in part to salinization and increased flooding from human-altered hydrology, sea-level rise, and subsidence. Significant financial resources have been committed toward planning and restoration efforts, including freshwater diversions and shoreline stabilization (U.S. Army Corps of Engineers, 2003). Restoration programs benefit from a mechanism to monitor and evaluate the effectiveness of project efforts, and from which to adapt continued management efforts. The traditional method is to use paired treatment and reference sites, but because of the extensive alteration to coasts like Louisiana, reference sites are difficult to find. Another approach may be to use a paleoecological method, to extrapolate characteristics of the marsh, such as water level or salinity, prior to disturbance from which to make comparisons.

Salinity and water level have a significant influence on the structure of coastal plant communities (Howard, 1996; Howard and Mendelssohn, 1999a, b, 2000; McKee and Mendelssohn, 1989; Wolanski et al., 2009). However, data on water level and salinity changes are limited both temporally and spatially. Analyses of currently available data often demonstrate both increases and decreases in salinity, without signifying a strict tendency of salinity increases toward wetland loss (Wiseman et al., 1990); however, historical records may not be long enough to identify trends. Decades of data are required to document long-term trends in sea-level rise and climate

variability. The lack of historical data on salinity and water level, both characteristics critical to coastal marsh ecology, is a significant gap in our attempt to understand processes controlling wetland instability and the impacts of environmental change. However, paleoecological methods that use a proxy for salinity and water level variations may provide a source of historical data that goes beyond recent monitoring efforts (Orson, 1996; Williams, 2011a).

Paleoecological analysis uses proxies (sometimes called paleoindicators) to reconstruct the ecosystems of the past. They have been an extremely useful tool for looking at long-term trends and impacts of climate change, sea-level rise, and anthropogenic disturbances. Diatoms, in particular have proven to be an excellent indicator of environmental change (Smol and Stoermer, 2010). They respond rapidly to changing environmental conditions and their frustules of silicon dioxide preserve well in most soils. Parsons et al. (1999a, b) examined salinity history for coastal marsh lakes using a diatom salinity index (DSI). The DSI was developed by identifying halophilic preferences of diatom species from literature. While demonstrating the utility of diatoms as environmental indicators in coastal areas, the authors acknowledge the limitations of using pre-defined knowledge of species preferences because of geographic variability. The transfer function procedure is a method that advances this concept by using knowledge on species optima and tolerance to environmental parameters from a modern training data set to quantify the environmental conditions of the past (Birks, 1995; Birks, 2010). The transfer function is developed from a statistical correlation between contemporary distributions of species and environmental conditions, which are then applied to fossil samples from the same geographic region.

A transfer function is developed by obtaining contemporary data on species distribution and density in relation to some environmental parameter, then using a backward approach, “transferring” that knowledge into an estimate of the environmental parameter from the assemblage of fossil species data. The contemporary data is often obtained by identifying the diatom assemblage from surface sediments collected at sites where environmental variables are measured.

The first quantitative paleo-reconstruction based on transfer functions was conducted by Imbri and Klip (1971). Developed first for paleo-oceanic studies, it was adopted by limnologists for reconstructing lake histories, and has received recent popularity in estuaries and coastal marshes for the study of sea-level rise. Diatoms have been used successfully in reconstructions of changing trends in pH (Birks et al., 1990), water quality (Dixit et al., 1999; Ramstack et al., 2003), temperature (Koç et al., 1993; Vyverman and Sabbe, 1995), and to identify significant stratigraphic events, such as tsunamis (Hayward et al., 2004; Hemphill-Haley, 1995). Recent attention has identified diatoms as a possible proxy for sea-level since species respond in predictable ways to marsh elevation, water level, and salinity (Denys and De Wolf, 1999; Horton et al., 2006; Palmer and Abbott, 1986; Roe et al., 2009; Sherrod, 1999; Szkornik et al., 2006).

While marsh elevation, per se, is unlikely to drive diatom species assemblages, the elevation of the marsh in relation to the tidal frame does influence many important marsh ecological characteristics that are important to diatoms, such as subaerial exposure, salinity, sediment temperature, turbidity, ratio of solutes, and macrophytic community (Morris, 1995; Nelson and Kashima, 1993). Diatom morphology is suitable for a specific ecological niche (Pappas and Stoermer, 1995) and there is evidence that

habitats may have a limited number of niches for species to occupy (Patrick, 1963), so as marsh ecology changes due to sea-level rise, the diatom community changes as well.

Examples of diatom-inferred sea-level reconstructions for coastal marsh systems are plentiful. Diatoms were found to have a high predictive capability for elevation in North Carolina (Horton et al., 2006; Kemp et al., 2009), Denmark (Szkornik et al., 2006), Canada (Roe et al., 2009), and the United Kingdom (Gehrels et al., 2001). Calibration data for these studies were sampled from transects, where sites are in close proximity, and authors suggest site-specific distributions of diatoms limit the application of regionally developed models (Horton et al., 2006). Woodroffe and Long (2009) support this assertion through their analysis of combined data sets for two sites in West Greenland, suggesting that differences in species distributions between sites would increase model error. However, spatial autocorrelation from closely sampled calibration data and cross-validation may generate over-optimistic estimates of model errors (Telford and Birks, 2005). Therefore, it is necessary to examine alternatives to transect-based calibration data.

Gehrels et al. (2001) applied a multi-proxy approach (diatoms, foraminifera, and testate amoebae) to infer tidal flooding. They determined that the pattern of intertidal zonation of micro-organisms is variable between sites. However, regional training sets increase the likelihood that environmental information from calibration data accurately reflects palaeoenvironmental conditions. While elevation is a more common variable used in sea-level studies, it is important to recognize that the effect of elevation will be dependent on geographic location because it will be tied to freshwater flow and tidal

range, therefore examining salinity, water level, and tidal flooding may provide more consistent results. This is particularly true for a location such as southern Louisiana, which is experiencing high rates of subsidence (Boesch et al., 1983; Dokka, 2006) and complicated interactions between elevation, water level, and salinity.

Reconstruction of salinity and tidal flooding can also support wetlands restoration objectives. Many wetland restoration projects have the objective of repairing natural hydrologic conditions and moderating salinity levels (Orson, 1996; Reed and Wilson, 2004; Vairin, 1997). However, because of the lack of historical data on water levels, salinity, and wetland productivity, objectives are often based on minimal quantitative knowledge of pre-existing wetland condition. Diatom-inferred salinity, water level and tidal flooding reconstructions can provide a historical perspective on restoration projects, and provide an essential tool for evaluating restoration success.

The purpose of this study is to explore the assemblage of diatoms as proxy for sea level and create a regional transfer function that can be used to reconstruct sea level for coastal marsh of the Chenier plain in southwest Louisiana. First, it must be determined that measurable characteristics of sea level (water level, marsh surface elevation, salinity, etc.) are a primary driver of diatom species assemblage in the Chenier plain. Gradient analysis on contemporary diatom assemblage for samples located throughout the Chenier plain identified salinity and water level (mean height of the water surface relative to NAVD88) as the most significant environmental variables influencing diatom assemblage (Chapter 4) supporting the development of a transfer function. In addition, these analyses concluded that the sample design was not significantly influenced by spatial autocorrelation. I chose to also look at marsh elevation (height of the marsh

surface in relation to vertical datum NAVD88), because it was significant in one variable analyses (Chapter 4), and tidal flooding (percent of measurements water level was higher than marsh elevation) since these variables are features of sea-level rise which may relate closely to marsh loss. While performing analyses on both tidal flooding and mean water level may seem redundant, both were included in an effort to enhance comparisons to other studies and provide a discussion on physical hydrologic parameters in coastal marsh and their influence on diatom species distributions. In addition, chronology (assigning an approximate date to historic sediments) provides an essential tool for comparing temporally consistent reconstruction results to historic data and records. Chronology for several sediment cores was determined using radioactive isotopes ^{210}Pb and ^{137}Cs (Chapter 3).

Sediment cores were collected at Rockefeller Wildlife Refuge (RWR). Beginning in 1984, refuge staff began collecting salinity and water level data at several locations. Although the sediment cores will span many decades further into the past, the data can be used to confirm general historic patterns revealed by diatom reconstructions.

Regional Setting

The Chenier plain extends from Vermillion Bay in south-central Louisiana to the Texas Louisiana border. It consists of over 6,000 km^2 of marsh, open water, and chenier habitats. The marshes began forming during periods when the Mississippi River followed a more westerly course, approximately 4,000 year ago (Gosselink et al., 1979). The reworking of Mississippi deltaic deposits formed a series of beach ridges; the relics of these ridges are called ‘cheniers’. Throughout the Chenier plain, man-made channels and water-control structures are prevalent and have greatly altered the natural hydrology (Gosselink et al., 1979).

Subsidence and sea level rise coupled with human-altered hydrology and subsurface oil and water extraction have caused large-scale wetlands loss and marsh instability (Boesch et al., 1994; Louisiana Coastal Wetlands Conservation and Restoration Task Force and the Wetlands Conservation and Restoration Authority, 1998). As a result, wetland restoration projects have sought to improve drainage and mitigate saltwater intrusion.

Methods

Calibration Data

Surface sediment sampling procedures for contemporary data were the same as previously described (Chapter 2). Briefly, a shallow push core (10-cm in diameter) was collected at each site. The top 2-cm was extracted, placed in plastic bags, and kept cool until samples could be processed in the lab. Sites were chosen to represent the range of salinity and elevation found within the marshes of the Chenier plain.

Hydrologic data were obtained from the CRMS program for each sample site. Marsh elevation is documented by detailed field surveys and rod surface elevation tables (RSET; Cahoon et al., 2002). Water level and salinity data are recorded at 15-min increments using a data sonde (i.e. InSitu Aquatroll 200). Sedimentation rate and seasonal variability are likely to influence diatom species and density within the sampled sediment interval. Based on estimated site sedimentation rates (< 2 cm yr^{-1}), two to three years of water level and salinity data will likely be sufficient to capture the temporal and seasonal variability of the sampled sediment, properly characterizing the environmental conditions which the diatom assemblage would have encountered. Therefore, 2 to 3 years of 15-min water level and salinity data were averaged to obtain a single estimate, mean salinity and mean water level, from which to characterize sites.

Using the same time period, tidal flooding was calculated as the percent of time water levels were higher than marsh elevation.

Marsh Sediment Cores

To test the validity of transfer functions, diatom assemblage data from three marsh cores were used to reconstruct past hydrologic conditions (Figure 5-1). Cores were collected during April of 2009 at Rockefeller Wildlife Refuge and were located along a transect perpendicular to the Gulf of Mexico. Core collection is described in detail in Chapter 2.

The cores were sealed and transported to the lab, where they were x-radiographed and sliced at 2-cm intervals. Compaction ranged from 3 to 33%, which is not uncommon for loosely consolidated marsh cores (Chapter 2). Detailed analysis of x-radiographs and radioisotope profiles (^{210}Pb and ^{137}Cs) provided sedimentation rates and geochronology for each core (methodology described in Chapter 3). Hurricane deposited sediments were identified in all three cores (Chapter 2). The diatom assemblage of these sediments differs significantly from the assemblage found in sediments prior to the hurricane, and are likely composed of allochthonous taxa due to turbulence and transport of sediments (Chapter 2). Therefore, reconstructions from hurricane deposits do not provide relevant predictions of environmental conditions at the sediment core sampling site (diatoms were likely transported from another location) and should be ignored when examining site-level trends.

Multivariate statistical procedures

A detrended canonical correspondence analysis (DCCA) was performed on the environmental variables to determine if unimodal methods were appropriate. Simpson (2012) suggests that if the DCCA gradient lengths are greater than 2 SD (Hill's standard

deviation units of compositional turnover), then several of the taxa in the calibration set have their optima located within the gradient and unimodal-based methods are appropriate. The program CANOCO (Version 4; ter Braak and Šmilauer, 1998) was used to perform DCCA.

Transfer functions were developed using a unimodal-based technique called weighted averaging (WA) regression (Braak and Juggins, 1993) using the program C2 (version 1.7.2; http://www.staff.ncl.ac.uk/staff/stephen.juggins/software/C2Home.htm). WA is based on the concept of niche-space partitioning and ecological optima of species by calculating weighted averages of species optima and tolerances. There are two types of WA in addition to the 'standard' WA: weighted average partial least squares (WA-PLS) and weighted averaging with tolerance downweighting (WA-Tol). WA-PLS is an extension of the WA method using partial least squares (PLS) and is appropriate for species rich, compositional data with many zero-abundances, such as in the case of most diatom assemblage data. In WA-Tol, taxa with a narrow range (tolerance) or amplitude (optima) can be given a greater weight than taxa with a wide tolerance to the environmental parameter through a tolerance downweighted regression. The WA-Tol downweights the weighted averaging equation by the squared tolerance (Battarbee et al., 1999; Juggins, 1992).

All three WA methods are performed in three parts: WA regression, WA calibration, and an additional 'deshrinking' regression (ter Braak et al., 1993). The WA regression uses the contemporary training data to calculate a weighted average to estimate species optima and tolerance to a specific environmental parameter (e.g. salinity). The weighted average is calculated from all the locations where the species is

present and is weighted by the taxon's density. Tolerance values are estimated by the standard deviation of the weighted averages. The second step, the WA calibration, estimates the environmental parameter for sites by the weighted averaging of species optima determined by the WA regression. Because averages are taken twice, the range of the estimated environmental parameters is reduced. The amount of 'shrinkage' in the estimate of the environmental parameter can be estimated from the training set using regression, either through inverse regression ($_{inv}$) or classical regression ($_{cla}$) (Birks et al., 1990). The classical regression technique 'deshrinks' the estimated environmental variable by calculating an error term from the regression of the calculated values for the environmental parameter against the observed values. The inverse regression minimizes the error of the mean square error in the calibration data set, but at the cost of introducing bias at the endpoints (ter Braak et al., 1993). Both WA and WA-Tol use either classical or inverse regression for 'deshrinking', however WA-PLS uses the inverse regression for calculating the amount of shrinkage and its first component (WA-PLS_1) is equivalent to the WA_{inv}, but with updated species optima. The additional components of WA-PLS improve species optima by utilizing the residual structure of species data and have been demonstrated to reduce the 'noise' of very complex, species rich data (ter Braak and Juggins, 1993). For this reason, WA-PLS is the most common procedure used in diatom-based transfer functions.

Results from multiple WA methods (WA_{inv}, WA_{cla}, WA-Tol_{inv}, WA-Tol_{cla}) and four components of WA-PLS are reported to establish transfer function performance and provide insight into model selection. Performance of the transfer functions are assessed in terms of root-mean square error (RMSE) and the square correlation (r^2) of observed

versus predicted values. The RMSE is a measure of the pair-wise differences between the observed and predicted values, whereas the r^2 measures the strength of the relationship. A jackknife cross-validation was also performed. A jackknife estimator is obtained by re-computing the estimate leaving out one observation at a time, allowing the bias and variance of the statistic to be calculated (Efron, 1983). The jackknife validation provides a less biased measure of the overall predictive capability of the dataset and will be assessed by using $RMSE_{jack}$ and r^2_{jack} statistics, as well. Scatter plots of estimated versus observed values for both the model and jackknifed cross-validation provide an illustration of how well the model predicts the actual measurements. The scatter plots also illustrate any trends that may be relevant regarding samples and model prediction, such as how well the transfer function predicts samples that are under-represented. Plots of residuals (predicted minus observed) provide insight on model biases (trends to over- or under-predict values). Plots of jackknifed estimates and residuals provide similar insights into model performance and demonstrate the sensitivity of the model to the removal of any one sample.

The influence of individual taxa can be evaluated by examining the species coefficients: the species optima, tolerance, and N2. N2 is analogous to Hill's N2 diversity measure (Hill, 1973) and is defined as the "effective number of occurrences". Line et al. (1994, p.148) provides an example of how optima and N2 are estimated: "A taxon with 6 actual occurrences with values of say, 70%, 1%, 0.9%, 0.7%, 0.5%, and 0.1% will have its WA optimum effectively determined by the sample in which it occurs with an abundance of 70%. The N2 for this taxon is thus close to 1."

Results

Transfer functions

Results from the single-constraining variable DCCA's indicate that for salinity (p-value = 0.001, DCCA axis 1 = 2.69 SD) the optima of a significant number of diatom taxa are contained within the data set and unimodel-methods are appropriate. Similar analyses for water level, tidal flooding and elevation had short gradient length (SD < 2) and failed significance tests (p-value = 0.118, 0.860 and 0.105, respectively). Water level and flooding were not considered further, whereas elevation regressions were conducted to further examine the predictive capacity of a transfer function.

Results for the WA regression methods are shown in Table 4-2. For the salinity model, the WA-PLS second component (WA-PLS_2) provides the most parsimonious model since it is the lowest acceptable component given the prediction statistics (RMSE = 2.35; $r^2_{apparent}$ = 0.808) and jackknifed validation errors (r^2_{jack} = 0.451). The WA-PLS third component is the best model for elevation (RMSE 0.04; $r^2_{apparent}$ = 0.887). The apparent prediction is higher than for the salinity model; however, the jackknifed versus observed correlation (r^2_{jack} = 0.05) is much lower than for salinity, indicating a greater sensitivity to the removal of samples.

Plots of observed salinity and elevation versus predicted values and residuals are provided in Figure 5-2. The model provides strong predictions for low to moderate salinity; however, it tends to under-predict at high salinity sites (salinity > 12.5). Only four sites had an average salinity value greater than 15‰. The salinity model is also sensitive to the removal of samples, which can be seen in the greater degree of spread for the samples in the jackknifed estimates versus observed values plot. Jackknifed residual plots also show that removing samples causes the model to under-predict high

salinity sites even more. Plots of observed versus predicted elevation show very few samples from sites with greater than 0.5 m range. The residual versus observed plot for elevation shows a great deal of over and under prediction, particularly on the extremes (high elevation and very low elevation). Jackknifed plots reflect the sensitivity of the model to sample removal and the tendency to over-predict sites with low elevation and under-predict sites with high elevation.

Species coefficients (optima and tolerance) for taxa occurring in at least 5 samples with an abundance of 3% or more were calculated from weighted averages and are included in Table 5-3. Many of the species were counted in over 20 samples and 30 species have an effective occurrence of over 30 samples. None of the species listed have a high salinity optimum (> 18‰) and only a few species have salinity optima greater than 10‰. Also, many of the species have a similar elevation of approximately 0.30m.

Additional calibration data covering a greater range of marsh locations could improve knowledge on species affinities and the predicative capability of the transfer function. The elevation transfer function tended to over-predict samples from low elevations, and the salinity transfer functions tended to under-predict samples from high salinity locations. Both transfer functions were sensitive to the removal of samples. However, the elevation transfer function was even more sensitive than the salinity transfer function, showing both under- and over-predictions at the high and low elevations, respectively. The performance of the salinity transfer function would likely improve with an additional 15-20 samples from high salinity locations (where average salinity is greater than 15‰), to provide a more robust species assemblage with high

salinity optima. The prediction for elevation had difficulty at both extremes. Species optima and tolerance data show that many diatom species had similar elevation optima, so either the sampling scheme did not characterize the full tolerance range of a significant number of species (perhaps only a few species respond to changes in marsh elevation), as suggested by the low gradient length from the DCCA.

Reconstruction

Based on gradient analyses, variability in diatom assemblages is influenced by elevation (Cahpter 4), however jackknifed estimates of model performance show that the models developed from this calibration data set is extremely sensitive to the removal of sites and tends to both over- and under-predict values at the extremes, likely due to few examples of representative sites with extreme elevations and few species with optima at these ranges. Based on the prediction and jackknifed performance, a transfer function for elevation is not recommended and will not be reconstructed using sediment cores. The salinity transfer function is also sensitive to the removal of sites. However, the error is largely limited to high-salinity inferences. Reconstructions can still be conducted, as long as this weakness is carefully considered with regards to interpretation of results. Therefore, the WA-PLS_2 salinity transfer function was applied to three sediment cores, where sediment representing the past 80-100 yrs was recovered.

Overall, species found in the sediment cores were represented in the contemporary calibration data. Only one diatom species, *Frustulia interposita* (Lewis) De Toni, (found in both core 4 and 9) did not have an analogous representative in the contemporary samples. The species was represented in extremely low density (<1%) and may be geographically isolated, uncommon, or allochthonous. Literature indicates the species may be largely freshwater (Patrick and Reimer, 1966a), however Williams

(1962) describes finding this species on bare mudflats in Sapelo Island, Georgia, and Pyle et al. (1998) document it in Florida Bay (however, uncommon), evidence that the species is found in intertidal habitats as well.

The first reconstruction (core 4) was located closest to the Gulf of Mexico, and had a thick hurricane deposit at the surface, approximately 13 cm in depth (Figure 4-3). Dominant species include the brackish epipelic taxa *Tryblionella granulata* (Grünow) Mann, *Diploneis smithii* var. *dilatata* (Peragallo) Terry, *D. crabro* (Ehrenberg) Ehrenberg, *Achnanthes brevipes* Agardh, and *Navicula peregrina* (Ehrenberg) Kützing; and marine/brackish planktonic species *Thalassiosira baltica* (Günow) Ostenfeld, *Actinoptychus senarius* (Ehrenberg) Ehrenberg, and *Cyclotella meneghiniana* Kützing. *Pinnularia viridis* (Nitzsch) Ehrenberg is typically found within freshwater, most notably rivers and streams. The species is present in high density below 40 cm, or prior to approximately 1950. This suggests that the site received freshwater in sufficient supply to host a large population of freshwater *Pinnularia* species.

The second reconstruction, located 3-km inland, was the least variable site, dominated primarily by a brackish generalist *T. granulata* (Figure 4-4). A storm sediment deposit was not as substantial as found in core 4 (approximately 9cm thick). Salinity estimates from diatom assemblage were constant from approximately 1935 to 2000, however there is a change in species composition at around 1950, as indicated by a decrease in *C. formosa* and *N. peregrina* and an increase in an unidentified *Diploneis* species (this specimen appears similar to *D. bombus*, as indicated, but it has a distinct morphology that is easy to differentiate; it may be a subspecies). This particular species was identified in only 5 contemporary samples, most in low densities, and has an

effective occurrence of only 3.42. The reconstruction shows a slight increase in salinity below the Hurricane Rita sediment deposit; however, this is largely due to a dominance of the species *T. granulata* (75% of counts). Prior to 1930, it appears salinity may have been low, as shown by the presence of *Caloneis formosa* (Gregory) Cleve, *Navicula peregrina* and *Pinnularia viridis*.

The final site is located approximately 6 km from the Gulf of Mexico shoreline (Figure 4-5). Samples from this core were dominated by planktonic generalists *C. meneghiniana*, *A. senarius* and an unidentified *Thalassiosira* species. Prior to 1950, the marsh was dominated by brackish species with lower salinity tolerances (notably *Nitzschia scalaris* (Ehrenberg) W. Smith and *N. obtusa* W. Smith). Around 1950, the reconstruction indicates an increase in marsh salinity, through an increase in brackish taxa with a higher tolerance for salinity (*C. formosa* and *N. peregrina*); however, x-radiographs and sediment profile data indicate that sediment samples for 23- and 25-cm depth are higher in density than above and below layers, indicating possible storm sedimentation. Radioisotopes date this layer as between 1950 and 1964. Species which dominate a zone from 15-20cm include two brackish epipelan species *Amphora proteus* Gregory and *Seminavis eulensteinii* (Grünow) Danielidis, Ford and Kennett.

Discussion

Salinity reconstructions for two sites support the assertion that salinity has increased since the 1950s. These results are in close agreement with local records and may have been initiated by several events. Salinity readings collected by RWR since 1984 show an increasing trend from approximately 8‰ in 1984 to almost 15‰ in 2012 (Figure 5-6) and the increasing salinity trend is reflected in core reconstructions. Shoreline erosion has been a significant issue in declining wetland area and

comparisons between recent imagery and historic (1956) marsh data suggest that the shoreline of Rockefeller has eroded and advanced northward by approximately 800 meters. In addition, a highway, lock and channel system was constructed to the north of the site during the 1950s that reduced freshwater flow south into the study site (Clark and Mazourek, 2005). Freshwater diversion structures that allow freshwater flow south of the highway were installed recently in order to attenuate salinity spikes (http://lacoast.gov/reports/project/ME-16%20PCR.pdf, accessed September 30, 2012). The impact of this diversion cannot be determined from these data because cores were collected shortly after project completion and the surface sediments (and diatoms) reflect deposition from recent storms rather than site-specific salinity changes. If more recent samples were collected and the freshwater diversion has indeed lowered salinity for these marshes, estimates from diatom assemblage should reflect these changing conditions. The rapid response of diatom assemblages makes diatom proxies an excellent method for examining post-restoration impacts.

The lack of salinity change in the results of core 6 may be due to regular fluxes of tides, since that site was close to a source of saltwater. A regular flush of tidal waters may ‘regulate’ the salinity of this site. Despite no change in estimated salinity, diatom composition does change during the 1950s, as a species of *Diploneis* increases in density. *Diploneis* is generally a brackish species that can tolerate higher salinities, so the sampled site may not have undergone a significant change in salinity. However, it does demonstrate a possible response to some perturbation, but limited knowledge on this species’ distribution and preferences can limit the interpretation of the significance of its appearance at this exact time period. This example demonstrates that salinity

reconstructions need to be interpreted in connection with the diatom species data and distribution in order to fully recognize the significance of events. Like the other two sites, the change in diatom species composition may reflect the impact of reduced freshwater flow from upland areas; however, perhaps salinity was not altered substantially and diatom species are responding to some other change in environmental condition caused by reduced freshwater flow, such as water level. Or perhaps the sensitivity of the transfer function to under-predict high salinity estimates may indicate that indeed salinity has increased at this site but the tendency of the transfer function to under-predict high salinity influenced the result. The estimated salinity prior to 1930 is lower than subsequent years, supporting the conclusion that salinity has increased at this site, although the exact timing and cause is subject to some speculation.

A transfer function for salinity using diatoms was created and salinity reconstructions for three sediment cores present reasonable salinity estimates for the past 90-100 years. Validating salinity reconstructions is difficult due to limited observational data for southern Louisiana marshes. Ancillary data for this study site was acquired for approximately 25 years and salinity reconstructions reveal the same general trend observed in the site measured data. Vegetation mapping data from 1948 to present also depict an interior advancement of saline marsh (http://lacoast.gov/crms_viewer/; accessed on October 10th, 2012). In addition, taking into account the historical information and geomorphology of the site, the reconstructions present a reasonable estimate of salinity, showing salinity increases from brackish to a more saline environment. This change is likely due to a decrease in freshwater flow from upland regions caused by construction of a highway rather than

the northward advancement of the shoreline due to coastal erosion and sea-level rise. Evidence to support this hypothesis is the consistent estimate of low salinity (5-10‰) prior to 1950 with a dramatic increase in salinity after 1950. In addition, mean sea level data for Eugene Island, LA (http://tidesandcurrents.noaa.gov/sltrends/sltrends_station.shtml?stnid=8764311; accessed October 9th, 2012) shows the same general increasing trend both before and after 1950. However, insufficient data exists in pre-1950 shoreline trends and erosion rates, but the dramatic change in post-1950 reconstructed salinity indicate dramatic even rather than a continuous gradual change.

The reconstruction results highlight the significance of anthropogenic disturbance as a primary cause of marsh salinization. This indication is significant because wetland restoration is unlikely to stop marsh loss due to sea-level rise, hurricanes or climate change; however, restoration and wetland management activities may succeed in reducing wetland loss by removing or remediating anthropogenic impacts (such as levees, impoundments, canals, etc.) which can exacerbate future long-term environmental changes.

Further research should focus on applying the salinity transfer function to sediment cores from locations with a more extensive field sampling record, to examine reconstructions against field and observational data. All evidence suggests that the diatom reconstructions presented here may present a valid estimate of past salinity. The comparison of diatom-based reconstruction with field measured values is important in order to increase confidence in reconstruction estimates and identify critical gaps in species calibration data. There are a limited number of sites in coastal Louisiana with

40-50 years of salinity readings (Wiseman et al., 1990). Additional samples, particularly from high salinity environments, would greatly improve the transfer function by describing the salinity optima of some taxa more accurately. In addition, these samples may provide sufficient data for developing water level or elevation transfer function for examining long-term sea-level trends. Transfer functions could also be tested in locations undergoing significant rates of marsh loss. By combining diatom-based salinity and water level interpretations for multiple cores with a spatial analysis of marsh loss using historic aerial photos and vegetation field surveys (Visser et al., 2000), the interrelated processes of salinity and marsh submergence could be more thoroughly examined. The relationship of salinity and water level to climate and sea-level rise are complex and spatially variable. It is likely that marsh morphology and landscape factors, such as distance from tidal source, will influence the impact of sea-level rise and salinity changes on coastal marsh. A series of deeper, accurately dated cores from additional sites are needed to draw inferences on the effects of sea-level rise on coastal marsh in southwest Louisiana.

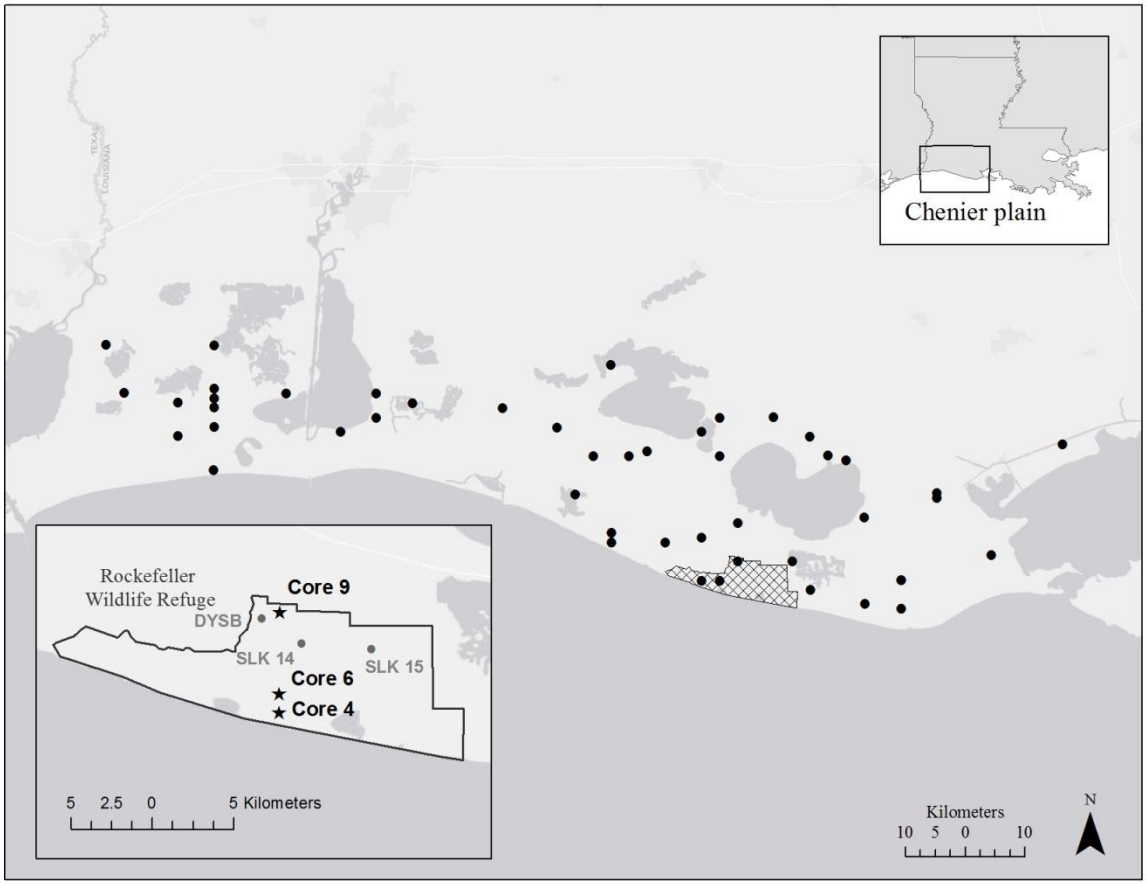

Figure 5-1. Map of surface sediment and sediment core sample locations. Forty-six contemporary surface sediment samples (black points) were collected throughout the Chenier plain. Three marsh cores (black stars; inset map) were sampled from Rockefeller Wildlife Refuge in southwest Louisiana, U.S.A. Monthly salinity and water level readings are collected by refuge staff at three locations noted in grey (DYSB, SLK 14, and SLK 15).

Table 5-1. Summary of descriptive statistics for modern calibration sample locations.

	Salinity (‰)	Elev (m NAVD88)	Water depth (meters)	Water level (meters)	Tidal range (meters)
Mean	7.386	0.321	0.236	0.388	0.333
Median	6.349	0.332	0.220	0.408	0.336
SD	5.356	0.114	0.085	0.096	0.086
Minimum	0.296	0.094	0.088	0.125	0.134
Maximum	22.840	0.579	0.408	0.561	0.626

SD = standard deviation; Elev = Elevation

Table 5-2. Performance of regression models for diatom-inferred salinity and elevation: WA_{inv}, weighted averaging with inverse deshrinking; WA_{cla}, weighted averaging with classical deshrinking; WA-Tol_{cla}, weighted averaging with classical deshrinking and tolerance downweighting; WA-Tol_{inv}, weighted averaging with inverse deshrinking and tolerance downweighting; WA-PLS_c, weighted averaging with partial least squares (c = principle components 1 through 4). The squared correlation between inferred and observed values ($r^2_{apparent}$) and between jackknife predicted and observed values (r^2_{jack}), as well as the root mean square error for the calibration data set (RMSE) and predication (RMSEP) are provided. The most parsimonious model for each parameter is in bold.

	Salinity (‰)				Elevation (m)			
Model	$r^2_{apparent}$	r^2_{jack}	RMSE	RMSEP	$r^2_{apparent}$	r^2_{jack}	RMSE	RMSEP
WA_{inv}	0.676	0.448	3.05	4.13	0.596	0.121	0.08	0.12
Wa_{cla}	0.676	0.454	3.71	4.48	0.596	0.131	0.12	0.15
WA-Tol_{cla}	0.711	0.439	2.88	4.37	0.656	0.089	0.08	0.13
WA-Tol_{inv}	0.711	0.446	3.41	4.60	0.656	0.099	0.10	0.16
WA-PLS_1	0.676	0.454	3.05	3.97	0.547	0.087	0.09	0.13
WA-PLS_2	**0.808**	**0.451**	2.35	4.03	0.798	0.071	0.06	0.14
WA-PLS_3	0.884	0.370	1.82	4.59	**0.887**	**0.053**	0.04	0.15
WA-PLS_4	0.938	0.267	1.34	5.48	0.948	0.037	0.03	0.17

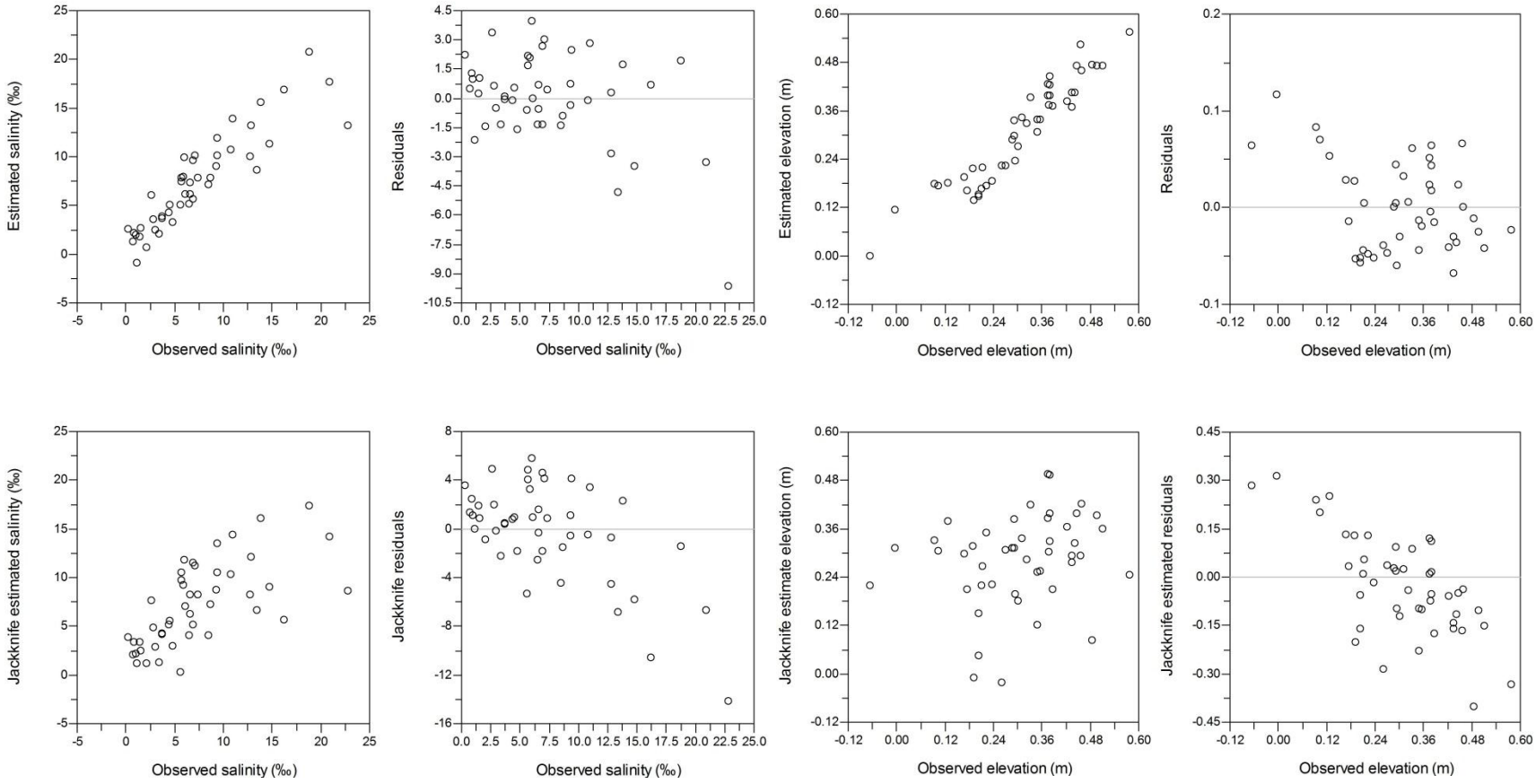

Figure 5-2. Graphs depicting the performance of transfer function developed from regional diatom calibration data set using weighted averaging partial least squares (WA-PLS) component 2 for salinity and WA-PLS component 3 for elevation.

Table 5-3. List of the 59 species with at least 3% abundance counted in at least five surface sediment samples, and their respective occurrences (Count), maximum relative abundance (Max), N2 (effective number of occurrences), and salinity and elevation optimum and tolerances.

					Salinity (‰)		Elevation (m)	
Code	Species name	Count	Max	N2	Optimum	Tolerance	Optimum	Tolerance
Cyc_mene	*Cyclotella meneghiniana*	45	29.94	28.24	7.30	5.26	0.35	0.13
Nit_sigm	*Nitzschia sigma*	42	11.01	24.51	7.51	4.87	0.30	0.11
Nit_cons	*Nitzschia constricta*	36	8.96	17.48	10.39	5.75	0.28	0.12
Nit_obtu	*Nitzschia obtusa*	36	37.74	13.04	4.11	3.24	0.35	0.14
Bac_para	*Bacillaria paradoxa*	35	19.69	15.10	6.19	4.59	0.29	0.10
Nit_scal	*Nitzschia scalaris*	35	3.75	20.43	5.60	4.19	0.29	0.12
Tha_lept	*Thalassiosira leptopus*	34	13.15	10.41	5.94	4.45	0.36	0.10
Act_sena	*Actinoptychus senarius*	33	12.01	16.78	8.96	5.42	0.37	0.11
Nav_trip	*Navicula tripunctata*	33	17.73	17.42	8.36	3.86	0.31	0.11
Tha_balt	*Thalassiosira baltica*	33	14.12	13.14	9.11	7.10	0.35	0.11
Nit_nana	*Nitzshia nana*	32	11.45	18.82	4.81	4.25	0.31	0.11
Amp_coff	*Amphora coffeaeformis*	31	14.67	17.55	6.62	4.30	0.30	0.11
Cal_form	*Caloneis formosa*	31	16.57	13.36	10.87	5.99	0.29	0.11
Dip_smit	*Diploneis smithii*	30	9.69	17.41	7.72	4.47	0.30	0.12
Nit_sgmo	*Nitzschia sigmoidea*	30	7.20	14.39	5.43	4.11	0.31	0.12
Nit_lieb	*Nitzschia liebtruthii*	29	3.72	19.47	6.37	3.70	0.31	0.10
Try_gran	*Tryblionella granulata*	29	33.55	8.75	13.63	6.57	0.33	0.12
Unk_Tha4	*Thalassiosira* spp. 4	29	6.88	16.01	9.13	5.57	0.35	0.12
Act_ocho	*Actinocyclus ochotensis*	28	10.07	9.65	6.02	5.10	0.34	0.11
Amp_oval	*Amphora ovalis*	28	7.89	14.52	10.17	5.85	0.28	0.12
Nit_fili	*Nitzschia filiformis*	28	10.76	16.81	6.68	5.09	0.28	0.11
Nav_pere	*Navicula peregrina*	26	4.86	14.49	6.32	3.73	0.32	0.09
Nit_litt	*Nitzschia littoralis*	26	6.01	11.91	8.29	4.29	0.27	0.12
Try_comp	*Tryblionella compressa*	26	5.56	11.56	8.05	4.75	0.35	0.13
Ent_alat	*Entomoneis alata*	25	5.45	8.81	9.72	4.95	0.30	0.10
Gyr_exil	*Gyrosigma exilis*	25	4.26	13.95	9.16	5.75	0.31	0.10
Shi_oest	*Shionodiscus oestrupii*	25	11.98	7.18	8.89	5.36	0.41	0.10
Tab_fasc	*Tabularia fasculata*	25	8.57	10.74	6.79	2.72	0.33	0.11
Act_octo	*Actinocyclus octonarius*	24	3.59	13.36	8.58	6.32	0.37	0.10
Nit_cf_dipp	*Nitzschia* cf. *dippelii*	24	5.26	11.43	7.03	3.65	0.29	0.11
Cos_spp	*Coscinodiscus* spp. 1	23	14.62	8.28	10.41	6.71	0.39	0.10
Dip_smdi	*Diploneis smithii* var. *dilatata*	23	23.80	7.59	7.57	3.60	0.38	0.10
Fal_pygm	*Fallacia pygmaea*	23	11.62	9.27	6.45	3.80	0.33	0.07
Nav_vene	*Navicula veneta*	23	6.16	12.09	6.21	3.65	0.31	0.11

Table 5-3. (Continued)

					Salinity (‰)		Tidal range (m)	
Code	Species name	Count	Max	N2	Optimum	Tolerance	Optimum	Tolerance
Pin_yarr	*Pinnunavis yarrensis*	23	13.42	5.82	13.40	5.80	0.33	0.11
Unk_Syn1	*Synedra* spp. 1	23	3.95	12.15	6.36	4.09	0.28	0.13
Mel_numm	*Melosira nummuloides*	21	6.40	12.11	9.23	5.00	0.24	0.11
Nit_debi	*Nitzschia debilis*	21	11.32	5.90	6.68	3.70	0.33	0.10
Gom_mexi	*Gomphomena mexicanum*	20	20.14	6.55	5.07	2.21	0.28	0.11
Ach_brev	*Achnanthes brevipes*	19	3.66	10.61	11.20	6.69	0.27	0.12
Mas_pumi	*Mastogloia pumila*	19	15.52	7.99	11.91	4.57	0.23	0.11
Nav_schr	*Navicula schroeteri*	19	20.94	8.80	2.70	2.37	0.27	0.09
Shi_oeve	*Shionodiscus oestrupii* var. *venrickae*	19	5.44	7.17	9.70	6.93	0.40	0.10
Amp_clev	*Seminavis eulensteinii*	18	17.17	6.32	11.82	5.41	0.22	0.10
Pin_viri	*Pinnularia viridis*	18	4.27	8.85	4.12	3.34	0.33	0.11
Dip_smpu	*Diploneis smithii* var. *pusilla*	17	12.06	6.82	5.74	4.01	0.33	0.15
Nit_egle	*Nitzschia eglei*	17	9.20	7.09	8.80	7.32	0.23	0.10
Eun_mono	*Eunotia monodon*	16	8.04	5.53	2.11	3.02	0.34	0.16
Gyr_balt	*Gyrosigma baltica*	16	3.83	7.34	10.57	6.28	0.36	0.06
Nit_brev	*Nitzschia brevissima*	16	17.42	6.16	3.99	2.85	0.30	0.09
Amp_prot	*Amphora proteus*	15	6.04	5.34	11.46	5.17	0.35	0.09
Ano_spha	*Anomoeoneis sphaerophora*	15	4.83	6.21	7.62	4.30	0.28	0.13
Sem_basi	*Seminavis basilica*	15	4.04	6.43	12.78	6.60	0.29	0.12
Nit_clau	*Nitzschia clausii*	14	6.37	6.44	5.85	5.52	0.27	0.14
Pin_micr	*Pinnularia microstauron*	12	3.03	8.03	2.64	2.13	0.33	0.10
Amp_stri	*Amphora strigosa*	9	3.13	5.13	4.15	2.50	0.26	0.09
Par_adna	*Parlibellus adnatus*	9	4.12	5.53	11.01	4.79	0.38	0.05
Rho_cf_musc	*Rhopalodia musculus*	9	4.86	5.23	8.27	3.47	0.38	0.12
Nav_erif	*Navicula erifuga*	8	3.86	5.61	7.72	3.12	0.24	0.14

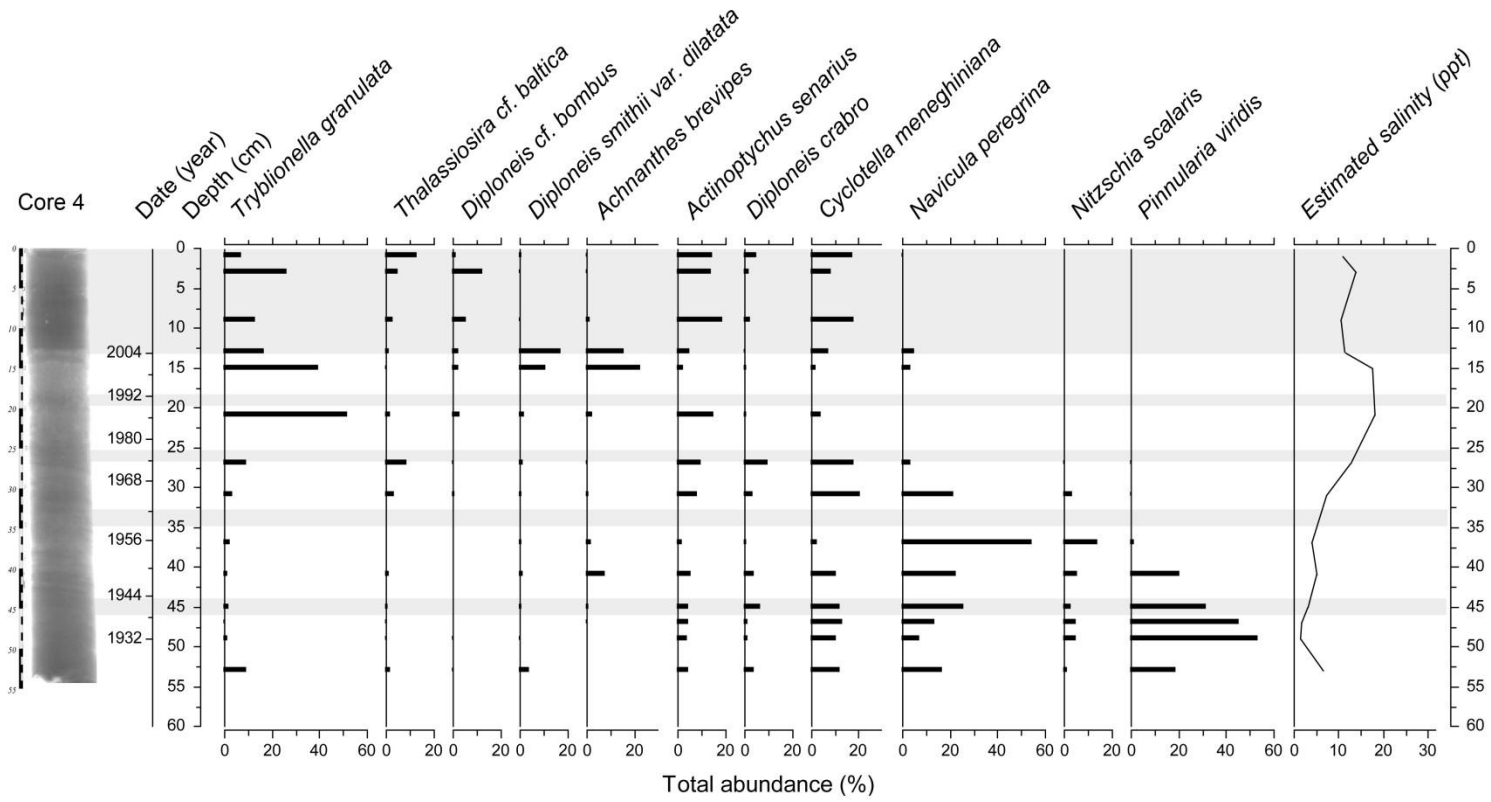

Figure 5-3. Diatom abundance diagram for sediment core 4 and salinity reconstruction based on weighted averaging partial least squares (WA-PLS) component 2 transfer-function developed from a regional calibration data set. Only the most abundant taxa are shown. Sediment core x-radiograph shows soil sediment characteristics (darker = high density, lighter = lower density). Hurricane sediment deposit is marked in grey and diatom assemblage is not reflective of true salinity. Vertical scale is present as a linear distance at depth from surface (cm).

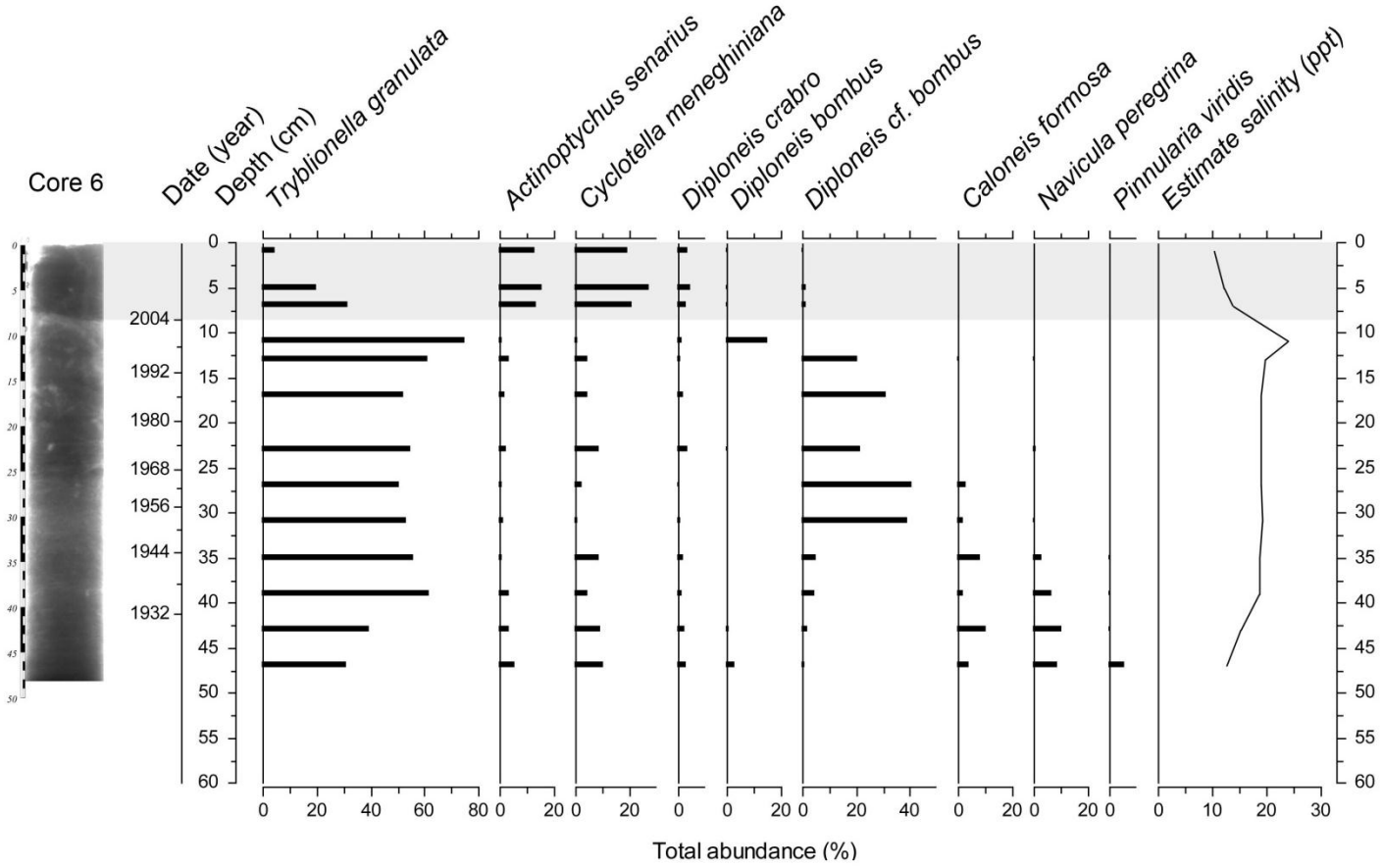

Figure 5-4. Diatom abundance diagram for sediment core 6 and salinity reconstruction based on weighted averaging partial least squares (WA-PLS) component 2 transfer-function developed from a regional calibration data set. Only the most abundant taxa are shown. Sediment core x-radiograph shows soil sediment characteristics (darker = high density, lighter = lower density). Hurricane sediment deposit is marked in grey and diatom assemblage is not reflective of true salinity. Vertical scale is present as a linear distance at depth from surface (cm).

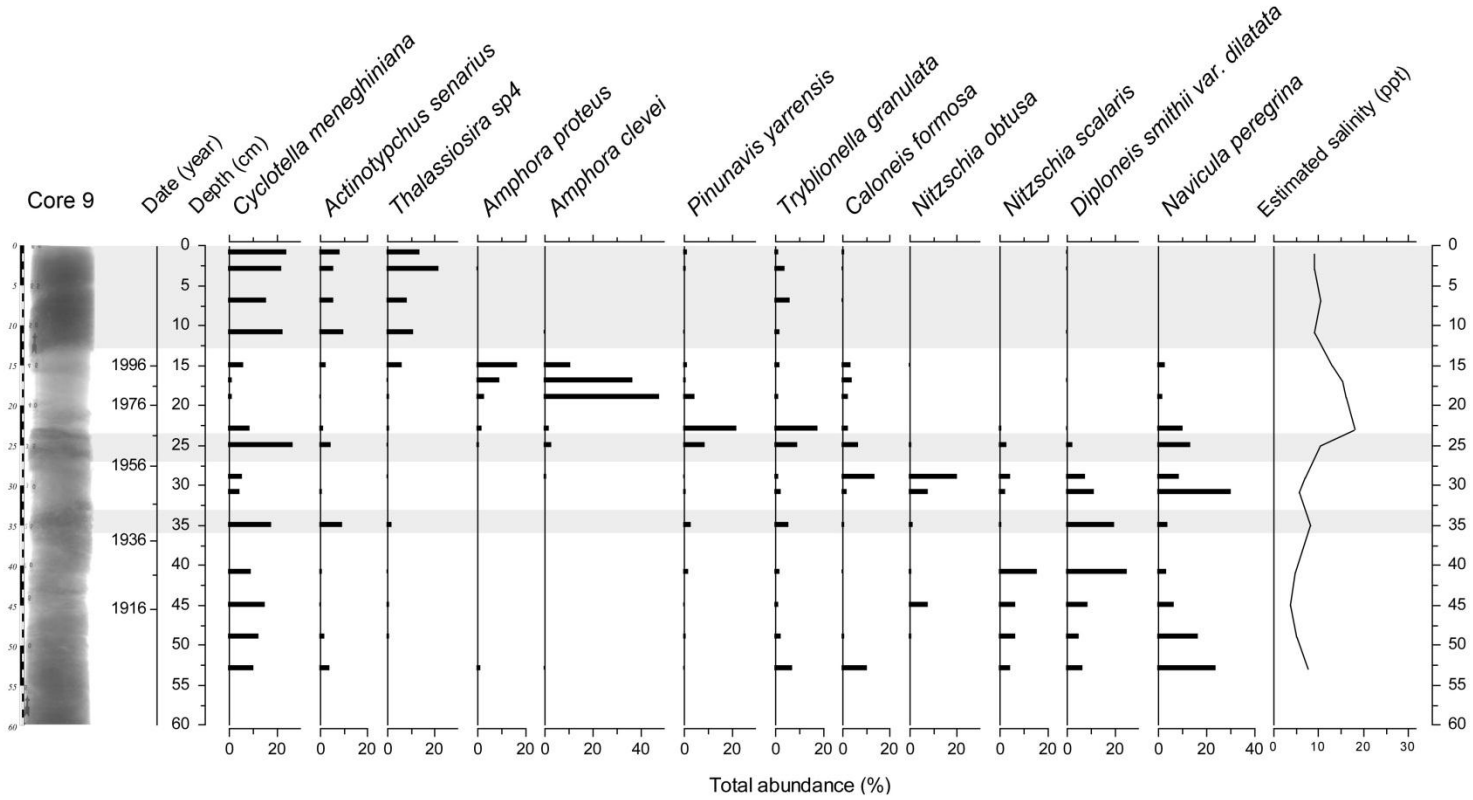

Figure 5-5. Diatom abundance diagram for sediment core 9 and salinity reconstruction based on weighted averaging partial least squares (WA-PLS) component 2 transfer-function developed from a regional calibration data set. Only the most abundant taxa are shown. Sediment core x-radiograph shows soil sediment characteristics (darker = high density, lighter = lower density). Hurricane sediment deposits are marked in grey and diatom assemblage is not reflective of true salinity. Vertical scale is present as a linear distance at depth from surface (cm).

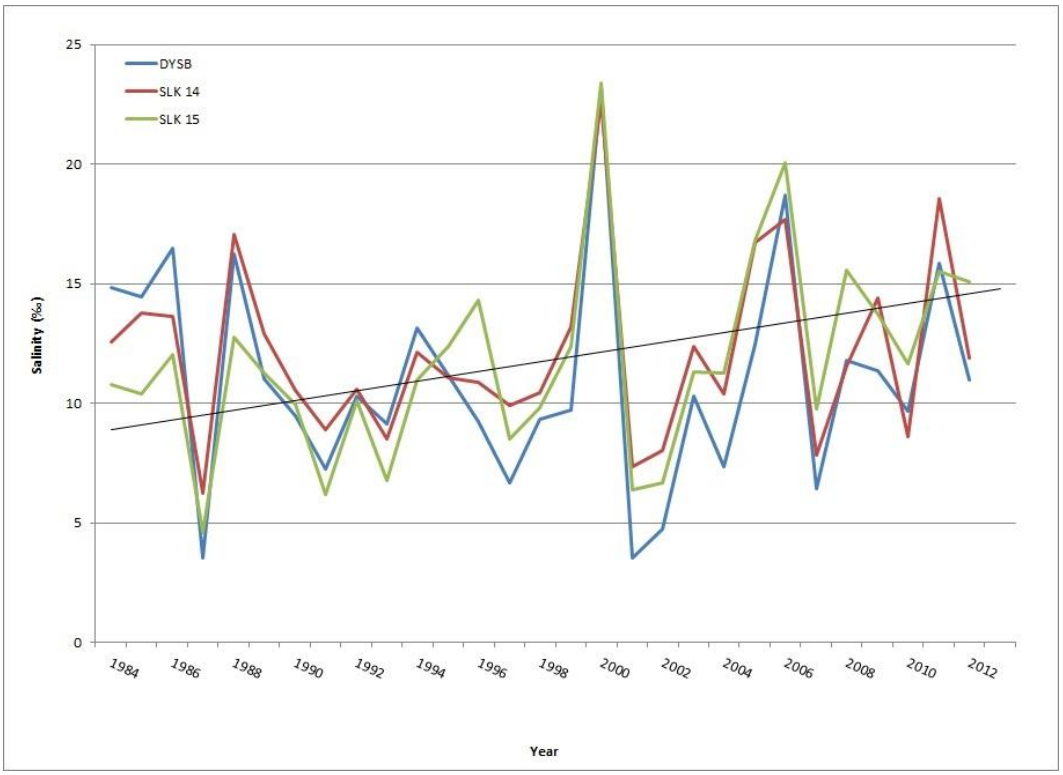

Figure 5-6. Salinity data collected on a monthly basis by Rockefeller Wildlife Refuge staff for three coastal marsh locations. The data were averaged by year and indicate an increasing trend.

CHAPTER 6
CONCLUSIONS

Diatoms are an important primary producer and are prevalent in the sediments, plants, and water column of coastal marsh. They are widely used to assess aquatic environmental conditions due to their species-specific correspondence to water characteristics. The silica walls of the diatom frustule do not decompose and are preserved in the sediment record, providing a record of past environmental conditions. Diatoms have the potential to provide a significant ecological indicator of current coastal wetland condition and a paleoecological tool for examining past environmental change. However the number of samples and the breadth of the conditions sampled must be sufficient to isolate the full tolerance and range of a significant number of species. Studies which compare sampling effort with its influence on gradient length and model predictive capacity could help clarify the number of samples and effort required to create effective transfer functions.

The application of salinity or water-level transfer functions for coastal wetlands are numerous, including setting goals and objectives for wetland restoration, examining the impacts of anthropogenic disturbances, looking at causes of subsidence and marsh loss, and research on sea-level rise. Despite the ubiquitous nature and valuable applications, there are very few studies that examine the relationships between the complex community structure of diatoms and environmental factors influencing their distribution and abundance in coastal marsh of the northern Gulf of Mexico. This study takes important steps toward identifying paleoecological and geochronological techniques to examine sedimentation from hurricanes and environmental change in the coastal marsh of southwest Louisiana.

Diatoms as Indicators of Hurricanes

The diatom community from hurricane sediments is different from non-storm sediments, and therefore shifts in diatom community may provide a method for identifying historic storms in the sediment record. Sharp increases in sand content are a common paleo-indicator of past storms for coastal marsh lakes in the northern Gulf of Mexico (Liu, 2004; Liu and Fearn, 2000a; Liu and Fearn, 1993, 2000b; Otvos, 1999). However, southwest Louisiana is dominated by fine-grained sediments and hurricane sediment deposition is also composed primarily of fine-grain sediments, but is differentiated from non-storm sediments by high bulk density due to low organic matter. Sediment with high bulk density and low organic matter is a common characteristic for many marsh locations; particularly marsh located nearby a tidal stream or the Gulf of Mexico where the regular deposition of mineral sediments from tidal flooding creates a dense sediment profile. Sediment cores from marsh sites located distant from tidal sources may provide the best locations for conducting research on past hurricane frequency because the dense, mineral sediments of hurricane deposition differentiates clearly from non-storm sediments in x-radiographs and sediment profiles. However, using diatoms as a paleo-indicator provides an additional method for identifying storm sediments and can greatly improve analysis in marsh locations dominated by regular mineral sedimentation where storm and non-storm sediments are similar in composition and other indicators are less distinct.

Diatom communities found in storm sediments differentiated from non-storm sediments and were composed primarily of *Tryblionella granulata*, *Actinocyclus senarius*, and *Cyclotella meneghiniana*. Similarities in diatom assemblage of storm sediments from three different marsh sites indicate that storm sedimentation may be

more uniform and less dependent on small-scale processes than non-storm sedimentation. Diatom composition in non-storm sediments varied between sites. Future work should focus on analyzing and comparing samples from historic storms identified deeper in the geologic record to resolve patterns in diatom composition and post-storm effects. Research should focus on answering the following questions: Is there a specific diatom composition that is indicative of storm deposition or does it vary between storms and with geographic location? Is post-storm diatom composition the same as pre-storm composition (i.e. do diatoms return to pre-storm population after landfall)? Due to the rapid response of diatom species to disturbance, it is likely a return or non-return to prior assemblage would also occur quickly. However, Parsons (1998) did not see a return to pre-storm community two years after landfall of Hurricane Andrew, and Pannard et al. (2008) suggest that the diatom community of lakes do not return to pre-event assemblage due to physical and chemical changes induced by meteorological forcing. Climatic events can have a significant role in coastal wetland development and short-term disturbances, such as hurricanes, can have immediate and delayed reactions (Thomson et al., 2001; Woodroffe, 2002). This “pulse” or “perturbation” theory suggests that large climatic events, such as hurricanes, can trigger dramatic long-term changes in ecosystems by altering vegetation (Thomson et al., 2001) and geomorphology (Warren and Niering, 1993). The impact of these events may take many years to fully equilibrate. Increases in the frequency or intensity of storms, as suggested by future climate models, can have substantial impact of the resilience of coastal wetlands. Scientists can gain a more complete understanding of the complex

nature and response times of coastal wetlands to short-term disturbances as more pre-storm and post-storm diatom data are analyzed.

Another question that requires evaluation is how do elements of storm sediment preservation (burial rate, mixing, and deposition depth) influence the diatom composition of storm sediments and diatoms as a paleo-indicator? Factors which influence sediment deposit preservation would also influence diatom assemblage preservation.

Geochronology of Event-driven System

The vertical distribution and inventories of radioisotopes ^{210}Pb and ^{137}Cs were used to calculate vertical accretion rates and estimate chronology for nine sediment cores. Lead-210 inventories for most marsh locations were within the expected atmospheric fallout inventory and do not indicate sediment focusing or excess ^{210}Pb inputs other than atmospheric sources, despite significant hurricane sedimentation. If sediment deposition from storms increases ^{210}Pb inventory, loss from other factors, such as erosion, must have been equivalent to gains to offset hurricane inputs. Sediment erosion is the likely cause for depleted inventories and obscured $^{210}Pb_{xs}$ peak activity below recent hurricane deposition layer for one site, however little indication of erosion was identified at other sites. And contrary to ^{210}Pb inventories, ^{137}Cs inventory was higher than expected for three sites. The inflated inventories are attributed to Hurricane Audrey (1957) since indications of storm deposition are seen in sediment core x-radiographs, so although storm deposition inflated inventories for ^{137}Cs, storm inputs of ^{210}Pb were not significant to alter inventories beyond expected levels.

Despite strong indications of changes in sedimentation and potential variable $_{210}$Pb flux, the ^{210}Pb model constant flux: constant sedimentation most closely

approximately the ^{137}Cs peak for most sites and is likely the most reliable ^{210}Pb model. Most likely the results suggest that despite variations in sedimentation and flux, the long-term depositional trend is largely consistent, except for sites with significant tidal influence.

Hurricane sedimentation alone is unlikely to provide sufficient mineral sediments for coastal marsh to keep pace with sea level. Hurricane sedimentation contributed up to 50% of vertical sediment accumulation, however vertical accretion for most of the sites was less than mean sea-level rise for this region. The marsh locations found to have vertical accretion rates similar to relative sea-level rise were dominated by mineral sedimentation and likely received significant tidal sedimentation.

Furthermore, hurricane impacts may cause compaction or sediment erosion equivalent to gains from deposition. Diatom composition of recent storm sediments suggest a marine source, however dominant species are also prevalent within saline marsh samples. Additional data on the diatom species composition of surrounding open water habitats (nearshore Gulf of Mexico, estuaries, and lakes) may provide more evidence to differentiate whether storm deposition is from saline marsh or open water habitats.

Diatoms and Environmental Gradients

Salinity, water level, and elevation had a significant influence on diatom assemblage. Contemporary diatom assemblages were examined for 46 sites from the coastal marsh of the Chenier plain. Samples were obtained from a very large geographic area representing sites that are several kilometers distant. Among these samples, 173 taxa were identified with 94 of these species having a total abundance of over 10%, showing a well-represented regional diatom population. The variance of

diatom assemblage was significantly correlated with salinity, bulk density, organic matter, and water level. The influence of salinity, bulk density, and organic matter were largely inter-related, also water level and elevation were positively correlated; however, the influence of water level and elevation on diatom assemblages was largely independent of the other three variables. These results show great promise for the development of regional transfer functions for salinity and sea-level parameters because previous transect-based studies on diatoms as sea-level proxies may have issues with spatial autocorrelation and a confounding influence of salinity and elevation or water level. At the local scale where sites are meters apart, elevation and water level are more likely to be correlated with salinity since tidal and freshwater sources are the same for all sites and largely influenced by distance from the source, whereas at a regional-scale fresh and saline water inputs and fluctuations are more likely to vary greatly between sites. A regionally-developed modern analogue for sea-level parameters (salinity, water level and marsh surface elevation) can provide a substantial tool for examining coastal change. Rates of change can be identified by examining changes within the sediment column with chronological data.

Diatom-based Reconstruction

Salinity reconstructions using a diatom transfer function for Rockefeller Wildlife Refuge demonstrate marsh salinization occurring since the 1950s, likely due to the construction of a highway which restricted upland freshwater runoff. Species within the fossil data set were well represented in the contemporary distribution, evidence that a salinity transfer function developed from a regional data set provides sufficient analogues for characterizing environmental conditions. For two of the cores, the salinity reconstruction was in close agreement with available field sampled salinity data and

with the history of salinization of the marsh due to a highway construction which impeded upland freshwater flow. Although the third core did not reflect a similar salinity trend, the diatom data showed a change in dominant species at a similar time frame. This change in community composition exemplifies the importance of examining species density data in conjunction with reconstruction estimates because an impact of the change in freshwater flow was reflected in the diatom record, but not reflected in the salinity reconstruction. Perhaps the salinity transfer function was not robust enough to reflect the change in salinity at this particular site, the salinity change was insubstantial, or some other environmental variable, such as water level, caused species assemblage to change. Water level or elevation reconstructions were not created because the data set did not contain the optima for a significant number of diatom taxa, and was highly sensitive to the removal of samples. Although the data were used to reconstruct several sites and ancillary data and information suggests that the reconstruction is plausible, performance tests suggest the salinity model is also sensitive to the removal of samples and may tend to under-predict high salinity samples. Therefore additional samples are recommended in order to provide a more informative analogue.

Future Research

Future research should focus on improving the diatom-proxy method for identifying historic hurricane sediments. Analysis of recent storm sedimentation has demonstrated that diatom assemblage in storm sediments is distinct from non-storm sediments. Past storms were not clearly identified as having similar assemblage as recent storms; however, few historic storms could be differentiated from non-storm sediments since only one core was analyzed from interior marsh. Analysis of additional sites, where storm sediments can be clearly identified and sampled, would provide a

more robust data set from which to make general conclusions. Future efforts should focus on collecting deeper cores from interior marsh where multiple historic hurricane sediments can be clearly differentiated and sampled. Sampling should be done such that hurricane sediments are sampled exclusively whenever possible, rather than a set sampling interval (such as 1- or 2-cm sediment core “slices” as was performed in this study) where storm and non-storm sediments may be combined and homogenized, tempering the storm-diatom “signal”. Diatom analysis on storm and non-storm sediments should focus on species shifts that are unique to storm sediments at specific locations and across the landscape, with the objective of providing a concrete diatom proxy for storms so that storm sediments can be more clearly differentiated in marsh areas where mineral deposition precludes other storm proxies.

Additional research should expand the contemporary sampling in southwest Louisiana to identify the distribution and environmental preferences for more diatom species, particularly focusing on marsh locations with high salinity. Statistical tests indicate the salinity transfer function was sensitive to removal of samples and may under-predict high-salinity reconstruction estimates. The reconstructions discussed here show that a diatom proxy for salinity shows great potential for reconstructing past sea level, providing a tool for identifying wetland restoration guidelines and evaluating success, and examining the effects of anthropogenic, climatic, and geologic forces in coastal marsh. High salinity may be the most important environmental values to interpret correctly since a change to high salinity could be indicative of marsh salinization and submergence. The diatom-based salinity transfer function will be improved by expanding this contemporary sampling effort, particularly in high salinity

marsh locations. In addition, analysis also demonstrated that the gradient of species preferences to water level and elevation were not fully elucidated within the current sampling effort. Additional samples may provide data on the full range of environmental tolerance for a larger number of species. Expanding on this data set would not be an overly difficult task since the network of sites from which the original sampling was conducted contains an additional 60 sampling stations that are visited regularly.

Not only has this research provided significant data on the distribution and ecology of diatoms in coastal Louisiana, it demonstrates the usefulness of diatoms as a paleo-indicator of storms and changes in salinity in the coastal marsh of southwest Louisiana. Diatom paleo-analysis provides a significant tool for examining past environments and impacts of catastrophic events, environmental change, and anthropogenic alterations on wetland development and long-term sustainability. A diatom transfer function was applied to reconstruct a reasonable estimate of historical salinity for a refuge located in southwest Louisiana. The refuge was impacted by reduction in freshwater flows due road construction, and restoration objectives were focused on restoring freshwater flow through diversions. Diatom analysis suggests that salinity levels were much lower prior to 1950 and averaged as low as 10‰. While this may not be identified as the restoration target, it does provide a historical perspective otherwise unavailable without this kind of analysis.

The techniques developed in this study provide a foundation for future research on the paleoecology of coastal marsh that can help answer many questions regarding long-term management issues. Prior to the early 20th century, land-building processes of the Louisiana coast provided sufficient sediment and vegetation production for marsh

development and maintenance. Due largely to anthropogenic alterations and subsidence, the capability of these wetlands to maintain elevations sufficient to keep pace with sea-level rise no longer exists. Increases in sea-level rise and hurricane frequency and intensity due to climate change can further exacerbate the susceptibility of coastal marsh to submergence. Future wetland loss could be ameliorated by identifying critical rates of vertical accretion, organic and inorganic composition, and marsh elevation requirements to improve wetland resilience to sea-level rise and increasing intensity of storms. Future monitoring of coastal marsh to examine the response of coastal marsh elevation to environmental impacts, such as storms and sea-level rise, and estimating the long-term impact of ecological restoration will lead to improved prediction of future climatic changes. However, these measurements take time, and based on the rate of wetlands loss in coastal Louisiana, will result in many more acres of loss before management can make use of results from future studies. By combining future monitoring with paleoecological studies, we can utilize multiple tools and make immediate decisions regarding site-specific wetland management and restoration goals.

APPENDIX

WEIGHTED AVERAGES OF SELECT ENVIRONMENTAL VARIABLES FOR THE MOST ABUNDANT DIATOM SPECIES OBSERVED IN SEDIMENT SAMPLES

Weighted averages of environmental variables for the most abundant diatom species were calculated using the "wascores" command from the package "vegan" in R (Oksanen, 2011b). Data are relevant to gradient analyses performed in Chapter 4.

Species	Species name	Elev	WL	Sal	LOI	BD	Veg	Acc	Sed	GS	Clay	Sand	Flood
Ach_brev	*Achnanthes brevipes var. brevipes*	0.89	1.12	11.20	27.53	0.28	60.84	0.44	0.12	8.76	0.17	0.11	0.62
Act_ocho	*Actinocyclus ochotensis*	1.10	1.23	6.02	25.49	0.31	64.64	0.46	0.39	7.91	0.18	0.10	0.68
Act_octo	*Actinocyclus octonarius*	1.14	1.33	8.58	21.95	0.38	58.62	0.89	-0.03	11.07	0.17	0.15	0.69
Act_sena	*Actinoptychus senarius*	1.22	1.37	8.96	20.83	0.39	62.38	0.46	-0.05	9.89	0.17	0.13	0.64
Amp_clev	*Seminavis eulensteinii (?)*	0.72	0.90	11.82	23.90	0.31	61.11	0.65	0.05	7.58	0.19	0.07	0.47
Amp_oval	*Amphora ovalis var. libyca*	0.91	1.11	10.17	31.60	0.26	61.14	0.47	0.08	8.38	0.17	0.10	0.58
Amp_prot	*Amphora proteus*	1.16	1.21	11.46	31.65	0.25	55.39	0.24	-0.16	7.31	0.19	0.07	0.66
Amp_stri	*Amphora strigosa*	0.81	1.19	4.15	34.45	0.25	61.33	-0.43	-0.53	11.76	0.14	0.11	0.57
Amp_coff	*Halamphora (Amphora) coffeaeformis*	0.95	1.18	6.62	31.93	0.28	62.06	0.60	-0.16	8.51	0.18	0.10	0.67

Species	Species name	Elev	WL	Sal	LOI	BD	Veg	Acc	Sed	GS	Clay	Sand	Flood
Ano_spha	*Anomoeoneis sphaerophora*	0.91	1.10	7.61	34.83	0.27	55.97	0.85	0.23	6.84	0.20	0.07	0.59
Bac_para	*Bacillaria paradoxa*	0.84	1.06	6.19	33.68	0.25	59.00	0.64	0.16	8.68	0.17	0.09	0.61
Bid_rhom	*Biddulphia rhombus*	1.23	1.39	7.88	23.64	0.34	56.64	0.25	-0.08	11.02	0.16	0.14	0.51
Cal_bude	*Caloneis budensis*	1.10	1.28	3.68	52.11	0.16	51.82	0.79	0.83	15.72	0.12	0.17	0.74
Cal_form	*Caloneis formosa*	0.94	1.11	10.87	27.11	0.28	59.94	0.55	0.14	7.75	0.19	0.08	0.58
Cos_spp	*Coscinodiscus* spp.	1.26	1.53	10.41	17.34	0.44	66.22	0.52	-0.16	9.04	0.18	0.11	0.60
Cyc_lito	*Cyclotella litoralis*	0.70	0.70	14.40	24.58	0.23	65.14	0.52	0.18	8.46	0.18	0.08	0.32
Cyc_mene	*Cyclotella meneghiniana*	1.12	1.27	7.30	29.10	0.32	59.76	0.48	-0.02	10.16	0.17	0.14	0.65
Dip_bomb	*Diploneis bombus*	1.28	1.43	11.48	16.40	0.45	64.18	0.33	-0.02	8.96	0.18	0.12	0.63
Dip_smit	*Diploneis smithii* var. *dilatata*	0.99	1.20	7.72	27.36	0.30	59.38	0.45	0.12	7.82	0.18	0.09	0.64
Dip_smdi	*Diploneis smithii* var. *smithii*	1.05	1.19	7.57	28.52	0.29	58.70	0.71	0.60	9.42	0.17	0.10	0.54
Dip_smpu	*Diploneis smithii* var. *pumila*	0.99	1.12	5.74	34.90	0.26	59.07	0.92	0.14	8.56	0.18	0.10	0.63
Enc_min	*Encyonema minutum* var. *pseudogracilis*	1.03	1.36	1.91	49.60	0.16	57.92	0.17	-1.72	7.68	0.10	0.18	0.83
Ent_alat	*Entomoneis alata*	0.92	1.06	9.71	23.99	0.32	64.16	0.22	-0.01	8.46	0.18	0.08	0.69

Species	Species name	Elev	WL	Sal	LOI	BD	Veg	Acc	Sed	GS	Clay	Sand	Flood
Env_pseu	*Envekadea pseudo-crassirostris*	1.07	1.22	10.58	31.09	0.25	63.98	-0.06	0.82	6.82	0.19	0.06	0.54
Eun_flex	*Eunotia flexuosa*	0.80	1.11	1.04	69.43	0.11	62.71	-0.06	-0.17	17.22	0.08	0.16	0.49
Eun_mino	*Eunotia minor*	1.14	1.20	3.04	51.44	0.16	70.35	0.29	-0.58	9.94	0.14	0.11	0.55
Eun_mono	*Eunotia monodon*	1.07	1.22	2.11	53.82	0.14	62.88	0.33	-0.81	13.35	0.10	0.19	0.65
Eun_peun	*Eunotia pectinalis* var. *undulata*	0.92	1.20	2.24	57.34	0.14	61.45	0.16	-0.65	12.42	0.10	0.15	0.65
Fal_pygm	*Fallacia pygmaea*	1.01	1.12	6.45	43.47	0.20	62.33	0.67	-0.15	9.33	0.16	0.10	0.75
Fru_cras	*Frustulia crassinerva*	0.77	1.06	1.25	55.88	0.14	61.81	0.59	-0.81	9.98	0.11	0.13	0.63
Gom_grac	*Gomphonema gracile*	1.40	1.34	4.43	43.47	0.19	71.87	0.46	-0.46	10.45	0.17	0.12	0.60
Gom_mexi	*Gomphonema mexicanum*	0.84	1.12	5.07	37.57	0.25	57.26	0.82	-0.42	9.28	0.16	0.13	0.51
Gyr_balt	*Gyrosigma balticum*	1.18	1.23	10.56	31.12	0.25	57.85	0.36	0.08	7.63	0.19	0.08	0.61
Gyr_exil	*Gyrosigma exilis*	0.95	1.11	9.16	26.98	0.29	59.38	0.42	0.16	7.90	0.19	0.08	0.59
Mas_pumi	*Mastogloia pumila*	0.74	0.87	11.91	26.41	0.31	58.00	0.81	0.09	7.72	0.19	0.07	0.46
Mel_numm	*Melosira nummuloides*	0.78	0.99	9.23	30.19	0.31	58.21	0.27	-0.31	9.10	0.17	0.09	0.62
Nav_dela	*Navicula delawarensis*	1.22	1.25	6.20	36.13	0.23	50.48	0.87	0.19	13.76	0.14	0.19	0.67
Nav_erif	*Navicula erifuga*	0.80	1.04	7.72	29.00	0.35	55.46	0.60	-0.05	8.30	0.17	0.09	0.52

Species	Species name	Elev	WL	Sal	LOI	BD	Veg	Acc	Sed	GS	Clay	Sand	Flood
Nav_muta	*Luticola (Navicula) mutica*	1.17	1.22	7.34	30.82	0.30	54.36	0.26	0.12	12.76	0.15	0.18	0.70
Nav_pere	*Navicula peregrina*	1.03	1.28	6.32	34.12	0.26	57.92	0.50	0.04	8.62	0.17	0.10	0.64
Nav_rhyn	*Navicula rhynchocephala*	0.93	1.01	8.98	38.16	0.24	63.02	0.37	-0.34	8.35	0.17	0.09	0.71
Nav_schr	*Navicula escambia*	0.74	1.05	2.70	34.49	0.22	60.23	0.62	-0.04	10.09	0.16	0.10	0.67
Nav_secu	*Navicula secura*	0.87	1.15	4.21	29.46	0.27	61.01	0.40	-0.14	6.79	0.19	0.06	0.73
Nav_trip	*Navicula tripunctata*	0.96	1.07	8.36	33.95	0.24	61.62	0.37	-0.14	8.91	0.17	0.10	0.63
Nav_vene	*Navicula veneta*	1.05	1.15	6.21	38.78	0.22	56.60	0.72	0.13	10.29	0.16	0.12	0.73
Nit_brev	*Nitzschia brevissima*	0.76	0.96	3.99	32.54	0.24	68.02	0.66	-0.26	7.50	0.19	0.08	0.69
Nit_cf_dipp	*Nitzschia* cf. *dippelli*	0.92	1.14	7.03	31.38	0.26	58.87	0.57	-0.06	8.45	0.18	0.09	0.64
Nit_clau	*Nitzschia clausii*	0.89	1.05	5.85	33.18	0.26	61.27	0.67	-0.06	8.13	0.18	0.08	0.60
Nit_cons	*Nitzschia constricta*	0.91	1.08	10.39	29.46	0.28	62.67	0.51	0.15	8.03	0.18	0.09	0.52
Nit_debi	*Nitzschia debilis*	1.08	1.17	6.68	31.71	0.26	54.32	0.53	0.16	12.29	0.15	0.17	0.67
Nit_egle	*Nitzschia eglei*	0.72	1.00	8.80	32.90	0.29	59.66	0.01	0.14	10.92	0.16	0.11	0.65
Nit_fili	*Nitzschia filiformis* var. *filiformis*	0.82	1.01	6.68	39.00	0.23	60.72	0.43	-0.22	11.01	0.16	0.12	0.60
Nit_lieb	*Nitzschia liebtruthii*	0.98	1.17	6.37	39.95	0.21	58.08	0.45	-0.04	8.73	0.17	0.10	0.60
Nit_litt	*Nitzschia littoralis*	0.86	1.03	8.28	33.56	0.24	63.82	0.54	-0.24	8.24	0.18	0.09	0.55
Nit_nana	*Nitzschia nana*	0.86	1.09	4.81	41.19	0.20	57.13	0.73	-0.13	11.31	0.15	0.14	0.65
Nit_obtu	*Nitzschia obtusa*	1.10	1.23	4.11	44.46	0.18	59.45	0.46	-0.43	11.50	0.15	0.16	0.65

Species	Species name	Elev	WL	Sal	LOI	BD	Veg	Acc	Sed	GS	Clay	Sand	Flood
Nit_pand	*Nitzschia panduriformis var. panduriformis*	0.94	1.00	10.99	34.68	0.21	60.56	0.23	-0.49	7.02	0.19	0.07	0.61
Nit_scal	*Nitzschia scalaris*	0.93	1.17	5.59	38.22	0.23	60.87	0.51	-0.38	8.92	0.17	0.11	0.61
Nit_sigm	*Nitzschia sigma*	0.96	1.11	7.50	32.47	0.26	60.58	0.34	0.17	8.43	0.17	0.09	0.62
Nit_sgmo	*Nitzschia sigmoidea*	0.92	1.15	5.43	30.34	0.29	61.78	0.52	-0.25	11.13	0.16	0.13	0.67
Par_adna	*Parlibellus adnatus*	1.22	1.17	11.00	26.87	0.34	63.19	0.32	0.52	9.36	0.17	0.13	0.71
Pet_mari	*Petroneis marina*	1.25	1.20	15.78	26.81	0.28	54.62	-0.14	-0.19	7.08	0.21	0.08	0.69
Pin_micr	*Pinnularia microstauron*	1.03	1.28	2.64	58.42	0.14	60.45	-0.03	-0.26	12.79	0.11	0.14	0.67
Pin_viri	*Pinnularia viridis*	1.02	1.35	4.12	36.94	0.25	60.25	0.63	-0.48	10.24	0.17	0.13	0.58
Pin_vifo	*Pinnularia viridiformis*	1.31	1.27	2.44	51.50	0.15	68.78	0.19	-0.73	15.21	0.10	0.21	0.65
Pin_yarr	*Pinnunavis yarrensis*	1.06	1.13	13.40	27.06	0.27	54.27	0.40	0.08	6.85	0.21	0.07	0.60
Pln_deli	*Planothidium delicatulum*	0.65	1.03	3.03	52.17	0.15	48.07	1.31	0.45	8.16	0.17	0.10	0.75
Ple_laev	*Pleurosira laevis*	0.68	1.14	2.71	33.68	0.24	65.68	-0.07	-0.33	16.48	0.10	0.13	0.57
Rho_acum	*Rhopalodia acuminata*	1.13	1.36	6.92	43.17	0.21	58.02	0.27	0.13	10.34	0.15	0.11	0.78
Rho_cf_musc	*Rhopalodia* cf. *musculus*	1.25	1.29	8.27	22.27	0.31	58.90	0.16	0.33	7.23	0.19	0.08	0.55
Rho_paci	*Rhopalodia pacifica*	1.30	1.36	7.30	31.40	0.26	62.40	0.65	0.28	8.77	0.16	0.15	0.76

Species	Species name	Elev	WL	Sal	LOI	BD	Veg	Acc	Sed	GS	Clay	Sand	Flood
Sem_basi	*Seminavis basilica*	0.96	1.23	12.78	27.01	0.27	59.66	0.54	0.17	8.53	0.18	0.09	0.66
Shi_oeve	*Shionodiscus oestrupii var. venrickae*	1.31	1.40	9.70	26.36	0.35	65.63	0.61	0.32	8.24	0.16	0.13	0.74
Shi_oest	*Shionodiscus oestrupii* var. *oestrupii*	1.33	1.43	8.89	18.31	0.43	60.79	0.36	-0.21	12.75	0.16	0.17	0.65
Sta_phoe	*Stauroneis phoenicentron*	1.01	1.16	4.35	44.73	0.25	63.44	-0.04	-0.87	8.60	0.12	0.15	0.69
Sta_pach	*Stauroneis pachycephala*	1.06	1.39	2.43	76.27	0.09	54.15	-0.18	0.66	27.75	0.05	0.27	0.55
Tab_fasc	*Tabularia fasciculata*	1.07	1.28	6.79	35.75	0.25	58.99	0.47	-0.28	9.50	0.16	0.12	0.58
Tha_balt	*Thalassiosira* cf. *baltica*	1.13	1.33	9.11	22.94	0.37	61.27	0.32	-0.12	9.10	0.18	0.12	0.57
Tha_lept	*Thalassiosira* cf. *leptopus*	1.16	1.31	5.93	25.59	0.29	63.50	0.51	0.37	7.22	0.19	0.09	0.68
Tro_lepi	*Tropidoneis lepidoptera*	1.29	1.18	12.39	21.05	0.46	65.23	0.30	0.39	10.17	0.16	0.16	0.79
Try_comp	*Tryblionella compressa* var. *compressa*	1.12	1.23	8.05	30.15	0.28	58.92	0.34	0.12	8.53	0.18	0.09	0.61
Try_gran	*Tryblionella granulata*	1.09	1.30	13.63	22.25	0.34	61.26	0.31	-0.06	7.38	0.20	0.08	0.65
Unk_Cha1	*Unknown Chamaepinnularia* spp1	0.77	1.09	5.10	39.90	0.25	54.28	1.14	-0.24	10.19	0.16	0.13	0.45

Species	Species name	Elev	WL	Sal	LOI	BD	Veg	Acc	Sed	GS	Clay	Sand	Flood
Unk_Nav3	*Unknown Navicula* spp3	1.41	1.58	8.70	16.15	0.48	62.30	0.34	-0.56	14.90	0.15	0.20	0.64
Unk_Syn1	*Unknown Synedra* spp1	0.90	1.17	6.36	33.06	0.28	55.38	0.32	0.30	9.08	0.18	0.10	0.57
Unk_Tha4	*Unknown Thalassiosira* spp4	1.13	1.28	9.13	25.03	0.32	62.69	0.57	0.25	8.19	0.19	0.09	0.62

Elev = elevation (m); WL = water level (m); Sal = salinity (‰); LOI = loss-on-ignition (%); BD = bulk density; Veg = vegetation cover; ACC = vertical accretion (cm/yr); EC = Elevation change (cm/yr); GS = grain size (phi); Clay = percent clay (%); Sand = percent sand (%); Flood = time flooded (%)

LIST OF REFERENCES

Appleby, P.G., 2002. Chronostratigraphic techniques in recent sediments, in: Last, W.M., Smol, J.P. (Eds.), Tracking Environmental Change Using Lake Sediments. Springer Netherlands, pp. 171-203.

Appleby, P.G., Oldfield, F., 1978. The calculation of ^{210}Pb assuming a constant rate of supply of unsupported ^{210}Pb to the sediment. Catena 5, 1-8.

Appleby, P.G., Oldfield, F., 1992. Application of lead-210 to sedimentation studies, in: Ivanovich, I., Harman, R.S. (Eds.), Uranium-series disequilibrium: Application to earth, marine, and environmental sciences. Clarendon Press, Oxford, pp. 731-778.

Barnard, G.A., 1963. Contribution to the discussion of Professor Bartlett's paper. Journal of the Royal Statistical Society, Series B 25, 294.

Barras, J., 2006. Land area change in coastal Louisiana after the 2005 hurricanes—a series of three maps. U.S. Geological Survey.

Barras, J.A., Beville, S., Britsch, L.D., Hartley, S., Hawes, S.R., Johnston, J., Kemp, G.P., Kinler, Q., Martucci, A., Porthouse, J., Reed, D., Roy, K., Sapkota, S., Suhayda, J.N., 2003. Historical and projected coastal Louisiana land changes: 1978-2050, Louisiana Coastal Area (LCA), Louisiana: Ecosystem restoration study Appendix B. U. S. Geological Survey, Baton Rouge, LA, p. 39.

Barras, J.A., Bourgeois, P.E., Handley, L.R., 1994. Land loss in coastal Louisiana 1956-90. U.S. Geological Survey Open-File Report 94-01.

Baskaran, M., 2011. Po-210 and Pb-210 as atmospheric tracers and global atmospheric Pb-210 fallout: a Review. Journal of Environmental Radioactivity 102, 500-513.

Baskaran, M., Coleman, C.H., Santschi, P.H., 1993. Atmospheric depositional fluxes of ^{7}Be and ^{210}Pb at Galveston and College Station, Texas. Journal of Geophysical Research-Atmospheres 98, 20555-20571.

Battarbee, R.W., 1986. Diatom analysis, in: Berglund, B.E. (Ed.), Handbook of Holocene Palaeoecology and Palaeohydrology. John Wiley & Sons, Chichester, pp. 527-570.

Battarbee, R.W., Charles, D.F., Dixil, S.S., Renberg, I., 1999. Diatoms as indicators of surface water salinity, in: Smol, J.P., Stoemer, E.F. (Eds.), Diatoms: Applications for the Environmental and Earth Sciences. Cambridge University Press, Cambridge, pp. 85-121.

Battarbee, R.W., Jones, V.J., Flower, R.J., Cameron, N.G., Bennion, H., Carvalho, L., Juggins, S., 2011. Diatoms, in: Smol, J.P., Birks, H.J., Last, W.M. (Eds.), Tracking Environmental Change Using Lake Sediments: Volume 3: Terrestrial, Algal, and

Siliceous Indicators. Kluwer Academic Publishers, Dordrecht, The Netherlands, pp. 155-202.

Battarbee, R.W., 1973. A new method for the estimation of absolute microfossil number, with reference especially to diatoms. Limnology and Oceanography 18, 647-653.

Baumann, R.H., Day, J.W., Miller, C.A., 1984. Mississippi deltaic wetland survival - sedimentation versus coastal submergence. Science 224, 1093-1095.

Beall, A.O., 1968. Sedimentary processes operative along the western Louisiana shoreline. Journal of Sedimentary Research 38, 869-877.

Besag, J., Diggle, P.J., 1977. Simple Monte Carlo tests for spatial pattern. Journal of the Royal Statistical Society. Series C (Applied Statistics) 26, 327-333.

Birks, H.J.B., 1995. Quantitative palaeoenvironmental reconstructions, in: Maddy, D., Brews, J.S. (Eds.), Statistical Modelling of Quaternary Science Data. Quaternary Research Association, Cambridge, pp. 161-254.

Birks, H.J.B., Line, J.M., Juggins, S., Stevenson, A.C., Ter Braak, C.J.F., 1990. Diatoms and pH reconstruction. Philosophical Transactions Royal Society of London, B 327, 263-278.

Birks, H.J.B., Lotter, A.F., Juggins, S., Smol, J.P., 2012. Tracking Environmental Change Using Lake Sediments: Data Handling and Numerical Techniques. Springer.

Birks, J.B., 2010. Numerical methods for the analysis of diatom assemblage data, in: Smol, J.P., Stoermer, E.F. (Eds.), The Diatoms: Application for the Environmental and Earth Sciences, 2nd ed. Cambridge University Press, Cambridge, MA, pp. 23-46.

Blott, S., Pye, K., 2001. GRADISTAT: A grain size distribution and statistics package for the analysis of unconsolidated sediments. Earth Surface Processes and Landforms 26, 1237-1248.

Boesch, D.F., Josselyn, M.N., Mehta, A.J., Morris, J.T., Nuttle, W.K., Simenstad, C., Swift, D.J.P., 1994. Scientific assessment of coastal wetland loss, restoration and management in Louisiana. Coastal Education and Research Foundation, West Palm Beach, FL.

Boesch, D.F., Levin, D., Nummedal, D., Bowles, K., 1983. Subsidence in Coastal Louisiana: Causes, Rates and Effects on Wetlands. U.S. Fish and Wildlife Service, Washington, D.C., p. 39.

Boesch, D.F., Turner, R.E., 1984. Dependence of fishery species on salt marshes: The role of food and refuge. Estuaries 7, 460-468.

Boorman, L.A., Garbutt, A., Barratt, D., 1998. The role of vegetation in determining patterns of the accretion of salt marsh sediment. Geological Society, London, Special Publications 139, 389-399.

Borcard, D., Gillet, F.o., Legendre, P., 2011. Numerical ecology with R. Springer, New York.

Braak, C.J.F., Juggins, S., 1993. Weighted averaging partial least squares regression (WA-PLS): an improved method for reconstructing environmental variables from species assemblages. Hydrobiologia 269-270, 485-502.

Bray, J.R., Curtis, J.T., 1957. An ordination of the upland forest communities of southern Wisconsin. Ecological Monographs 27, 325-349.

Britsch, L.D., Dunbar, J.B., 1993. Land loss rates - Louisiana coastal plain. Journal of Coastal Research 9, 324-338.

Britsch, L.D., Kemp, E.B., III, 1990. Land loss rates : Mississippi River deltaic plain. U.S. Army Corps of Engineers Waterways Experiment Station, Vicksburg, MS, p. 25.

Byrnes, M.R., McBride, R.A., Tao, Q., Duvic, L., 1995. Historical shoreline dynamics along the Chenier Plain of southwestern Louisiana. Gulf Coast Association of Geological Societies Transactions XLV, 113-122.

Cahoon, D.R., Day, J.W., Jr., Reed, D.J., 1999. The influence of surface and shallow subsurface soil processes on wetland elevation; a synthesis, in: Patrick, W.H., Jr., Nyman, J.A. (Eds.), Current Topics in Wetland Biogeochemistry, vol.3, pp. 72-88.

Cahoon, D.R., Day, J.W., Jr., Reed, D.J., Young, R.S., 1998. Global climate change and sea-level rise: estimating the potential for submergence of coastal wetlands, in: Guntenspergen, G.R., Vairin, B.A. (Eds.), Vulnerability of Coastal Wetlands in the Southeastern United States: Climate Change Research Results, 1992-97. U.S. Geological Survey National Wetlands Research Center 1998-0002, Lafayette, LA, pp. 19-32.

Cahoon, D.R., Hensel, P., Rybczyk, J., McKee, K.L., Proffitt, C.E., Perez, B.C., 2003. Mass tree mortality leads to mangrove peat collapse at Bay Islands, Honduras after Hurricane Mitch. Journal of Ecology 91, 1093-1105.

Cahoon, D.R., Lynch, J.C., Perez, B.C., Segura, B., Holland, R.D., Stelly, C., Stephenson, G., Hensel, P., 2002. High-precision measurements of wetland sediment elevation: II. The rod surface elevation table. Journal of Sedimentary Research 72, 734-739.

Cahoon, D.R., Reed, D.J., Day, J.W., Jr., 1995a. Estimating shallow subsidence in microtidal salt marshes of the Southeastern United States; Kaye and Barghoorn revisited. Marine Geology 128, 1-9.

Cahoon, D.R., Reed, D.J., Day, J.W., Jr., Steyer, G.D., Boumans, R.M., Lynch, J.C., McNally, D., Latif, N., 1995b. The influence of Hurricane Andrew on sediment distribution in Louisiana coastal marshes, in: Stone, G.W., Finkl, C.W. (Eds.), Impacts of Hurricane Andrew on the coastal zones of Florida and Louisiana, 22-26 August 1992; Journal of coastal research special issue no. 21. Coastal Education and Research Foundation, West Palm Beach, FL, pp. 280-294.

Cahoon, D.R., Turner, R.E., 1989. Accretion and Canal Impacts in a Rapidly Subsiding Wetland II. Feldspar Marker Horizon Technique. Estuaries 12, 260-268.

Chabreck, R.H., 1963. Breeding habits of the Pied-billed grebe in an impounded coastal marsh in Louisiana. The Auk 80, 447-452.

Chabreck, R.H., Linscombe, J., 1997. Vegetation Type Map of the Louisiana Coastal Marshes. Louisiana Department of Wildlife and Fisheries, New Orleans, LA.

Chmura, G.L., Kosters, E.C., 1994. Storm deposition and Cs-137 accumulation in fine-grained marsh sediments of the Mississippi delta plain. Estuarine, Coastal and Shelf Science 39, 33-44.

Clark, D., Mazourek, J., 2005. Final environmental assessment: Water introduction south of LA Highway 82 project (ME-16). U.S. Fish and Wildlife Service, Lafayette.

Cochran, J.K., Hirschberg, D.J., Wang, J., Dere, C., 1998. Atmospheric deposition of metals to coastal waters (Long Island Sound, New York U.S.A.): Evidence from saltmarsh deposits. Estuarine, Coastal and Shelf Science 46, 503-522.

Collins, E.S., Scott, D.B., Gayes, P.T., 1999. Hurricane records on the South Carolina coast: Can they be detected in the sediment record? Quaternary International 56, 15-26.

Conner, W.H., Day, J.W., Baumann, R.H., Randall, J.M., 1989. Influence of hurricanes on coastal ecosystems along the northern Gulf of Mexico. Wetlands Ecology and Management 1, 45-56.

Costanza, R., Pérez-Maqueo, O., Martinez, M.L., Sutton, P., Anderson, S.J., Mulder, K., 2008. The value of coastal wetlands for hurricane protection. AMBIO: A Journal of the Human Environment 37, 241-248.

Cretini, K.F., Visser, J.M., Krauss, K.W., Steyer, G.D., 2011. CRMS vegetation analytical team framework: Methods for collection, deployment, and use of vegetation response variables. U.S. Geological Survey Open-File Report 2011-1097, p. 60.

Dahl, T.E., 2011. Status and trends of wetlands in the conterminous United States 2004 to 2009. U.S. Department of Interior, Fish and Wildlife Service, Washington D.C., p. 108.

Davis, D.W., 1992. Canals and the southern Louisiana landscape, in: Janelle, D.G. (Ed.), Geographical snapshots of North America : Commemorating the 27th Congress of the International Geographical Union and Assembly. Guilford Press, New York, pp. 375-379.

Day, J.W., Jr., Reed, D.J., Suhayda, J.N., Kemp, G.P., Cahoon, D., Boumans, R.M., Latif, N., 1994. Physical processes of marsh deterioration, in: Roberts, H.H. (Ed.), Final Report : Critical Physical Processes of Wetland Loss, 1988-1994. The Institute, Baton Rouge, La., pp. 5.1-5.40.

Day, J.W., Jr., Shaffer, G.P., Britsch, L.D., Reed, D.J., Hawes, S.R., Cahoon, D., 1999. Pattern and process of land loss in the Louisiana coastal zone: an analysis of spatial and temporal patterns of wetland habitat change, in: Rozas, L.P., Nyman, J.A., Proffitt, C.E., others, a. (Eds.), Recent Research in Coastal Louisiana: Natural System Function and Response to Human Influence: A Symposium Convened by the Louisiana Universities Marine Consortium, Lafayette, LA, February 3-5, 1998, pp. 193-201.

Day, J.W., Jr., Shaffer, G.P., Britsch, L.D., Reed, D.J., Hawes, S.R., Cahoon, D., 2000. Pattern and process of land loss in the Mississippi Delta: A spatial and temporal analysis of wetland habitat change. Estuaries 23, 425-438.

de Knegt, H.J., van Langevelde, F., Coughenour, M.B., Skidmore, A.K., de Boer, W.F., Heitkönig, I.M.A., Knox, N.M., Slotow, R., van der Waal, C., Prins, H.H.T., 2009. Spatial autocorrelation and the scaling of species–environment relationships. Ecology 91, 2455-2465.

Dean, J., W. E., 1974. Determination of carbonate and organic matter in calcareous sediments and sedimentary rocks by loss on ignition: comparison with other methods. Journal of Sedimentary Petrology 44, 242-248.

DeLaune, R.D., Baumann, R.H., G., G.J., 1983. Relationships among vertical accretion, coastal submergence, and erosion in a Louisiana Gulf Coast marsh. Journal of Sedimentary Petrology 53, 147-157.

DeLaune, R.D., Nyman, J.A., Patrick, W.H., Jr., 1994. Peat collapse, ponding and wetland loss in a rapidly submerging coastal marsh. Journal of Coastal Research 10, 1021-1030.

Delaune, R.D., Patrick, W.H., Jr., Buresh, R.J., 1978. Sedimentation rates determined by ^{173}Cs dating in a rapidly accreting salt marsh. Nature 275, 532-533.

DeLaune, R.D., Reddy, C.N., Patrick, W.H., Jr., 1981. Accumulation of plant nutrients and heavy metals through sedimentation processes and accretion in a Louisiana salt marsh. Estuaries 4, 328-334.

Delaune, R.D., Smith, C.J., Patrick, W.H., 1986. Sedimentation patterns in a gulf coast backbarrier marsh: Response to increasing submergence. Earth Surface Processes and Landforms 11, 485-490.

DeLaune, R.D., Whitcomb, J.H., Patrick, W.H., Jr., Pardue, J.H., Pezeshki, S.R., 1989. Accretion and canal impacts in a rapidly subsiding wetland. I. ^{137}Cs and ^{210}Pb techniques. Estuaries 12, 247-259.

Denys, L., De Wolf, H., 1999. Diatoms as indicators of coastal paleo-environments and relative sea-level change, in: Stoermer, E.F., Smol, J.P. (Eds.), The Diatoms: Application for the Environmental and Earth Sciences. Cambridge University Press, Cambridge, pp. 277-297.

Dingler, J.R., Hsu, S.A., Foote, A.L., 1995. Wind shear stress measurements in a coastal marsh during Hurricane Andrew, in: Stone, G.W., Finkl, C.W. (Eds.), Impacts of Hurricane Andrew on the Coastal Zones of Florida and Louisiana, 22-26 August 1992; Journal of Coastal Research Special Issue No. 21. Coastal Education and Research Foundation, Fort Lauderdale, FL, pp. 295-305.

Dixit, S.S., Smol, J.P., Charles, D.F., Hughes, R.M., Paulsen, S.G., Collins, G.B., 1999. Assessing water quality changes in the lakes of the northeastern United States using sediment diatoms. Canadian Journal of Fisheries and Aquatic Sciences 56, 131-152.

Dokka, R.K., 2006. Modern-day tectonic subsidence in coastal Louisiana. Geology 34, 281-284.

Donnelly, J.P., Bryant, S.S., Butler, J., Dowling, J., Fan, L., Hausmann, N., Newby, P., Shuman, B., Stern, J., Westover, K., Webb, T., 2001. 700 yr sedimentary record of intense hurricane landfalls in southern New England. Geological Society of America Bulletin 113, 714-727.

Doyle, T.W., Keeland, B.D., Gorham, L.E., Johnson, D.J., 1995. Structural impact of Hurricane Andrew on the forested wetlands of the Atchafalaya Basin in south Louisiana, in: Stone, G.W., Finkl, C.W. (Eds.), Impacts of Hurricane Andrew on the Coastal Zones of Florida and Louisiana, 22-26 August 1992; Journal of Coastal Research Special Issue No. 21. Coastal Education and Research Foundation, West Palm Beach, FL, pp. 354-364.

Draut, A.E., Kineke, G.C., Velasco, D.W., Allison, M.A., Prime, R.J., 2005. Influence of the Atchafalaya River on recent evolution of the chenier-plain inner continental shelf, northern Gulf of Mexico. Continental Shelf Research 25, 91-112.

Dunbar, J.B., Britsch, L.D., Kemp, E.B., III, 1990. Land loss rates: Report 2. Louisiana Chenier plain. U.S. Army Corps of Engineers Waterways Experiment Station, Vicksburg, MS.

Dunbar, J.B., Britsch, L.D., Kemp, E.B., III, 1992. Land loss rates: Report 3. Louisiana coastal plain. U.S. Army Engineer Waterways Experiment Station, Vicksburg, MS.

Ebersole, B.A., Westerink, J.J., Bunya, S., Dietrich, J.C., Cialone, M.A., 2010. Development of storm surge which led to flooding in St. Bernard Polder during Hurricane Katrina. Ocean Engineering 37, 91-103.

Efron, B., 1983. Estimating the error rate of a prediction rule: Improvement on cross-validation. Journal of the American Statistical Association 78, 316-331.

Everitt, B., 2011. Cluster Analysis. Wiley, Chichester, West Sussex, U.K.

Ezekiel, M., 1941. Methods of Correlation Analysis, 2nd ed. J. Wiley & Sons, New York; Chapman & Hall, London.

Faith, D.P., Minchin, P.R., Belbin, L., 1987. Compositional dissimilarity as a robust measure of ecological distance. Plant Ecology 69, 57-68.

Fisk, H.M., McClelland, B., 1959. Geology of the continental shelf off Lousiana: Its influence on offshore foundation design. Geological Society of America Bulletin 70, 1369-1394.

Fletcher III, C.H., Van Pelt, J.E., Brush, G.S., Sherman, J., 1993. Tidal wetland record of holocene sea-level movements and climate history. Palaeogeography, Palaeoclimatology, Palaeoecology 102, 177-213.

Folk, R.L., 1974. Petrology of Sedimentary Rock. Hemphill Publishing Company, Austin, Texas.

Folse, T.M., West, J.L., Hymel, M.K., Troutman, J.P., Sharp, L.A., Weifenbach, D., McGinnis, T.E., Rodrigue, L.B., Boshart, W.M., Richardi, C., Miller, C.M., Wood, W.B., 2008, revised 2012. A standard operating prcedures manual for the Coast-wide Reference and Monitoring System-WETLANDS: Methods for site establishment, data collection, and quality assurance control. Louisiana Coastal Protection and Restoration Authority, Baton Rouge, LA, p. 207.

Fritts, H.C., Blasing, T.J., Hayden, B.P., Kutzbach, J.E., 1971. Multivariate techniques for specifying tree-growth and climate relationships and for reconstructing anomalies in paleoclimate. Journal of Applied Meteorology 10, 845-864.

Fritz, S.C., Juggins, S., Battarbee, R.W., Engstrom, D.R., 1991. Reconstruction of past changed in salinity and climate using a diatom-based transfer function. Nature 352, 706-708.

Gagliano, S.M., Kemp, E.B., III, Wicker, K.M., Wiltenmuth, K.S., Sabate, R.W., 2003. Neo-tectonic framework of southeast Louisiana and applications to coastal restoration. Transactions of the Gulf Coast Association of Geological Societies 53, 262-276.

Gehrels, W.R., Roe, H.M., Charman, D.J., 2001. Foraminifera, testate amoebae and diatoms as sea-level indicators in UK saltmarshes: A quantitative multiproxy approach. Journal of Quaternary Science 16, 201-220.

Goldenberg, S.B., Landsea, C.W., Mestas-Nunez, A.M., Gray, W.M., 2001. The recent increase in Atlantic hurricane activity: Causes and implications. Science 293, 474-479.

Gosselink, J.G., Cordes, C.L., Parsons, J.W., 1979. An ecological characterization study of the Chenier Plain coastal ecosystem of Louisiana and Texas. U.S. Fish and Wildlife Service Office of Biological Services, FWS/OBS-78/9 through 78/11 (3 volumes).

Guiot, J., de Vernal, A., 2007. Transfer functions: Methods for quantitative paleoceanography based on microfossils, in: Claude Hillaire–Marcel and Anne De, V. (Ed.), Developments in Marine Geology. Elsevier, pp. 523-563.

Guntenspergen, G.R., 1998. The impact of Hurricane Andrew on Louisiana's coastal landscape, in: Mac, M.J., Opler, P.A., Puckett, C.E. (Eds.), Status and Trends of the Nation's Biological Resources. U.S. Geological Survey, Reston, VA, pp. 20-22.

Guntenspergen, G.R., Cahoon, D.R., Grace, J., Steyer, G.D., Fournet, S., Townson, M.A., Foote, A.L., 1995. Disturbance and recovery of the Louisiana coastal marsh landscape from the impacts of Hurricane Andrew, in: Stone, G.W., Finkl, C.W. (Eds.), Impacts of Hurricane Andrew on the Coastal Zones of Florida and Louisiana, 22-26 August 1992; Journal of Coastal Research Special Issue No. 21. Coastal Education and Research Foundation, West Palm Beach, FL, pp. 324-339.

Guntenspergen, G.R., Vairin, B.A., 1996. Willful winds: Hurricane Andrew and Louisiana's coast. Louisiana Sea Grant College Program and U.S. Dept. of the Interior National Biological Service, Baton Rouge, LA.

Harvey, J.W., Odum, W.E., 1990. The influence of tidal marshes on upland groundwater discharge to estuaries. Biogeochemistry 10, 217-236.

Hassan, G.S., Espinosa, M.A., Isla, F.I., 2008. Fidelity Of Dead Diatom Assemblages In Estuarine Sediments: How Much Environmental Information Is Preserved? PALAIOS 23, 112-120.

Hatton, R.S., DeLaune, R.D., Patrick, W., 1983. Sedimentation, accretion, and subsidence in marshes of Barataria Basin, Louisiana. Limnology and Oceanography 28, 494-502.

Hayes, M.O., 1978. Impact of hurricanes on sedimentation in estuaries, bays, and lagoons., in: Wiley, M.L. (Ed.), Estuarine Interactions. Academic Press, News York, pp. 323-346.

Hayward, B.W., Cochran, U., Southall, K., Wiggins, E., Grenfell, H.R., Sabaa, A., Shane, P.R., Gehrels, R., 2004. Micropalaeontological evidence for the Holocene earthquake history of the eastern Bay of Plenty, New Zealand, and a new index for determining the land elevation record. Quaternary Science Reviews 23, 1651-1667.

Hemond, H.F., Nuttle, W.K., Burke, R.W., Stolzenbach, K.D., 1984. Surface infiltration in salt marshes: Theory, measurement, and biogeochemical implications. Water Resources Research 20, 591-600.

Hemphill-Haley, E., 1995. Diatom evidence for earthquake-induced subsidence and tsunami 300 yr ago in southern coastal Washington. Geological Society of America Bulletin 107, 367-378.

Hill, M.O., 1973. Diversity and evenness: A unifying notation and its consequences. Ecology 54, 427-432.

Hill, M.O., Gauch, H.G., 1980. Detrended correspondence analysis: An improved ordination technique. Plant Ecology 42, 47-58.

Hinchey, J.V., Green, O.R., 1994. A guide to the extraction of fossil diatoms from lithified or partially consolidated sediments. Micropaleontology 40, 368-372.

Hippensteel, S.P., Martin, R.E., Harris, M.S., 2005. Records of prehistoric hurricanes on the South Carolina coast based on micropaleontological and sedimentological evidence, with comparison to other Atlantic Coast records: Discussion. Geological Society of America Bulletin 117, 250-253.

Hook, D.D., Buford, M.A., Williams, T.M., 1991. Impact of Hurricane Hugo on the South Carolina coastal plain forest, in: Finkl, C.W., Pilkey, O.H. (Eds.), Impacts of Hurricane Hugo: September 10-22, 1989; Journal of Coastal Research Special Issue No. 8. Coastal Education and Research Foundation, West Palm Beach, FL, pp. 291-300.

Horton, B.P., Corbett, R., Culver, S.J., Edwards, R.J., Hillier, C., 2006. Modern saltmarsh diatom distributions of the Outer Banks, North Carolina, and the development of a transfer function for high resolution reconstructions of sea level. Estuarine, Coastal and Shelf Science 69, 381-394.

Horton, B.P., Edwards, R.J., 2006. Quantifying Holocene sea-level change using intertidal foraminifera: lessons from the British Isles. Cushman Foundation for Foraminiferal Research, 1-97.

Horton, B.P., Rossi, V., Hawkes, A.D., 2009. The sedimentary record of the 2005 hurricane season from the Mississippi and Alabama coastlines. Quaternary International 195, 15-30.

Horton, B.P., Sawai, Y., 2010. Diatoms as indicators of former sea levels, earthquakes, tsunamis, and hurricanes, in: Smol, J.P., Stoermer, E.F. (Eds.), The Diatoms: Applications for the Environmental and Earth Sciences, 2nd ed. Cambridge University Press, Cambridge, MA, pp. 357-372.

Horton, B.P., Zong, Y., Hillier, C., Engelhart, S., 2007. Diatoms from Indonesian mangroves and their suitability as sea-level indicators for tropical environments. Marine Micropaleontology 63, 155-168.

Howard, R.J., 1996. Relative salinity tolerance of common plants in oligohaline marshes of the northern Gulf of Mexico. U.S. Department of the Interior, National Biological Survey, p. 4.

Howard, R.J., Mendelssohn, I.A., 1999a. Salinity as a constraint on growth of oligohaline marsh macrophytes. I. Species variation in stress tolerance. American Journal of Botany 86, 785-794.

Howard, R.J., Mendelssohn, I.A., 1999b. Salinity as a constraint on growth of oligohaline marsh macrophytes. II. Salt pulses and recovery potential. American Journal of Botany 86, 795-806.

Howard, R.J., Mendelssohn, I.A., 2000. Structure and composition of oligohaline marsh plant communities exposed to salinity pulses. Aquatic Botany 68, 143-164.

Imbrie, J., Kipp, N.G., 1971. A new micropaleontological method for quantitative paleoclimatology; application to a late Pleistocene Caribbean core, in: Turekian, K.K. (Ed.), Late Cenozoic Glacial Ages. Yale University Press, New Haven, pp. 71-181.

Intergovernmental Panel on Climate Change, 2007. Climate change 2007: Impacts, adaptation and vulnerability: Working Group II contribution to the fourth assessment report of the Intergovernmental Panel on Climate Change. Cambridge University Press, Cambridge.

Jackson, L.L., Foote, A.L., Ballistrieri, L.S., 1995. Hydrological, geomorphological, and chemical effects of Hurricane Andrew on coastal marshes of Louisiana, in: Stone, G.W., Finkl, C.W. (Eds.), Impacts of Hurricane Andrew on the Coastal Zones of Florida and Louisiana, 22-26 August 1992; Journal of Coastal Research Special Issue No. 21. Coastal Education and Research Foundation, West Palm Beach, FL, pp. 306-323.

Jarvis, J.C., 2010. Vertical accretion rates in coastal Louisiana: A review of the scientific literature. Army Corps of Engineers, Vicksburg, p. 14.

Joanen, T., McNease, L., 1970. A telemetric study of nesting female alligators on Rockefeller Refuge, Louisiana. Proceedings of the Annual Conference of Southeast Game and Fish Commission 24:175-193.

Jordan, R.W., Stickley, C.E., 2010. Diatoms as indicators of paleooceanographic events, in: Smol, J.P., Stoermer, E.F. (Eds.), The Diatoms: Applications for the Environmental and Earth Sciences, 2nd ed. Cambridge University Press, Cambridge, UK, pp. 424-453.

Juggins, S., 1992. Diatoms in the Thames estuary, England. Bibliotheca Diatomologica 25, 1-216.

Kang, W.J., Trefry, J.H., 2003. Retrospective analysis of the impacts of major hurricanes on sediments in the lower Everglades and Florida Bay. Environmental Geology 44, 771-780.

Kaye, C.A., Barghoorn, E.S., 1964. Late Quaternary sea-level change and crustal rise at Boston, Massachusetts, with notes on the autocompaction of peat. Geological Society of America Bulletin 75, 63-80.

Kearney, M.S., Stevenson, J.C., Ward, L.G., 1994. Spatial and temporal changed in marsh vertical accretion rates at Monie Bay: Implications for sea-level rise. Journal of Coastal Research 10, 1010-1020.

Kemp, A.C., Horton, B.P., Corbett, D.R., Culver, S.J., Edwards, R.J., van de Plassche, O., 2009. The relative utility of foraminifera and diatoms for reconstructing late Holocene sea-level change in North Carolina, USA. Quaternary Research 71, 9-21.

Knott, J.F., Nuttle, W.K., Hemond, H.F., 1987. Hydrologic parameters of salt marsh peat. Hydrological Processes 1, 211-220.

Ko, J.-Y., Day, J.W., 2004. A review of ecological impacts of oil and gas development on coastal ecosystems in the Mississippi Delta. Ocean & Coastal Management 47, 597-623.

Kolbe, R.W., 1927. Zur Ökologie, Morphologie und Systematik der Brackwasser-Diatomeen: die Kieselalgen des Sperenberger Salzgebiets, Volume 7. G. Fischer.

Koç, N., Jansen, E., Haflidason, H., 1993. Paleoceanographic reconstructions of surface ocean conditions in the Greenland, Iceland and Norwegian seas through the last 14 ka based on diatoms. Quaternary Science Reviews 12, 115-140.

Krammer, K., Lange-Bertalot, H., 1990-2009. Süßwasserflora von Mitteleuropa, Bd 02/1-4: Bacillariophyceae. Spektrum Akademischer Verlag, Berlin.

Kulp, M., Penland, S., Williams, S.J., Jenkins, C.J., Flocks, J.G., Kindinger, J.L., 2005. Geological framework, evolution, and sediment resources for restoration of the Louisiana coastal zone, in: Finkl, C.W., Khalil, S.M. (Eds.), Saving America's Wetland: Strategies for Restoration of Louisiana's Coastal Wetlands and Barrier Islands; Journal of Coastal Research Special Issue No. 44. Coastal Education and Research Foundation, West Palm Beach, Fl, pp. 56-71.

Legendre, P., 1993. Spatial autocorrelation: Trouble or new paradigm? Ecology 74, 1659-1673.

Legendre, P., Anderson, M., 1999. Distance-based redundancy analysis: Testing multispecies responses in multifactorial ecological experiments. Ecological Monographs 69, 1-24.

Legendre, P., Fortin, M., 1989. Spatial pattern and ecological analysis. Vegetatio 80, 107-138.

Legendre, P., Gallagher, E., 2001. Ecologically meaningful transformations for ordination of species data. Oecologia 129, 271-280.

Legendre, P., Legendre, L., 1998. Numerical Ecology, 2nd English ed. Elsevier, Amsterdam ; New York.

Leonard, L.A., Luther, M.E., 1995. Flow Hydrodynamics in tidal marsh canopies. Limnology and Oceanography 40, 1474-1484.

Lewis, R.C., Coale, K.H., Edwards, B.D., Marot, M., Douglas, J.N., Burton, E.J., 2002. Accumulation rates and mixing of shelf sediments in the Monteray Bay National Marine Sanctuary. Marine Geology 181, 157-169.

Line, J.M., Braak, C.J.F., Birks, H.J.B., 1994. WACALIB version 3.3 — a computer program to reconstruct environmental variables from fossil assemblages by weighted averaging and to derive sample-specific errors of prediction. Journal of Paleolimnology 10, 147-152.

Liu, K.-B., 2004. Paleotempestology: Principles, methods, and examples from Gulf Coast lake sediments, in: Murnane, R.J., Liu, K.-B. (Eds.), Hurricanes and Typhoons Past, Present, and Future. Columbia University Press, New York, pp. 13-57.

Liu, K.-b., Fearn, M., 2000a. Holocene history of catastrophic hurricane landfalls along the Gulf of Mexico coast reconstructed from coastal lake and marsh sediments, in: Ning, Z.H., Abdollahi, K.K. (Eds.), Current Stresses and Potential Vulnerabilities: Implications of Global Change for the Gulf Coast Region of the United States. Franklin Press, Inc., Baton Rouge, LA, pp. 38-47.

Liu, K.-b., Fearn, M.L., 1993. Lake-sediment record of late Holocene hurricane activities from coastal Alabama. Geology 21, 793-796.

Liu, K.-b., Fearn, M.L., 2000b. Reconstruction of prehistoric landfall frequencies of catastrophic hurricanes in northwestern Florida from lake sediment records. Quaternary Research 54, 238-245.

Louisiana Coastal Wetlands Conservation and Restoration Task Force, 2002. Hydrologic investigation of the Louisiana Chenier plain. Louisiana Department of Natural Resources, Coastal Restoration Division, Baton Rouge, LA, p. 135.

Louisiana Coastal Wetlands Conservation and Restoration Task Force and the Wetlands Conservation and Restoration Authority, 1998. Coast 2050: toward a more sustainable coastal Louisiana. Louisiana Department of Natural Resources, Baton Rouge, LA, p. 161.

McBride, R.A., Taylor, M.J., Byrnes, M.R., 2007. Coastal morphodynamics and Chenier plain evolution in southwestern Louisiana, USA: A geomorphic model. Geomorphology 88, 367-422.

McKee, K., Cherry, J., 2009. Hurricane Katrina sediment slowed elevation loss in subsiding brackish marshes of the Mississippi River delta. Wetlands 29, 2-15.

McKee, K.L., Mendelssohn, I.A., 1989. Response of a freshwater marsh plant community to increased salinity and increased water level. Aquatic Botany 34, 301-316.

Mendelssohn, I.A., Morris, J.T., 2002. Eco-Physiological Controls on the Productivity of Spartina Alterniflora Loisel., in: Weinstein, M.P., Kreeger, D.A. (Eds.) Concepts and Controversies in Tidal Marsh Ecology. Springer Netherlands, pp. 59-80.

Merrill, J.Z., Cornwell, J.C., 2002. The role of oligohaline marshes in estuarine nutrient cycling., in: Weinstein, M.P., Kreeger, D.A. (Eds.) Concepts and Controversies in Tidal Marsh Ecology. Springer Netherlands, pp. 425-441.

Michener, W.K., 1997. Climate change, hurricanes and tropical storms and rising sea level in coastal wetlands. Ecological applications 7, 770-801.

Milan, C.S., Swenson, E.M., Turner, R.E., Lee, J.M., 1995. Assessment of the ^{137}Cs method for estimating sediment accumulation rates: Louisiana salt marshes. Journal of Coastal Research 11, 296-307.

Moore, D.M., Reynolds, R.C., 1989. Diffraction and the Identification and Analysis of Clay Minerals. Oxford University Press, Oxford.

Morgan, J.P., Nichols, L.G., Wright, M., 1958. Morphological Effects of Hurricane Audrey on the Louisiana Coast. Louisiana State University Coastal Studies Institute, Baton Rouge, pp. iv, 53.

Morris, J., 1995. The mass balance of salt and water in intertidal sediments: Results from North Inlet, South Carolina. Estuaries and Coasts 18, 556-567.

Morton, R.A., Barras, J.A., 2011. Hurricane impacts on coastal wetlands: A half-century record of hurricane generated-features from southern Louisiana. Journal of Coastal Research 27, 27-43.

Morton, R.A., Purcell, N.A., Peterson, R.L., 2001. Shallow stratigraphic evidence of subsidence and faulting induced by hydrocarbon production in coastal Southeast Texas. U.S. Geological Survey Open-File Report 01-274.

Mudd, S.M., Howell, S.M., Morris, J.T., 2009. Impact of dynamic feedbacks between sedimentation, sea-level rise, and biomass production on near-surface marsh stratigraphy and carbon accumulation. Estuarine, Coastal and Shelf Science 82, 377-389.

Nelson, A.R., Kashima, K., 1993. Diatom zonation in southern Oregon tidal marshes relative to vascular plants, foraminifera, and sea level. Journal of Coastal Research 9, 673-697.

Nicholls, R.J., Hoozemans, F.M.J., Marchand, M., 1999. Increasing flood risk and wetland losses due to global sea-level rise: regional and global analyses. Global Environmental Change-Human and Policy Dimensions 9, S69-S87.

Nyman, J.A., Crozier, C.R., DeLaune, R.D., 1995. Roles and patterns of hurricane sedimentation in an estuarine marsh landscape. Estuarine, Coastal and Shelf Science 40, 665-679.

Nyman, J.A., DeLaune, R.D., Patrick, W.H., Jr., 1990. Wetland soil formation in the rapidly subsiding Mississippi River deltaic plain: mineral and organic matter relationships. Estuarine Coastal and Shelf Science 31, 57-69.

Nyman, J.A., Delaune, R.D., Roberts, H.H., Patrick, W.H., 1993. Relationship between vegetation and soil formation in a rapidly submerging coastal marsh. Marine Ecology Progress Series 96, 269-279.

Oksanen, J., 2011a. Multivariate Analysis of Ecological Communities in R: vegan tutorial, p. 43 p.

Oksanen, J., 2011b. Vegan: Community Ecology Package for R, 2.0-1 ed.

Olsen, C.R., Larsen, I.L., Lowry, P.D., Cutshall, N.H., Todd, J.F., Wong, G.T.F., Casey, W.H., 1985. Atmospheric fluxes and marsh-soil inventories of ^{7}Be and ^{210}P. Journal of Geophysical Research 90, 10487-10495.

Olsson, I.U., 1987. Radiometric dating, in: Berglund, B.E. (Ed.), Handbook of Holocene Palaeoecology and Palaeohydrology. John Wiley & Sons Ltd., New York, pp. 313-312.

Orson, R.A., 1996. Some applications of paleoecology to the management of tidal marshes. Estuaries 19, 238-246.

Otvos, E.G., Jr., 1999. Quaternary coastal history, basin geometry and assumed evidence for hurricane activity, northeastern Gulf of Mexico coastal plain. Journal of Coastal Research 15, 438-443.

Otvos, E.G., Jr., Liu, K., Fearn, M.L., 2002. Prehistoric landfall frequencies of catastrophic hurricanes in northwestern Florida from lake sediment records; discussion and reply. Quaternary Research 57, 425-431.

Palmer, A.J.M., Abbott, W.H., 1986. Diatoms as indicators of sea-level change, in: van de Plassche, O. (Ed.), Sea-level research: A manual for the collection and evaluation of data. Free University, Amsterdam, pp. 457-481.

Pannard, A., Bormans, M., Lagadeuc, Y., 2008. Phytoplankton species turnover controlled by physical forcing at different time scales. Canadian Journal of Fisheries and Aquatic Sciences 65, 47-60.

Pappas, J.L., Stoermer, E.F., 1995. Multidimensional analysis of diatom morphologic and morphometric phenotypic variation and relation to niche. Ecoscience 2, 357-367.

Parsons, M.L., 1998. Salt marsh sedimentary record of the landfall of Hurricane Andrew on the Louisiana coast: Diatoms and other paleoindicators. Journal of Coastal Research 14, 939-950.

Parsons, M.L., Dortch, Q., Turner, R.E., Rabalais, N.N., 1999a. Salinity history of coastal marshes reconstructed from diatom remains. Estuaries 22, 1078-1089.

Parsons, M.L., Dortch, Q., Turner, R.E., Rabalais, N.N., 1999b. The use of diatom remains as a proxy of historical salinity changes in Airplane Lake, Louisiana, in: Rozas, L.P., Nyman, J.A., Proffitt, C.E., Rabalais, N.N., Reed, D.J., Turner, R.E. (Eds.), Recent Research in coastal Louisiana: Natural System Function and Response to Human Influence. Louisiana Sea Grant College Program, Baton Rouge, LA, pp. 65-78.

Patrick, R., 1963. The structure of diatom community under varying ecological conditions. Annals of the New York Academy of Science 108, 357-365.

Patrick, R., Reimer, C.W., 1966a. The diatoms of the United States, exclusive of Alaska and Hawaii: Vol. 1 : Fragilariaceae, Eunotiaceae, Achnanthaceae, Naviculaceae. Academy of Natural Sciences of Philadelphia.

Patrick, R., Reimer, C.W., 1966b. The diatoms of the United States, exclusive of Alaska and Hawaii: Vol. 2 : Entomoneidaceae, Cymbellaceae, Gomphonemaceae, Epithemiaceae. Academy of Natural Sciences of Philadelphia.

Patterson, R.T., Hutchinson, I., Guilbault, J.P., Clague, J.J., 2000. A comparison of the vertical zonation of diatom, foraminifera, and macrophyte assemblages in a coastal marsh: Implications for greater paleo-sea level resolution. Micropaleontology 46, 229-244.

Paulsen, S.C., List, E.J., Santschi, P.H., 1999. Modeling variability in ^{210}Pb and sediment fluxes near the Whites Point outfalls, Palos Verdes Shelf, California. Environmental Science & Technology 33, 3077-3085.

Penland, S., Mendelssohn, I.A., Wayne, L., Britsch, D., 1996. Natural and human causes of coastal land loss in Louisiana – Workshop summary. Coastal Studies Institute, Wetland Biochemistry Institute, Louisiana State University, Baton Rouge, p. 25.

Pethick, J.S., 1981. Long-term accretion rates on tidal salt marshes. Journal of Sedimentary Research 51, 571-577.

Pheiffer Madsen, P., Sørensen, J., 1979. Validation of the lead-210 dating method. Journal of Radioanalytical Chemistry 54, 39-48.

Phillips, L.A., 2002. Vertical accretion and marsh elevation dynamics on the Chenier plain, Louisiana. University of Louisiana at Lafayette, Lafayette, p. 123.

Pyle, L., Cooper, S.R., Huvane, J.K., 1998. Diatom paleoecology Pass Key core 37, Everglades National Park, Florida Bay. U.S. Geological Survey Open-File Report 98-522, Durham, NC, p. 40.

Ramsey, E.W., III, Laine, S., Werle, D., Tittley, B., Lapp, D., 1994. Monitoring Hurricane Andrew damage and recovery of the coastal Louisiana marsh using satellite remote sensing data, Coastal Zone Canada '94: Cooperation in the Coastal Zone. Dalhousie University, Halifax (Canada), 20-23 Sep 1994, pp. 1841-1852.

Ramstack, J.M., Fritz, S.C., Engstrom, D.R., Heiskary, S.A., 2003. The application of a diatom-based transfer function to evaluate regional water quality trends in Minnessota since 1970. Journal of Paleolimnology 29, 79-94.

Ravens, T.M., Roberts, K.A., Santschi, P.H., Thomas, R.C., 2009. Causes of salt marsh erosion in Galveston Bay, Texas. Journal of Coastal Research 25, 265+.

Reed, D., 1992. Effect of weirs on sediment deposition in Louisiana coastal marshes. Environmental Management 16, 55-65.

Reed, D., Spencer, T., Murray, A., French, J., Leonard, L., 1999. Marsh surface sediment deposition and the role of tidal creeks: Implications for created and managed coastal marshes. Journal of Coastal Conservation 5, 81-90.

Reed, D.J., 1989. Patterns of sediment deposition in subsiding coastal salt marshes, Terrebonne Bay, Louisiana - the role of winter storms. Estuaries 12, 222-227.

Reed, D.J., 1995. The response of coastal marshes to sea-level rise: Survival or submergence? Earth Surface Processes and Landforms 20, 39-48.

Reed, D.J., Wilson, L., 2004. Coast 2050: A new approach to restoration of Louisiana coastal wetlands. Physical geography 25, 4-21.

Rejmánek, M., Sasser, C.E., Peterson, G.W., 1988. Hurricane-induced sediment deposition in a gulf coast marsh. Estuarine, Coastal and Shelf Science 27, 217-222.

Reynolds, C.S., 1984. Phytoplankton periodicity: the interactions of form, function and environmental variability. Freshwater Biology 14, 111-142.

Robbins, J.A., 1978. Geochemical and geophysical applications of radioactive lead, in: Nriagu, J.O. (Ed.), The biogeochemistry of lead in the environment. Elsevier Scientific, Amsterdam, pp. 285-393.

Roberts, H.H., Bentley, S., Coleman, J.M., Hsu, S.A., Huh, O.K., Rotondo, K., Inoue, M., Rouse, L.J., Jr., Sheremet, A., Stone, G.W., Walker, N., Welsh, S., Wiseman, W.J., Jr., 2002. Geological framework and sedimentology of Recent mud deposition on the eastern chenier plain coast and adjacent inner shelf, western Louisiana. Transactions - Gulf Coast Association of Geological Societies 52, 849-859.

Roe, H.M., Doherty, C.T., Patterson, R.T., Swindles, G.T., 2009. Contemporary distributions of saltmarsh diatoms in the Seymour-Belize Inlet Complex, British Columbia, Canada: Implications for studies of sea-level change. Marine Micropaleontology 70, 134-150.

Roman, C.T., Peck, J.A., Allen, J.R., King, J.W., Appleby, P.G., 1997. Accretion of a New England (U.S.A) salt marsh in response to inlet migration, storms, and sea-level rise. Estuaries, Coastal and Shelf Science 45, 717-727.

Rousseeuw, P.J., 1987. Silhouettes: A graphical aid to the interpretation and validation of cluster analysis. Journal of Computational and Applied Mathematics 20, 53-65.

Rybczyk, J.M., Cahoon, D.R., 2002. Estimating the potential for submergence for two wetlands in the Mississippi River delta. Estuaries 25, 985-998.

Sachs, H.M., Webb, T., Clark, D.R., 1977. Paleoecological transfer functions. Annual Review of Earth and Planetary Sciences 5, 159-178.

Sallenger, A.H., Jr., Williams, S.J., 1993. Hurricanes and coastal erosion; the lessons of Andrew in Louisiana; United States Geological Survey yearbook, FY 1992. U.S. Geological Survey, United States, pp. 1-3.

Scavia, D., Field, J.C., Boesch, D.F., Buddemeier, R.W., Burkett, V., Cayan, D.R., Fogarty, M., Harwell, M.A., Howarth, R.W., Mason, C., Reed, D.J., Royer, T.C., Sallenger, A.H., Jr., Titus, J.G., 2002. Climate change impacts on US coastal and marine ecosystems. Estuaries 25, 149-164.

Shennan, I., Innes, J., Long, A., Zong, Y., 1995. Holocene relative sea-level changes and coastal vegetation history at Kentra-moss Argyll, Northwest Scotland. Marine Geology 124, 43-59.

Shepard, R., 1962. The analysis of proximities: Multidimensional scaling with an unknown distance function. I. Psychometrika 27, 125-140.

Sherrod, B.L., 1999. Gradient analysis of diatom assemblages in a Pudget Sound salt marsh: Can such assemblages be used for quantitative paleoecological reconstructions? Palaeogeography Palaeoclimatology Palaeoecology 149, 213-226.

Simpson, G.L., Hall, R.I., 2012. Human Impacts: Application of numerical methods to evaluate surface-water acidification and eutrophication, in: Birks, H.J.B., Lotter, A.F., Juggins, S., Smol, J.P. (Eds.), Tracking Environmental Change Using Lake Sediments: Data Handling and Numerical Techniques. Springer, Netherlands, pp. 431-494.

Smol, J.P., Stoermer, E.F., 2010. The Diatoms: Applications for the Environmental and Earth Sciences. Cambridge University Press.

Sneath, P.H.A., Sokal, R.R., 1973. Numerical Taxonomy: The Principles and Practice of Numerical Classification. Freeman, San Francisco.

Soukup, D.A., Buck, B.J., Harris, W., 2008. Preparing soils for mineralogical analysis, in: Ulery, A.L., Drees, L.R. (Eds.), Methods of Soil Analysis. Part 5, Mineralogical Methods. Soil Science Society of America, Madison, WI, pp. xvii, 521 p.

Stedman, S., Dahl, T.E., 2008. Status and trends of wetlands in the coastal watersheds of the Eastern United States 1998 to 2004. National Oceanic and Atmospheric Adminstration, National Marine Fisheries Service and U.S. Department of Interior, Fish and Wildlife Service, p. 32.

Stevenson, J.C., Kearney, M.S., Pendleton, E.C., 1985. Sedimentation and erosion in a Chesapeake Bay brackish marsh system. Marine Geology 67, 213-235.

Stevenson, R.J., Bothwell, M.L., Lowe, R.L., 1996. Algal ecology : freshwater benthic ecosystems. Academic Press, San Diego.

Steyer, G., Sasser, C., Visser, J., Swenson, E., Nyman, J., Raynie, R., 2003. A proposed coast-wide reference monitoring system for evaluating wetland restoration trajectories in Louisiana. Environmental Monitoring and Assessment 81, 107-117.

Steyer, G.D., 2010. Coastwide Reference Monitoring System (CRMS), in: Survey, U.S.G. (Ed.), Fact Sheet, p. 2.

Stidolph, S.R., Ferrenburg, F.A.S., Smith, K.E.L., Kraberg, A., 2012. Stuart R. Stidolph Diatom Atlas. U.S. Geological Survey Open-File Report 2012–1163, St. Petersburg, FL.

Stone, G.W., Grymes, J.M., Dingler, J.R., Pepper, D.A., 1997. Overview and significance of hurricanes on the Louisiana coast, USA. Journal of Coastal Research 13, 656-669.

Stone, G.W., Liu, B.Z., Pepper, D.A., Wang, P., 2004. The importance of extratropical and tropical cyclones on the short-term evolution of barrier islands along the northern Gulf of Mexico, USA. Marine Geology 210, 63-78.

Stone, G.W., Xu, J.P., Zhang, X., 1995. Estimation of the wave field during Hurricane Andrew and morphological change along the Louisiana coast, in: Stone, G.W., Finkl, C.W. (Eds.), Impacts of Hurricane Andrew on the Coastal Zones of Florida and Louisiana, 22-26 August 1992; Journal of Coastal Research Special Issue No. 21. Coastal Education and Research Foundation, West Palm Beach, FL, pp. 234-253.

Stumpf, R.P., 1983. The process of sedimentation on the surface of a salt marsh. Estuarine, Coastal and Shelf Science 17, 495-508.

Szkornik, K., Gehrels, W.R., Kirby, J.R., 2006. Salt-marsh diatom distributions in Ho Bugt (western Denmark) and the development of a transfer function for reconstructing Holocene sea-level changes. Marine Geology 235, 137-150.

Telford, R., Birks, H., 2005. The secret assumption of transfer functions: problems with spatial autocorrelation in evaluating model performance. Quaternary Science Reviews 24, 2173-2179.

Telford, R.J., Andersson, C., Birks, H.J.B., Juggins, S., 2004. Biases in the estimation of transfer function prediction errors. Paleoceanography 19, PA4014.

ter Braak, C.J.F., 1995a. Calibration, in: Jongman, R.H., ter Braak, C.J.F., Van Tongeren, O.F.R. (Eds.), Data Analysis in Community and Landscape Ecology. Cambridge University Press, Cambridge ; New York, pp. 78-90.

ter Braak, C.J.F., 1995b. Ordination, in: Jongman, R.H., ter Braak, C.J.F., Van Tongeren, O.F.R. (Eds.), Data Analysis in Community and Landscape Ecology. Cambridge University Press, Cambridge ; New York, pp. 91-173.

ter Braak, C.J.F., Juggins, S., 1993. Weighted averaging partial least squares regression (WA-PLS): An improved method for reconstructing environmental variables from species assemblages. Hydrobiologia 269-270, 485-502.

ter Braak, C.J.F., Juggins, S., Birks, H.J.B., Van der Voet, H., 1993. Weighted averaging partial least squares regression (WA-PLS): Definition and comparison with other methods for species-environment calibration, in: Patil, G.P., Rao, C.R. (Eds.), Multivariate Environmental Statistics, 2nd ed. Elsevier Science Publishers B.V. (North Holland), Amsterdam, pp. 525-560.

ter Braak, C.J.F., Šmilauer, P., 1998. CANOCO reference manual and User's guide to Canoco for Windows: Software for Canonical Community Ordination (Version 4). Microcomputer Power, Ithaca, N.Y.

Thomson, D.M., Shaffer, G.P., McCorquodale, J.A., 2001. A potential interaction between sea-level rise and global warming: implications for coastal stability on the Mississippi River Deltaic Plain. Global and Planetary Change 32, 49-59.

Turner, R.E., 1997. Wetland loss in the northern Gulf of Mexico: Multiple working hypotheses. Estuaries 20, 1-13.

Turner, R.E., Baustian, J.J., Swenson, E.M., Spicer, J.S., 2006a. Wetland sedimentation from hurricanes Katrina and Rita. Science 314, 449-452.

Turner, R.E., Milan, C.S., Swenson, E.M., 2006b. Recent volumetric changes in salt marsh soils. Estuarine, Coastal and Shelf Science 69, 352-359.

Turner, R.E., Swenson, E.M., Milan, C.S., Lee, J.M., 2007. Hurricane signals in salt marsh sediments: Inorganic sources and soil volume. Limnology and Oceanography 52, 1231-1238.

Twilley, R.R., 2003. Coastal Louisiana ecosystem assessment and restoration (CLEAR) model of Louisiana coastal area (LCA) comprehensive ecosystem restoration plan,

Volume 1: Tasks 1-8. Department of Natural Resources, Coastal Restoration Division, Baton Rouge, LA.

U.S. Army Corps of Engineers, 2003. Louisiana Coastal Area (LCA), Louisiana: Ecosystem Restoration Study. U.S. Army Corps of Engineers, New Orleans, p. 506.

Vairin, B.A., 1997. Caring for Coastal Wetlands: The Coastal Wetlands Planning, Protection and Restoration Act. U.S. Geological Survey, National Wetlands Research Center, Lafayette, LA.

van der Werff, A., 1956. A new method of concentrating and cleaning diatoms and other organisms. International Association of Theoretical and Applied Limnology 12, 276-277.

van der Werff, A., Huls, H., 1957-1974. Diatomeënflora van Nederland (reprinted 1976). Otto Koeltz Science Publishers, Koenigstein.

Van Heurck, H., 1896. A treatise on the Diatomaceae. William Wesley and Son, London, p. 558.

Visser, J.M., Sasser, C.E., Linscombe, R.G., Chabreck, R.H., 2000. Marsh vegetation types of the Chenier plain, Louisiana, USA. Estuaries 23, 318-327.

Vyverman, W., Sabbe, K., 1995. Diatom-temperature transfer functions based on the altitudinal zonation of diatom assemblages in Papua New Guinea: a possible tool in the reconstruction of regional palaeoclimatic changes. Journal of Paleolimnology 13, 65-77.

Wachnicka, A., Gaiser, E., Collins, L., Frankovich, T., Boyer, J., 2010. Distribution of Diatoms and Development of Diatom-Based Models for Inferring Salinity and Nutrient Concentrations in Florida Bay and Adjacent Coastal Wetlands of South Florida (USA). Estuaries and Coasts 33, 1080-1098.

Wagner, H., 2004. Direct multi-scale ordination with canonical correspondence analysis. Ecology 85, 342-351.

Warren, R.S., Niering, W.A., 1993. Vegetation change on a northeast tidal marsh: interaction of sea-level rise and marsh accretion. Ecology 74, 96-103.

Webb, T.I., Bryson, R.A., 1972. Late- and postglacial climatic change in the northern Midwest, USA: Quantitative estimates derived from fossil pollen spectra by multivariate statistical analysis. Quaternary Research 2, 70-115.

Webster, P.J., Holland, G.J., Curry, J.A., Chang, H.R., 2005. Changes in tropical cyclone number, duration, and intensity in a warming environment. Science 309, 1844-1846.

Wheatcroft, R.A., Drake, D.E., 2003. Post-depositional alteration and preservation of sedimentary event layers on continental margins, I. The role of episodic sedimentation. Marine Geology 199, 123-137.

Wicker, K.M., Roberts, D., Davis, D., 1983. Rockefeller State Wildlife Refuge and Game Preserve : Evaluation of Wetland Management Techniques. Louisiana Dept. of Natural Resources, Baton Rouge; Office of Coastal Zone Management, National Oceanic and Atmospheric Administration, Washington D.C., p. 106.

Williams, C.J., 2011a. A paleoecological perspective on wetland restoration wetlands, in: LePage, B.A. (Ed.). Wetlands: Integrating Multidisplinary Concepts. Springer Netherlands, pp. 67-91.

Williams, H.F.L., 2009. Stratigraphy, sedimentology, and microfossil content of Hurricane Rita storm surge deposits in southwest Louisiana. Journal of Coastal Research 25, 1041-1051.

Williams, H.F.L., 2010. Storm surge deposition by hurricane ike on the Mcfaddin National Wildlife Refuge, Texas: Implications for paleotempestology studies. Journal of Foraminiferal Research 40, 210-219.

Williams, H.F.L., 2011b. Stratigraphic record of Hurricanes Audrey, Rita, and Ike in the Chenier plain of southwest Louisiana. Journal of Coastal Research, Special Issue No. 64, 1921-1926.

Williams, H.F.L., Flanagan, W.M., 2009. Contribution of Hurricane Rita storm surge to long-term sedimentation in Louisiana coastal woodlands and marshes. Journal of Coastal Research, Special Issue No. 56, 1671-1675.

Williams, R.B., 1962. The Ecology of Diatom Populations in a Georgia Salt Marsh. Harvard University, Cambridge, p. 146.

Wiseman, W.J., Jr., Swenson, E.M., Power, J., 1990. Salinity trends in Louisiana estuaries. Estuaries 13, 265-271.

Witkowski, A., Lange-Bertalot, H., Netzeltin, D., 2000. Diatom Flora of Marine Coasts, I. A.R.G. Gantner, Konigstein.

Wolanski, E., Brinson, M.M., Cahoon, D.R., Perillo, G.M.E., 2009. Coastal wetlands: A synthesis. Coastal Wetlands: An integrated ecosystem approach, 1-43.

Woodroffe, C.D., 2002. Coasts: Form, Process, and Evolution. Cambridge University Press, Cambridge ; New York.

Woodroffe, S.A., Long, A.J., 2009. Reconstructing recent relative sea-level changes in West Greenland: Local diatom-based transfer functions are superior to regional models. Quaternary International 221, 91-103.

Wright, L.D., Swaye, F.J., Coleman, J.M., 1970. Effects of Hurricane Camille on the landscape of the Breton-Chandeleur Island chain and the eastern portion of the Lower Mississippi Delta. Louisiana State University, Coastal Studies Institute, Baton Rouge.

Zong, Y., 1997. Mid- and late-Holocene sea-level changes in Roudsea Marsh, northwest England: a diatom biostratigraphical investigation. Holocene 7, 311-323.

Zong, Y., Shennan, I., Combellick, R., Hamilton, S., Rutherford, M., 2003. Microfossil evidence for land movements associated with the AD 1964 Alaska earthquake. Holocene 13, 7-20.

Zong, Y., Tooley, M., 1996. Holocene sea-level changes and crustal movements in Morecambe Bay, northwest England. Journal of Quaternary Science 11, 43-58.

BIOGRAPHICAL SKETCH

Kathryn Enga Louise Smith was born in Minnesota to James and Darlene Smith. She gained a passion for the outdoors at an early age and was determined to become a scientist. As an honor student at Champlin Park High School, she took college classes at North Hennepin Community College and obtained an Associate of Arts degree, then went on to pursue her Bachelor of Science in Natural Resources and Environmental Studies at the University of Minnesota, Twin Cities. After graduation, she worked for the Minnesota Department of Natural Resources where she honed her skills in spatial analysis and data management, but desired more scientific challenges. She moved to Gainesville in 1999 to pursue a Master of Science in Wildlife Ecology, with emphasis on landscape ecology. Upon graduation, she began work for the U.S. Geological Survey where she learned to combine her passion for science with her natural skills in technology and geographic information systems. Again, looking for greater challenges, she enrolled at the University of Florida, College of Engineering Sciences because she read a paper on intertidal marshes by her advisor, Clay Montague, and, after talking with him, was inspired by his enthusiasm for science and learning. Kathryn continues to work for the U.S. Geological Survey Coastal and Marine Science Center in Saint Petersburg, Florida, where she hopes to find more opportunities to apply paleoecological methods to explore the societal implications related to environmental change and impacts on coastal ecosystems.